

University of Alberta

A Design Guide for Steel Plate Shear Walls in Canada

by

Joseph Stankevicius

A thesis submitted to the Faculty of Graduate Studies and Research
in partial fulfillment of the requirements for the degree of

Master of Science

in

Structural Engineering

Department of Civil and Environmental Engineering

©Joseph Stankevicius

Spring 2011

Edmonton, Alberta

Permission is hereby granted to the University of Alberta Libraries to reproduce single copies of this thesis and to lend or sell such copies for private, scholarly or scientific research purposes only. Where the thesis is converted to, or otherwise made available in digital form, the University of Alberta will advise potential users of the thesis of these terms.

The author reserves all other publication and other rights in association with the copyright in the thesis and, except as herein before provided, neither the thesis nor any substantial portion thereof may be printed or otherwise reproduced in any material form whatsoever without the author's prior written permission.

Examining Committee

Dr. Gilbert Grondin, Department of Civil and Environmental Engineering

Dr. Samer Adeeb, Department of Civil and Environmental Engineering

Dr. Pierre Mertiny, Department of Mechanical Engineering

Abstract

Steel plate shear walls have typically been analyzed using quasi static and monotonic pushover analysis; however, dynamic excitations during an earthquake elicit different behaviour from the structure due to the nature of the loading.

This report outlines the design and analysis of a steel plate shear wall according to NBCC and S16-09 requirements. For lateral loading, wind and seismic forces are considered.

The NBCC recognizes two procedures for determining seismic loading, the equivalent static force procedure and dynamic analysis. An analytical model was created in SAP2000® using capacity design principals and the strip model. The dynamic analysis uses bi-directional tension strips to resist load reversals and was validated against a finite element analysis using ABAQUS®.

The dynamic analysis provided an effective means of designing the steel plate shear wall. The equivalent static force procedure resulted in a similar design; however, the structure required stiffening to meet the deflection requirements.

Acknowledgements

I would like to sincerely thank Dr. Gilbert Y. Grondin for his guidance and encouragement during my graduate studies.

Financial support for the author of this project was provided by the Natural Sciences and Engineering Research Council of Canada (NSERC) IPS Scholarship, the G.L. Kulak Scholarship for Steel Structures Research, and the Cohos-Evamy Graduate Scholarship.

The author would also like to thank Empire Iron Ltd., especially the Edmonton branch, for sponsoring the NSERC IPS Scholarship and providing valuable insight into the steel welding and fabrication process.

Thank you to my officemates and colleagues who provided useful and interesting insights, and helped to make the graduate experience enjoyable.

Finally, I would like to thank my family, Lucy, Claire, Ella, and Peter, my parents and sister, and my extended family, for their support and encouragement during my studies. Their continued support and understanding have made this dissertation possible.

Table of Contents

1. STEEL PLATE SHEAR WALLS.....	1
1.1 Introduction	1
1.2 Description.....	1
1.3 Applications.....	2
1.3.1 Usage in Canada.....	2
1.3.2 Usage in the United States	3
1.3.3 Usage in Japan and Mexico	4
1.4 Objectives and Scope.....	4
1.5 Chapter Overview.....	6
2. BACKGROUND	14
2.1 Introduction	14
2.2 Takahashi <i>et al.</i> (1973).....	14
2.3 Mimura and Akiyama (1977).....	16
2.4 Thorburn <i>et al.</i> (1983).....	17
2.5 Timler and Kulak (1983).....	18
2.6 Tromposch and Kulak (1987)	20
2.7 Elgaaly and Caccese (1990)	21
2.8 Chen (1991).....	22
2.9 Xue and Lu (1994).....	23
2.10 Driver <i>et al.</i> (1997; 1998a,b)	24
2.11 Lubell (1997).....	26
2.12 Timler <i>et al.</i> (1998)	28

2.13	Schumacher <i>et al.</i> (1999)	29
2.14	Rezai (1999).....	30
2.15	Kulak <i>et al.</i> (2001).....	31
2.16	Astaneh-Asl (2001)	32
2.17	Behbahanifard <i>et al.</i> (2003)	33
2.18	Berman and Bruneau (2003)	34
2.19	Kharrazi <i>et al.</i> (2004).....	35
2.20	Shishkin <i>et al.</i> (2005)	35
2.21	Berman and Bruneau (2008)	37
2.22	Bhowmick <i>et al.</i> (2009)	37
2.23	Bing and Bruneau (2009)	39
2.24	Neilson <i>et al.</i> (2010).....	41
2.25	Infill Panel with Circular and Cut Out Sections.....	43
3.	DESIGN PROCEDURE.....	63
3.1	Introduction	63
3.2	Design Forces	63
3.2.1	General Loading.....	63
3.2.2	Seismic Loading.....	64
3.3	CSA-S16-09 Design Requirements.....	71
3.3.1	General Design.....	71
3.3.2	Seismic Design	73
3.4	AISC 2005	78
3.4.1	General Design.....	79
3.4.2	Seismic Design	81
4.	ANALYSIS	83

4.1	Introduction	83
4.2	Lateral Loading	83
4.3	Description of Software and Analysis Method.....	85
4.3.1	Direct Integration Analysis	86
4.3.2	Time History Records	88
4.3.3	Geometric and Material Nonlinearities	88
4.4	Model Generation and Analysis	93
5.	DESIGN EXAMPLE	106
5.1	General.....	106
5.2	Building Information.....	106
5.3	Design Procedure	107
5.4	Static Design.....	107
5.4.1	Wind Loading.....	107
5.4.2	Seismic Loading-Equivalent Static Force Procedure	108
5.4.3	Preliminary Design	112
5.4.4	Detailed Design.....	122
5.4.5	Analysis Results.....	125
5.5	Dynamic Analysis	125
5.5.1	Design.....	126
5.6	Connection and Welding Details	127
5.6.1	Connection Details.....	127
5.6.2	Infill Panel Welding	133
5.6.3	Miscellaneous Requirements	135
6.	DISCUSSION.....	151
6.1	Introduction	151

6.2	Validation of the Dynamic Model.....	151
6.3	Analysis Results	154
6.3.1	Storey Displacement	154
6.3.2	Structure and Element Force Effects	155
6.3.3	Capacity Design Forces.....	157
6.3.4	System Overstrength	158
6.4	Comparisons of Analysis Methods	158
7.	SUMMARY AND CONCLUSIONS	171
7.1	Summary	171
7.2	Conclusions	173
7.3	Future Research.....	174
	REFERENCES	176

List of Tables

Table 4.1 - Reference Point Coordinates for Axial Hinge	98
Table 4.2 - Reference Point Coordinates for Moment Axial Interaction Hinge.....	98
Table 5.1 - Dead Loads	137
Table 5.2 - Storey Weights and Seismic Information for a Single SPSW	137
Table 5.3 - Initial Infill, Beam and Column Selection	138
Table 5.4 - Preliminary Element Selection	139
Table 5.5 - Preliminary Design Force Effects	140
Table 5.6 - Final Element Selection.....	141
Table 5.7 - Final Design Force Effects.....	142
Table 5.8 - Dynamic Analysis Results	143
Table 5.9 - Peak Interstorey Displacements in Millimeters.....	143
Table 6.1 - Comparison of 15-Storey Models; Shell Model and Strip Model	160
Table 6.2 - Periods of SPSWs	160
Table 6.3 - Drift Values from Static Analyses; Final Design	160
Table 6.4 - Interstorey Drift Values from Dynamic Analysis.....	161
Table 6.5 - Base Reactions and Top Storey Displacements of Dynamic and Static Models	161
Table 6.6 - Storey Shear Ratio; Dynamic Analysis/ESFP.....	162
Table 6.7 - Storey Moment Ratio; Dynamic Analysis/ESFP	162

List of Figures

Figure 1.1 - Steel Plate Shear Wall Elements (Courtesy of Canam Manac Group).....	7
Figure 1.2 - Steel Plate Shear Wall; a) Unloaded, b) Loaded.....	8
Figure 1.3 - SPSW Mid Span Splice, ING Building (Courtesy of Group Teknika).....	9
Figure 1.4 - Steel Plate Shear Wall Base Anchorage, ING Building (Courtesy of Group Teknika)	10
Figure 1.5 - Edmonton International Airport Control Tower Steel Plate Shear Wall (Courtesy of Dialog).....	11
Figure 1.6 - U.S. Federal Court House, Seattle (Courtesy of Magnusson Klemencic Associates, Seattle)	12
Figure 1.7 - 22 Storey Condominium Steel Plate Shear Wall in Mexico (Courtesy of Martinez-Romero, 2003)	13
Figure 2.1 - Hysteresis Model Proposed by Mimura and Akiyama (1977).....	45
Figure 2.2 - Strip Model proposed by Thorburn et al. (1983)	46
Figure 2.3 - Equivalent Brace Model proposed by Thorburn et al. (1983).....	46
Figure 2.4 - Single Storey Test Specimen from Timler and Kulak (1983)	47
Figure 2.5 - Hysteresis Model Proposed by Tromposch and Kulak (1987).....	48
Figure 2.6 – 3-Storey Model used by Chen (1991)	48
Figure 2.7 – 4-Storey Specimen (Driver et al. 1997; 1998a).....	49
Figure 2.8 - Single Storey Test Specimens (Lubell 1997): (a) SPSW1; and (b) SPSW2.....	50
Figure 2.9 - 4-Storey Test Specimen (Lubell 1997)	51
Figure 2.10 - Staggered Strip (a) and Cross Hatching Method (b).....	52
Figure 2.11 - Corner Details Tested by Schumacher et al. (1999)	53
Figure 2.12 – 4-Storey Shake Table Specimen (Rezai 1999).....	54

Figure 2.13 - Simplified Strip Model (Rezai 1999)	55
Figure 2.14 - Hypothetical Vancouver Building Layout (Kulak et al. 2001)	56
Figure 2.15 - SPSW Failure Mechanism Hierarchy (Astaneh-Asl 2001).....	57
Figure 2.16 - Single Storey Collapse Mechanism (Berman and Bruneau 2003)	57
Figure 2.17 - Multi-Storey Collapse Mechanisms Proposed by Berman and Bruneau (2003): (a) Soft Storey Mechanism; and (b) Unified Collapse Mechanism..	58
Figure 2.18 - Column Free Body Diagrams (Berman and Bruneau 2008)	59
Figure 2.19 - Office Floor Plan and Elevation of 4-storey and 15-storey SPSW analysed by Bhowmick et al. (2009)	60
Figure 2.20 - Relationship Between system overstrength Ω_k and percentage of shear in infill panel κ (Bing and Bruneau 2009).....	61
Figure 2.21 - SPSW with Perforated Infill Panel (Vian 2005).....	61
Figure 2.22 - SPSW with Corner Cut-Outs (Vian 2005)	62
Figure 4.1 - Damping Ratio as a Function of Frequency	99
Figure 4.2 - Vancouver Spectrum Compatible Ground Motion Histories	100
Figure 4.3 - Original Ground Motion Histories (Bhowmick 2009)	101
Figure 4.4 - FEMA Axial Hinge definition (FEMA 356, 2000)	102
Figure 4.5 - Axial Hinge Definition	102
Figure 4.6 – Axial-Moment Interaction.....	103
Figure 4.7 – Axial-Moment Interaction Hinge Definition.....	103
Figure 4.8 - Hypothetical Office Building Adapted from Bhowmick et al. (2009).....	104
Figure 4.9 - 4-Storey Scaling Example: a) initial single storey; b) single storey replicated above initial storey; c) 4-storey created using 2-storey replication	105
Figure 5.1 - Example Building Layout.....	144
Figure 5.2 - Beam Forces Due to Infill Plate Yielding	144
Figure 5.3 - Column Forces from Yielding of Infill Panel	145

Figure 5.4 - 15-Storey Analysis Model Using; a) ESFP and b) Dynamic Analysis	146
Figure 5.5 - Vancouver Spectrum Compatible Ground Motion Histories	147
Figure 5.6 - CISC Seismic Connection Guide Shear and Moment Definitions (CISC 2008)	148
Figure 5.7 - Bolted Stiffened Connection Detail (CISC 2008).....	149
Figure 5.8 - Fish Plate Detail - Schumacher et al. (1999)	150
Figure 6.1 - 140% Tarzana Hill Ground Displacement Record	163
Figure 6.2 - Time History Comparison of Top Storey Displacement from the 4-storey Model; 140% Tarzana Hill Record (Bhowmick et al., 2009).....	163
Figure 6.3 - Time History Comparison of the Top Storey Displacement from the 15-Storey Model (El Centro Earthquake)	164
Figure 6.4 - Time History Comparison of the Base Moment from the 15-Storey Model (El Centro Earthquake)	164
Figure 6.5 - Time History Comparison of the Base Shear from the 15-Storey Model (El Centro Earthquake)	165
Figure 6.6 - Interstorey Drift from Dynamic and Static Analyses, and NBCC Limit.....	165
Figure 6.7 - Peak Storey Moments.....	166
Figure 6.8 - Peak Storey Shears	166
Figure 6.9 - Maximum Moment; Left Column	167
Figure 6.10 - Maximum Moment; Right Column	167
Figure 6.11 - Maximum and Minimum Axial Load; Left Column	168
Figure 6.12 - Maximum and Minimum Axial Load; Right Column	168
Figure 6.13 - Capacity Design and Analysis Force Effects; Column Axial Loads	169
Figure 6.14 - Capacity Design and Analysis Force Effects; Column Moments.....	169
Figure 6.15 - Capacity Design and Analysis Force Effects; Column Shear	170

List of Symbols

A	Area of equivalent brace, area
A_b	Area of beam, area of bolt
A_c	Area of column
A_g	Gross area
A_s	Area of tension strip
A_t	Tributary area of column
A_w	Effective throat area of a weld
a_0	Proportionally scaled coefficient for the mass matrix
a_1	Proportionally scaled coefficient for the stiffness matrix
B	Torsional sensitivity parameter, seismic amplification factor
B_f	Bearing capacity of beam flanges
B_r	Bearing capacity of the column
B_x	Storey torsional sensitivity parameter at level x
b_b	Width of beam
b_c	Width of column
b_{el}	Width of compression element
b_t	Tributary width for beams
C	Structure damping matrix
C_a	Shape factor
C_b	Basic roof snow load factor
C_d	Deflection amplification factor

C_e	Exposure factor
C_f	Factored axial force
C_g	Gust factor
C_p	External pressure coefficient
C_{pr}	Factor to account for connection conditions
C_s	Slope factor
C_w	Wind exposure factor
C_y	Axial yield resistance, strength ratio defined by CISC
D	Dead load, circular cut-out diameter, weld size
D_{nx}	Plan dimension of building at floor level x
d	Distance from the shear center to the SPSW
d_b	Depth of beam
d_{bt}	Bolt diameter
d_c	Depth of column
d_{SF}	Deformation scale factor
E	Modulus of elasticity, earthquake load
e_x	Distance between centre of mass and centre of rigidity
F_a	Acceleration based site coefficient
F_i	Seismic loads from plastic collapse mechanism
F_t	Portion of design base shear concentrated at the top storey
F_u	Specified minimum tensile strength, tensile strength of bolt
F_v	Velocity based site coefficient
F_x	Applied lateral load at storey x

$F_{x,total}$	Total lateral loading for storey x
F_y	Yield strength
F_{yc}	Yield strength of column
$F(t)$	Time-dependent applied loads or accelerations matrix
f_n	Frequency of the n^{th} mode
H	Height above base
h	Storey height
h_n	Height of structure in meters
h_s	Interstorey height
h_{sx}	Storey height immediately below level x
I_b	Beam moment of Inertia
I_c	Column moment of Inertia
I_E	Building importance factor
I_s	Snow load importance factor
I_w	Wind load importance factor
J	Numerical reduction coefficient for base overturning moment
J_x	Numerical reduction coefficient for level x overturning moment
K	Stiffness matrix, stiffness of bracing element
L	Bay width, live load, length of element
L_{cf}	Clear distance between column flanges
L_{cr}	Allowable laterally unsupported bracing length
L_i	Width of bay under consideration
L_{SF}	Load scale factor

M	Moment, diagonal mass matrix
M_{beam}	Beam design moment
$M_{beam(gravity)}$	Moment in beam due to gravity loads
$M_{beam(infill)}$	Moment in beam due to yielding of the infill panel
M_{cf}	Moment at the column centerline
M_{column}	Column design moment
$M_{column(beam)}$	Moment in column from beam shear
$M_{column(infill)}$	Moment in column due to yielding of infill panel
$M_{column(MF)}$	Moment in column from plastic hinging of beams
M_{pb}	Nominal plastic moment resistance of beam
M_{prli}, M_{prri}	Left and right beam plastic moments
M_{rpb}	Reduced plastic moment capacity for beam section
M_u	Factored seismic overturning moment at base
M_v	Higher mode adjustment factor for base shear
M_w	Strength reduction factor for multi-orientation fillet welds
M_x	Overturning moment at level x
M_x^*	Amplified overturning moment at storey x
n	Number of tension strips in bay
P	Axial load
P_{beam}	Beam design axial force
$P_{beam(infill)}$	Axial forces in the beam from yielding of the infill panel
$P_{beam(column)}$	Axial forces in the beam from the column

P_{bli}, P_{bri}	Left and right beam axial forces
P_{cf}	Load from moment at column centerline
P_{column}	Column design axial force
$P_{column(beam)}$	Axial force in column from beam loading
$P_{column(g)}$	Axial force in column from gravity loads
$P_{column(infill)}$	Axial force in column from yielding of infill panel
P_x	Total gravity load on structure above and including level x
p	Wind loading
p_t	Total pressure on tributary area
q	Reference velocity pressure
R	Seismic response modification coefficient
R_d	Ductility-related force modification factor
R_o	Overstrength-related force modification factor
R_y	Probable yield stress factor
$R_{yl}, R_{xl}, R_{yr}, R_{xr}$	Left and right column reaction components
r_{SF}	Rotation scale factor
r_y	Radius of gyration about weak axis
S	Snow load
S_e	Elastic section modulus
SF	Scale factor
$S(T)$	Design spectral response acceleration for period T
$S_a(T)$	5% damped spectral response acceleration for period T
S_{diag}	Shortest distance between perforations

S_r	1-in-50-year rain load
S_s	1-in-50-year ground snow load
T_a	Fundamental lateral period
T_b	Minimum bolt tension
T_f	Tensile capacity of beam flanges
T_r	Tensile capacity of the column
T_x	Torsional moment
T_y	Probable yield of infill plate unit strip
t_b	Beam flange thickness
t_c	Column flange thickness
t_p	Thickness of the end plate
U_2	Second order effect amplification factor
u	Structure displacements matrix
\dot{u}	Structure velocities matrix
\ddot{u}	Structure accelerations matrix
V	Probable storey shear strength
V_{beam}	Beam design shear force
$V_{beam(gravity)}$	Shear force in beam from gravity load
$V_{beam(MF)}$	Shear force in the beam from plastic hinge formation in beam
$V_{beam(infill)}$	Shear force in the beam due to yielding of the infill panel
V_{column}	Column design shear force
$V_{column(beam)}$	Shear force in the column from beams
$V_{column(infill)}$	Shear force in the column due to yielding of the infill panel

V_f	Factored shear force
V_h	Shear at the plastic hinge location
V_{max}	Maximum value of base shear
V_n	Nominal lateral storey shear
$V_{r,weld\ metal}$	Required shear resistance of weld
V_u	Factored seismic base shear
V_x	Design storey shear at storey x
V_x^*	Amplified design storey shear
V'	Shear at column joint panel zone
W	Weight of structure, wind load, minimum effective width
W_i	Individual floor weight at floor i
w	Thickness of infill plate,
w_i	Width of building orthogonal to wind loading at storey i
w_g	Factored distributed gravity load
w'	Required column web thickness
X_u	Ultimate strength of weld metal
x	Storey level
Z_x	Plastic section modulus about strong axis
α	Angle of tension field, numerical solver constant
Δ_f	First order lateral displacement of storey
Δ_{mx}	Maximum inelastic storey drift of the storey below level x
Δt	Small equal time intervals

Δt_w	Difference in the infill panel thicknesses bounding a beam
Δ_x	Tension strip spacing
δ	Lateral deflection
δ_{ave}	Average displacement of the structure at level x
δ_{max}	Maximum displacement of the structure at level x
δ_y	Yield deflection
η	Reduction ratio for reduced beam sections
θ	Angle of axis of weld with respect to line of action of force
θ_x	Stability factor
κ	Percentage of design shear assigned to infill, end moment ratio
ξ	Structure damping
ϕ	Acute angle between brace and columns, resistance factor
ϕ_{bi}	Bearing resistance factor
ϕ_w	Weld resistance factor
Ω_κ	Modified overstrength factor for design shear
Ω_s	System overstrength factor
ω	Distributed load on beam from yielding of infill panel
ω_h	Column flexibility parameter
ω_L	Beam flexibility parameter
ω_n	Angular frequency of the structure
ω_{xb}, ω_{yb}	Components of distributed load on beam from yielding of infill
ω_{xc}, ω_{yc}	Components of distributed load on column from yielding of infill

List of Abbreviations

<i>AISC</i>	American Institute of Steel Construction
<i>ASCE</i>	American Society of Civil Engineers
<i>ASTM</i>	American Society for Testing and Materials
<i>ATC</i>	Applied Technology Council
<i>CISC</i>	Canadian Institute of Steel Construction
<i>CP</i>	Collapse Prevention
<i>CSA</i>	Canadian Standards Association
<i>ESFP</i>	Equivalent Static Force Procedure
<i>FE</i>	Finite Element
<i>FEA</i>	Finite Element Analysis
<i>FEM</i>	Finite Element Model
<i>FEMA</i>	Federal Emergency Management Agency
<i>IO</i>	Immediate Occupancy
<i>LS</i>	Life Safety
<i>M–PFI</i>	Modified-Plate Frame Interaction
<i>NBCC</i>	National Building Code of Canada
<i>SPSW</i>	Steel Plate Shear Wall

1. STEEL PLATE SHEAR WALLS

1.1 Introduction

Steel plate shear walls have long been used as a lateral load resisting system for wind loads and seismic loads. The steel plate shear wall system is composed of traditional beam and column frame elements, to which infill panels are connected as shown in Figure 1.1. There are several variations of SPSWs with variables such as stiffened and unstiffened infill panels, rigid and shear beam-to-column connections, perforated and non-perforated infill panels, bolted and welded infill panels, and several others. Once the system has been constructed, it exhibits high initial stiffness for service wind loads and excellent energy absorption capacity for extreme loading cases such as seismic events. This report deals with unstiffened, rigid frame, welded, thin infill panels steel plate shear walls as a primary lateral load resisting system and will be herein referred to as SPSWs.

1.2 Description

As a lateral load resisting system, the infill panel in the SPSW is the primary lateral load resisting element. The lateral loads are resisted primarily by the formation of a diagonal tension field in the infill plate as shown in Figure 1.2. The tension field that forms in a SPSW is similar to the tension field described by Basler (1961) for plate girders, and an analogy can be made with a cantilevered plate in a vertical position. The infill panel has traditionally been designed to resist the entire shear force from the lateral loading while the columns form a mechanism to resist the overturning moment. In unstiffened SPSWs, the compression strength of the infill plate is considered to be negligible as shear buckling occurs at low lateral forces. In addition to the infill panel acting as an energy dissipating element, the beams and columns may also form plastic hinges to dissipate energy during inelastic action when the beams and columns are connected together using moment resisting connections. The combination of the yielding of the infill panel and plastic hinging of the boundary elements allows SPSWs to perform in a ductile and robust manner with a high degree of redundancy. The system also provides good energy

dissipation capacity even when the beam-to-column connections are not designed to transfer moments.

1.3 Applications

Steel plate shear walls have been used in new construction projects ranging from residential buildings to high-rise structures, and for the rehabilitation of existing structures to increase their resistance to earthquakes. SPSWs offer many advantages over other lateral load resisting systems, including construction cost and speed (Timler *et al.*, 1998). Compared to concrete shear walls, SPSWs can be erected in significantly less time, occupy smaller floor areas, thus yielding larger usable floor area for the same building footprint, and have a significantly reduced mass, which aids in reducing foundation and other design aspects. Several structures have been designed and built using SPSWs as the primary lateral load resisting system in Canada, the United States, Japan, and elsewhere. Several structures using this system will be outlined here.

1.3.1 Usage in Canada

The lateral load resisting system designed for the Canam Manac Group expansion of the headquarters in St. Georges, Québec, utilized a 6-storey SPSW, shown in Figure 1.1 which was located around the elevator core with an irregular expansion footprint of 3700 m². The SPSW was constructed using 4.8 mm infill panels throughout and a bay width center-to-center for the columns of 2.6 m. The height of the SPSW was 23 m and was fabricated in two tiers, which were field spliced at mid height using a slip critical connection.

A SPSW was used as the lateral load resisting system for the 7-storey ING building in Ste-Hyacinthe, Québec. The structure was 24 m high with some walls fabricated fully in the shop while others were fabricated in half width segments which were bolted together by beam splices shown in Figure 1.3. The base of the wall was anchored to the foundation continuously as shown in Figure 1.4.

A 2-storey SPSW was also used for the construction of an additional two floors of Institut de Recherches Cliniques de Montréal, Québec. The extension consisted of a 2-

and 3-storey SPSW, both using 6.8 mm infill plates. The bay dimensions of SPSWs were 3.0 m x 3.5 m and 3.0 m x 4.8 m for the 2-, and 3-storey walls, respectively.

A SPSW system was adopted as the lateral load resisting system for the combined airport traffic control tower and office building structure at the Edmonton International Airport in Alberta (Figure 1.5). The tower and building consist of six SPSWs whose design was governed by wind loading. The east core supporting the control tower, which was also designed to allow for the accidental collapse of a boundary column, consists of two SPSWs with bay widths of 6.0 m and two SPSWs with bay widths of 2.9 m. The west core consists of two SPSWs with bay widths of 5.7 m. Each SPSW is 11-storeys tall and uses 5.0 mm infill panels bolted to the boundary elements.

1.3.2 Usage in the United States

In the United States, stiffened SPSWs have been used as early as the 1970's, but unstiffened SPSWs have been used only recently. The 50-storey, 170 m tall, Hyatt Regency hotel in Dallas, Texas, was constructed using a stiffened SPSW whose design was governed by wind loading. The SPSW structure uses bays 3.0 m x 7.8 m with 25.4 mm thick infill plates throughout. The infill plates in this case were reported to contribute to the gravity load support system, enabling the use of smaller boundary members (AISC, 2005).

The 55-storey, 200 m tall, Los Angeles Convention Center was constructed using an unstiffened SPSW as the lateral load resisting system. The SPSWs were built using infill plates varying from 6.35 mm to 9.53 mm (Yousseff *et al.*, 2009). The use of SPSWs was reported to have reduced the weight of the structure by 35% as well as reclaiming over 1850 mm² of real estate compared to a comparable concrete shear wall.

The SPSWs in the 23-storey, 107 m tall, US federal courthouse in Seattle Washington, shown in Figure 1.6, were selected due to space requirements, weight reductions, and construction time versus a traditional concrete shear wall (AISC 2005). The bounding columns of the SPSW were concrete filled circular columns to increase flexural rigidity and the SPSWs used were joined together by rigid beam connections to make the SPSWs work as a single unit.

The Olive View Medical Center at Sylmar was built to replace the hospital damaged by the 1971 San Fernando earthquake in California and used several 4-storey SPSWs. The building used both interior and perimeter shear walls constructed in 4.7 m by 7.6 m modules with infill plates varying from 15.9 mm to 19.1 mm. The hospital was subjected to the 1994 Northridge earthquake and no structural damage was reported.

1.3.3 Usage in Japan and Mexico

In Japan, buildings constructed with SPSWs as the lateral load resisting system have typically used stiffened SPSWs, which appeared as early as the 1970's. The stiffened SPSWs were designed to be used in conjunction with moment resisting frames for redundancy. The Shinjuku Nomura and Nippon Steel buildings are examples of high rise buildings built using stiffened SPSWs in the 1970's. The 51-storey Shinjuku Nomura building in Tokyo has a height of 211 m and used infill panels 3 m x 5 m connected to the boundary elements, which reportedly used 200 to 500 bolts (AISC 2005). The Nippon steel building in Tokyo is a 20-storey building, 84 m high, with 2.7 m x 3.7 m infill panels ranging from 4.5 mm to 12.0 mm thick.

The 35-storey Kobe city hall building located in Kobe, Japan, was constructed in 1989 and is 130 m tall. The Kobe building also used a stiffened SPSW and it was reported that minor local buckling occurred in the 26th storey plate wall after the Kobe earthquake of 1995 (Fujitani *et al.*, 1996). Two 22-storey buildings were constructed in Mexico in the early 2000's using thin, unstiffened, SPSWs after it was determined that SPSWs offered a more economical design compared with a reinforced concrete structure. The SPSWs, shown in Figure 1.7, were designed according to the Canadian standard CAN/CSA S16.1 (CSA 2001).

1.4 Objectives and Scope

The objective of this research project is to provide background information on the past research on SPSW and provide a design guide for the design and analysis of a SPSW constructed to Canadian standards following the NBCC 2005 and S16-09.

Steel plate shear walls as lateral load resisting system have been studied as early as the 1970's (Takahashi *et al.*, 1973; Mimura and Akiyama, 1977). Initial research focused on

stiffened panels or thick infill panels designed to resist the lateral forces without buckling. Starting with the work of Thorburn *et al.* (1983) the focus has shifted to thin, unstiffened, panels which are expected to resist the lateral forces through tension field action that develops after the infill plates have buckled. The compressive strength of the thin infill plate is usually considered to be negligible. When the loading direction is reversed, the panel buckles in the other direction and the tension field reforms to resist that cycle. The ability of the panel to undergo several load reversals leads to a robust lateral load resisting system which has significant overstrength and ductility.

The design of a SPSW in Canada is done in accordance to the National Building Code of Canada (NBCC 2005) and CSA-S16-09 to determine the loading and design requirements. The NBCC outlines the lateral wind and seismic loading on the building.

The NBCC design load requirements and the provisions of CSA-S16-09 to ensure ductile behaviour of SPSWs are reviewed and illustrated in this document. While the NBCC allows the design loads to be determined using a static method for certain buildings, a dynamic design is required for buildings that exceed a certain height. S16-09 recognizes the strip model proposed by Thorburn *et al.* (1983) as the model that should be used for analysis purposes. Although the strip model has been validated as an effective model to conduct push over analysis, its use for cyclic dynamic analysis has not received much attention. Non-linear dynamic analysis of SPSWs has been conducted using shell element models implemented in highly advanced general purpose finite element software more commonly used by research engineers than design engineers (Bhowmick *et al.*, 2009; Kurban and Topkaya, 2009). However, the ability of the strip model to predict the cyclic behaviour of SPSWs accurately has not yet been demonstrated. It is therefore one of the main objectives of this research project to test the strip model with a dynamic non-linear analysis using software packages commonly used by design engineers.

An example is presented to illustrate the design procedure for a SPSWs using wind and seismic loads and two methods of analysis. The example uses a 15-storey office building located in Vancouver, Canada, designed according to the NBCC and S16-09.

1.5 Chapter Overview

This report consists of seven chapters outlined in this section.

Chapter 2: a brief review of the research conducted on SPSWs over the past 40 years is presented. The chapter covers the development of SPSW research with a focus on theoretical and experimental tests of unstiffened SPSWs using thin infill panels.

Chapter 3: the current method of SPSW design is outlined, citing the NBCC (NRCC 2005), S16-09 and AISC (2005). The NBCC covers the procedures for the determination of the lateral loads on SPSWs, which include wind and seismic loading. S16-09 and AISC are concerned with the design of the SPSWs under the given loading to ensure that the desired behaviour and performance of the SPSW is achieved. The S16-09 design criteria are covered in detail while the coverage of the AISC guide highlights the differences between the two approaches.

Chapter 4: an analysis method used in the design of a SPSW is described. The analysis focuses on the use of a dynamic non-linear time history method. The analysis method was developed for use with SAP 2000®, although any software with non-linear time history analysis capability can be used to perform the analysis.

Chapter 5: details the design of a SPSW for use in a commercial building located in Vancouver, Canada. The wind and seismic loads on the building are calculated using NBCC. The seismic loading for this process is determined by two methods, namely, the equivalent static force procedure and a dynamic analysis. The design method for the SPSW utilizes capacity design principles as requires by S16-09.

Chapter 6: the results of the design and analyses from Chapter 5 are discussed and compared with a similar analysis performed using a shell element model implemented in ABAQUS® for a similar structure.

Chapter 7: summary, conclusions, and recommendations for future work are presented.

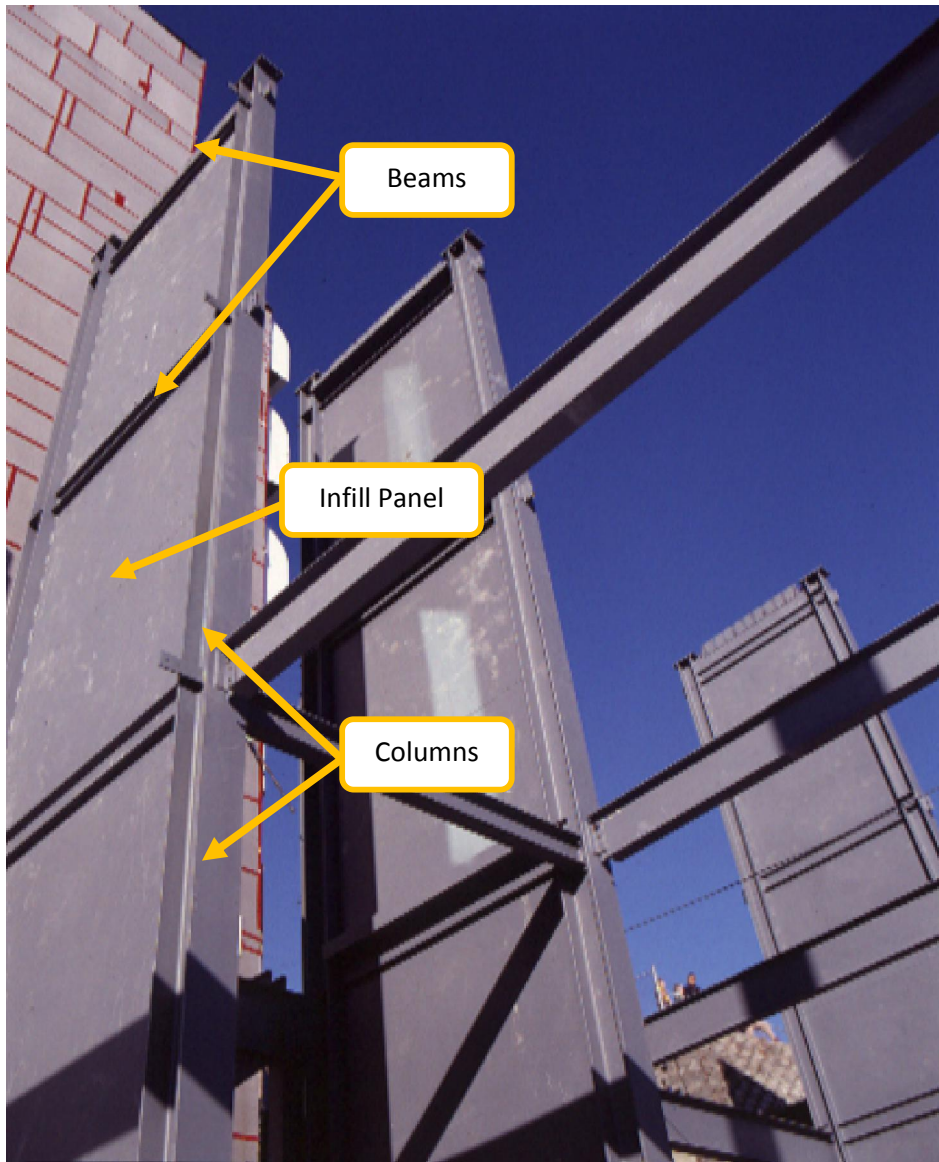


Figure 1.1 - Steel Plate Shear Wall Elements (Courtesy of Canam Manac Group)

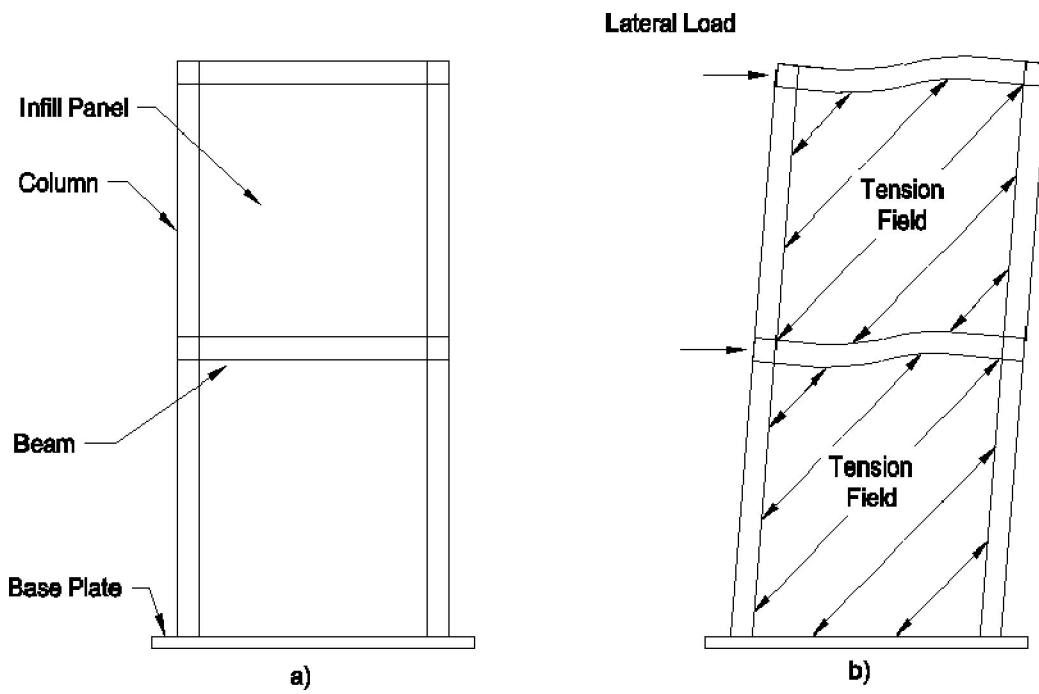


Figure 1.2 - Steel Plate Shear Wall; a) Unloaded, b) Loaded



Figure 1.3 - SPSW Mid Span Splice, ING Building (Courtesy of Group Teknika)



Figure 1.4 - Steel Plate Shear Wall Base Anchorage, ING Building (Courtesy of Group Teknika)



*Figure 1.5 - Edmonton International Airport Control Tower Steel Plate Shear Wall
(Courtesy of Dialog)*



Figure 1.6 - U.S. Federal Court House, Seattle (Courtesy of Magnusson Klemencic Associates, Seattle)



Figure 1.7 – 22-Storey Condominium Steel Plate Shear Wall in Mexico (Courtesy of Martinez-Romero, 2003)

2. BACKGROUND

2.1 Introduction

Research on steel plate shear walls (SPSW) has been conducted since the early 1970's and the underlying theory has been studied since 1931. The system was found to be an economical and effective system for resisting lateral loading due to wind and seismic forces on buildings. The early studies focused on preventing the shear buckling of the plate. Japanese engineers used stiffening techniques to prevent the infill plate from buckling while engineers in the United States relied on thicker infill panels. In both cases, the post-buckling capacity of the infill panel was neglected.

Over the past three decades, research has focused on the post-buckling capacity of SPSWs and the increase in lateral load resistance that is gained from this phenomenon. Early work by Wagner (1931) and Kuhn *et al.* (1952) demonstrated that an in-plane diagonal tension field forms after buckling of a shear panel, which provides resistance to the shear force. The shear capacity can be taken as a combination of pure shear and the inclined tension field. Based on this work, Basler (1961) developed a diagonal tension field model to predict the shear capacity of steel plate girders using the diagonal tension field model. SPSWs can be seen as an extension of steel plate girders in the fact that a SPSW can be seen as a vertical cantilevered plate girder.

This chapter describes some of the primary research on thin unstiffened SPSWs. The chapter follows the early development of SPSWs to the current research. Some of the topics covered are the development(s) of analysis models and their implementation, large and small scale testing, finite element and planar frame methods of analysis, and loading techniques (static, nonlinear and time history).

2.2 Takahashi *et al.* (1973)

Takahashi *et al.* (1973) conducted the first experimental research program on steel plate shear walls. The experiment focused on panels stiffened in various configurations. The test program was designed to determine the suitability of stiffened steel plate shear walls as a lateral load resisting system by imposing inelastic load cycles.

The testing program consisted of two parts. The first part focused on cyclic testing of 12 panels with an aspect ratio, L/h , of 1.33 (1200 mm x 900 mm). The test program used variable plate thickness, 2.3 mm to 4.5 mm, and stiffener arrangements. The control panel was an unstiffened plate, which was part of a frame with bolted shear beam-to-column connections. Four to six shear loading cycles were applied with increasing deformation. While the stiffened panels dissipated more energy than the unstiffened panels, it was noted that both panels performed in a stable and ductile manner, with panels stiffened on both sides providing the most stability.

It was recommended that stiffened panels be designed to force buckling to occur between stiffeners while avoiding elastic buckling. Guidance was provided to achieve these recommendations.

The second portion of the test program consisted of tests on two full scale, single bay and 2-storey stiffened SPSW sections taken from the design of a 32-storey building. One frame had a stiffened door opening and used a 6 mm infill plate while the other frame was continuous with a 6 mm infill plate. Lateral in-plane loads were applied to the top of the specimens in one direction with a few fully reversed loading cycles inserted between loading and unloading. Both shear walls responded with good energy dissipation and ductility.

An attempt was made to model the full scale test specimens analytically using an elasto-plastic material model with von Mises yield criteria. The test specimens were represented as planar frames to avoid modelling plate buckling. Although the analysis used monotonic loading, good agreement was achieved between the model and the envelope of the load vs. deflection curve from the shear wall tests.

From this test program, it was determined that the stiffness of the panels could be predicted using conventional shear theory and the equations developed for the stiffener spacing was proposed for design.

2.3 Mimura and Akiyama (1977)

Mimura and Akiyama (1977) investigated the behaviour of unstiffened SPSWs and developed models to predict the monotonic and hysteretic response to loading. The models assumed that the infill plate buckles prior to reaching their shear capacity. The method describing the monotonic loading for SPSWs considered the strength contribution of the infill panel to be separate from the contributions of the boundary members.

In the model proposed by Mimura and Akiyama the shear buckling capacity of the infill plate for the monotonic loading case is calculated using classical plate buckling theory with a pinned boundary assumption. After the infill panel buckles, tension field action (Wagner 1931) becomes the load resisting mechanism, with the yield and ultimate shear strength calculated based on pure diagonal tension field action. The contributions of the moment resisting frame can be determined by an elasto-plastic analysis of the frame. The sum of the contributions from both the infill panel and the moment resisting frame gives the overall monotonic load vs. deflection behaviour from which a hysteresis model is developed to predict the cyclic performance of SPSWs.

Mimura and Akiyama (1977) made several assumptions in the development of the hysteresis model illustrated in Figure 2.1. The main assumption was that the deformation required to re-form the tension field upon load reversal is equal to half the plastic deformation from the previous cycle. A constant tension field angle of 45° and a plastic Poisson's ratio of 0.5 were also assumed. The proposed hysteresis model indicates the lateral deflection, δ , as a result of the applied lateral force, Q . The initial loading of the SPSW is shown by path OAB , followed by the unloading path BC' parallel to OA . The panel is being loaded in the opposite direction on path $C'C$, upon where shear buckling of the panel is considered to occur at point C followed by a re-formation of the tension field at point D . The result of the Poisson's ratio assumption can be seen in line DD' , which is parallel to OA' , that divides the deformation between O and C' in half. The deformation from further reverse loading from point D follows an empirical linear path to point A' , which is equal and opposite to point A . Further loading deforms the panel along the path $A'E$ which is parallel to path AB until the panel returns to

point F' after unloading at an arbitrary point E . The loading cycle begins again at point F' followed by plate buckling at point F until loading is resumed at point G . Point G is determined using the previously mentioned Poisson's ratio assumption to locate point G' , and a line parallel to path OA . Further loading from point G is assumed to be linear to previous unloading point B , followed by increasing inelastic deformation along path BH .

2.4 Thorburn *et al.* (1983)

Thorburn *et al.* (1983) noted that SPSWs with thin infill panels can resist considerable loads through post buckling behaviour, despite the infill panel buckling at very low in-plane shear loads. An analytical model, termed the strip model, was proposed that neglects the shear resistance of the panel prior to buckling and considers only the post-buckling resistance of the panel. The lateral resistance of the SPSWs is obtained from the formation of the diagonal tension field based on pure diagonal tension developed by Wagner (1931).

The researchers proposed a strip model that represented the diagonal tension field by a series of pin-connected strips oriented parallel to the tension field, at an angle α from the vertical. A typical inner storey modelled using the proposed strip model method can be seen in Figure 2.2. The subdivision of the infill plate into multiple strips dictates that the compressive stresses perpendicular to the tension field is negligible. The bounding beams connected to the infill panel are assumed to be infinitely stiff. This assumption is valid for an interior beam with infill panels both above and below. The proposed strip model was based on pinned beam to column connections where the tensile yield strength of the infill plate was considered to be the limiting stress. The researchers demonstrated that 10 strips per panel would be sufficiently accurate to describe the behaviour of the tension field. However, the analysis was limited to elastic material behaviour. Using the principle of least work, the equation to calculate the tension field angle α was determined to be:

$$\tan^4 \alpha = \left[\frac{1 + \frac{Lw}{2A_c}}{1 + \frac{hw}{A_b}} \right] \quad 2.1$$

where L is the frame width; h is the storey height; w is the infill plate thickness; and A_b and A_c are the beam and column cross-sectional areas, respectively.

Thorburn *et al.* (1983) also described an equivalent brace model used to simplify the plate as a single diagonal tension strut, which intersects the working points of the frame as shown in Figure 2.3. This simplified model was proposed for the preliminary analysis of steel plate shear walls in order to speed up the design process. The single brace is based on rigid boundary members and represents the stiffness characteristics of the tension field that develops in the infill plate. The equation proposed for the area of the equivalent brace is as follows:

$$A = \frac{wL \sin 2\alpha}{2 \sin \phi \sin 2\phi} \quad 2.2$$

where ϕ is the acute angle described by the brace and the columns and all other terms as previously defined.

Based on the research findings from Thorburn *et al.* (1983), CSA-S16-01 recommended the strip and equivalent brace models as a design and preliminary design tool, respectively, for the development and analysis of SPSWs.

2.5 Timler and Kulak (1983)

Timler and Kulak (1983) tested a SPSW to verify the strip model technique proposed by Thorburn *et al.* (1983). The test specimen consisted of a pair of conjoined single story SPSWs with vertically oriented beams and horizontally oriented columns as shown in Figure 2.4. The SPSW had an aspect ratio of 1.5, an infill plate thickness of 5 mm and used rigid beam-to-column connections for the interior beam and pinned connections for the outer beam.

The testing procedure consisted of statically loading the frame with three complete cycles to achieve the service load deflection limit of $h_s / 400$ or 6.25 mm. Under these

initial load cycles, the specimen remained in the elastic region, after which the SPSW was loaded in one direction to determine the ultimate capacity. The test setup did not include gravity loads to the columns. Timler and Kulak (1983) noted that the performance of the SPSW and thus the value of the angle α from Thorburn *et al.* (1983) had a significant dependence on the flexural stiffness of the bounding columns and thus modified the equation for α to include the column flexural stiffness. The equation for the angle of inclination of the tension field, α , proposed by Thorburn *et al.* (1983) was modified to account for flexible columns as follows:

$$\tan^4 \alpha = \left[\frac{1 + \frac{Lw}{2A_c}}{1 + hw \left(\frac{1}{A_b} + \frac{h^3}{360I_c L} \right)} \right] \quad 2.3$$

where I_c is the moment of inertia for the column and all other parameters are as defined earlier.

The equation for α was also re-derived for the top panel of the SPSW as the top panel does not have a panel above the beam to help anchor the tension field. As before, the proposed equation was derived for pinned beam-to-column connections and takes the form:

$$\tan^4 \alpha = \left[\frac{1 + Lw \left(\frac{1}{2A_c} + \frac{L^3}{120I_b h} \right)}{1 + hw \left(\frac{1}{2A_b} + \frac{h^3}{360I_c L} \right)} \right] \quad 2.4$$

where I_b is the moment of inertia of the beam about the axis orthogonal to the infill panel.

The strip model was used to analyze the test specimen using an elastic analysis program. In order to include inelastic behaviour, modifications were made to the boundary and strip elements. The beam and column cross sectional areas were iteratively reduced and the stresses in the tension strips were limited to their experimentally tested static yield strength. The model was found to provide good correlation with the experimental results for the axial strains, infill plate stresses and load vs. deflection behaviour. The

proposed equation for the angle α was adopted by the Canadian steel design standard (CAN/CSA S16-01).

2.6 Tromposch and Kulak (1987)

Tromposch and Kulak (1987) conducted a cyclic test on a SPSW specimen to examine the strip model proposed by Thorburn *et al.* (1983) and to examine the hysteretic behaviour. The test setup was similar to that of Timler and Kulak (1983) with the exception that the beam-to-column connections were bolted and a thinner infill plate was used (3.25mm). The upper and lower beam sections of the test specimen were very stiff beams to anchor the tension field that would develop under cyclic loading and simulate the behaviour of an inner storey panel.

The test procedure consisted of preloading the columns to represent gravity loads of a taller structure, followed by cyclic loading laterally. Fully reversed cycles with an amplitude of 17 mm, which represented 2/3 of the predicted ultimate capacity of the structure which was the capacity limit for the testing frame. After 28 cycles, the test was completed under monotonic loading in one direction to determine the ultimate capacity of the frame.

The SPSW specimen performed in a ductile manner, but severe pinching of the hysteresis loops was observed. This was attributed to the thin infill plate and relatively flexible boundary members. The hysteretic behaviour model proposed by Mimura and Akiyama (1973) was used to model the test specimen response with two modifications as shown by the dotted lines in Figure 2.5. The first modification was to neglect the strength of the infill plate prior to buckling. This modification implies that the line CC' in Figure 2.1 would have zero length. The second modification was that until the tension field develops, the stiffness of the shear wall was taken to be the elastic stiffness of the bounding frame. This adjustment can be seen when comparing line CD of Figure 2.1 and Figure 2.5.

The SPSW was analysed using a strip model with both pinned and rigid beam-to-column connections and compared to the test results. The model using the rigid and pinned frame provided an upper and lower bound solution respectively and the test specimen

fell in between the two extremes. The strip model using pinned boundary elements underestimated the initial stiffness and the ultimate capacity of the specimen by 40% and 16% respectively, while the model with rigid beam-to-column connections underestimated the initial stiffness by 17% and overestimated the ultimate capacity of the specimen by 11%. The eccentricity of the fish plate with respect to the boundary elements was also examined and it was concluded that the eccentricity had no noticeable effect on the performance of the SPSW.

2.7 Elgaaly and Caccese (1990)

Elgaaly and Caccese (1990) conducted an experimental program with 10 quarter scale SPSWs subjected to cyclic loading. Their test results were examined in detail and an analytical study of the specimens were presented in Caccese *et al.* (1993) and Elgaaly *et al.* (1993). The parameters that were varied in the tests were the beam-to-column connections and infill plate thickness. The beam-to-column connections were fabricated as moment or shear connections and the plate thickness ranged from 0.76 mm to 2.66 mm.

The specimens were loaded with a single in-plane load at the top of the shear wall. The test specimens were loaded cyclically with gradually increasing deflection increments by 6 mm up to 2% drift (51 mm). The specimens were subjected to 24 fully reversed cycles to reach the 2% drift which was then repeated for 48 cycles, followed by monotonic loading to determine the ultimate capacity.

Two analytical models were developed to reproduce the experimental results. The first model used a finite element method with beam and shell elements to describe the SPSW. The second model replaced the shell elements with elasto-plastic truss elements oriented in the principal tensile and compressive stress directions. The finite element model overestimated the initial stiffness and ultimate strength up to 40% and 26%, respectively, which was attributed to the coarseness of the mesh and initial out-of-plane deformations of the infill panel in the test specimens. Further refinements of the mesh resulted in a model that was beyond the computational resources available and thus the model was abandoned. The compression members in the truss model were assumed to

buckle at the onset of loading and thus the model was similar to the tension strip model proposed by Thorburn *et al.* (1983). The truss model gave good predictions of the ultimate strength although the initial stiffness was overestimated.

The researchers concluded that beam to column connection type does not have a significant impact on the performance of SPSW and the infill plate thickness reaches an optimum value beyond which the strength remains constant and the failure mode of the SPSW becomes either column yielding or buckling.

Kulak *et al.* (1994) noted that due to several differences between specimens such as plate thickness and material properties, as well as a failed weld connection in one specimen, a direct comparison could not be made between the test specimens. The analytical study of Tromposch and Kulak (1987) also indicated that the type of beam-to-column connection has a significant effect on the energy dissipation characteristics of the SPSW. Kennedy *et al.* (1994) noted that the second conclusion regarding the infill plate thickness could not be considered the general case as the columns can be designed to resist the loads transferred from the other elements of the structure, in this case, a thicker infill plate.

2.8 Chen (1991)

Chen (1991) conducted an experimental program that consisted of ten quarter scale, 3-storey, single bay SPSWs that were subjected to cyclic loading. The structure used in the experiment can be seen in Figure 2.6. The beam-to-column connections were constructed as either rigid or simple and the infill plate thickness ranged from 0.76 mm to 2.66 mm. The effect of plate wall openings and aspect ratios, L/h , was also considered. The loading procedure consisted of 24 fully reversed cycles of increasing displacement up to a maximum specimen drift of 2%, or approximately 50 mm. This loading procedure was applied twice to each frame followed by a monotonic test to determine the ultimate capacity if possible. A frame without an infill plate was also tested as a lower bound comparison. The SPSW performed in a very ductile manner and displayed a high initial stiffness with high energy dissipation.

The analysis identified two failure modes, plate yielding and column buckling or fracture. With very thin infill plates, the columns were relatively stiff and provided rigid boundary conditions, forcing the plate to yield before yielding of the columns. For thicker plates, the initial stiffness was higher, but the relatively flexible boundary members were likely to yield or fracture before any plate yielding occurred. It was therefore concluded that the selection of infill plate thickness is essential as it would influence the type of failure for a given size of column. For a given set of boundary members, the strength of the SPSW increases as the plate thickness increases. However, Chen also observed that an optimal infill plate thickness exists beyond which the resistance remained constant and column buckling limited the capacity.

The work of Chen (1991) also indicated that the type of beam-to-column connection had no effect on overall strength of SPSWs. It was observed that an increase in the aspect ratio resulted in an increase in the strength of the SPSW, although the extent of the capacity increase was not thoroughly investigated.

2.9 Xue and Lu (1994)

Xue and Lu (1994) conducted an analytical study on four 12-storey steel plate shear walls with three bays designed for seismic loading. The models consisted of a hybrid system utilizing moment resisting frames combined with SPSWs. In each of the models, the exterior bay frame connections were rigid beam-to-column connections while the interior bay contained the infill plate with different types of connections. Two infill plate to boundary members connection details were investigated, namely, the infill plate was connected to all the boundary members, or to the beams only. The models were then compared to a lower and upper bound specimens. The lower bound model consisted of moment resisting exterior frames, and an interior frame with simple beam-to-column connections and no infill plates. The interior frame of the upper bound specimen consisted of an infill plate fully welded to all boundary members and was not assumed to buckle. Rigid beam-to-column connections were used for the upper bound model.

The exterior and interior bays were 9144 mm and 3658 mm wide, respectively, while the first floor and remaining floor heights were 4572 mm and 3658 mm, respectively.

These dimensions resulted in aspect ratios (b/h) of 0.8 and 1.0. The infill plate thickness was varied from 2.2 mm at the top storey to 2.8 mm at the bottom storey. All the SPSWs were modelled using beam elements for the boundary members and shell elements for the infill plate. Monotonic lateral loading was applied at the floor levels without the addition of gravity loads.

Xue and Lu (1994) found that the type of beam-to-column connection for the inner frame had a small effect on the lateral stiffness of the frame. It was also found that the stiffness of the SPSW with the infill plate connected to both the beams and columns approached the results of the upper bound solution. The stiffness of the specimen with the infill plate connected to only the beams was lower than fully connected infill plate specimen, but still provided a significant increase over the case with no infill plate. Despite the reduction in lateral stiffness, it was recommended that the plates be connected to the beam elements only. This was suggested as the analysis results indicated that due to the high stiffness of the system, the columns would be required to carry a larger portion of the storey shears, which could result in an early failure of the columns. By using a structure with a lower stiffness (infill plate connected to beam elements only), more of the infill plate was engaged in resisting the storey shear, resulting in an increase of their effectiveness and a reduction in the demand on the columns. No tests were performed to verify the results of the numerical study.

2.10 Driver *et al.* (1997; 1998a,b)

Driver *et al.* (1997; 1998a) conducted a large scale test of a 4-storey single bay unstiffened steel plate shear wall. The beam-to-column connections for the specimen shown in Figure 2.7 were designed as rigid connections and the infill plate was 4.8 mm thick in the bottom two storeys and 3.4 mm in the top two storeys. Welded fish plates were used to connect the infill plates to the beams and columns of the frame. Gravity loads were applied to the columns and lateral loads were applied at each floor level as specified by ATC-24 (Applied Technology Council 1992).

A total of 30 load cycles were applied with the last 20 being in the inelastic range of the SPSW with a yield deflection (δ_y) of 8.5 mm. The specimen behaviour was robust and

demonstrated a high initial stiffness, excellent ductility and high energy dissipation. The ultimate strength of the frame was reached at five times the yield deflection where the columns buckled locally at the base and eventually fractured. After the ultimate strength was reached, the subsequent cycles had a reduced load carrying capacity, but the deterioration was gradual and stable. The peak deflection of the lowest storey prior to failure was nine times the yield deflection.

Driver *et al.* (1997;1998b) modelled the 4-storey specimen using two FEA methods. The first model was developed using ABAQUS® which incorporated shell elements for the infill panel and beam elements for the beam and column members. The infill plate model included initial imperfections based on the first buckling mode. The modelling of the boundary members included residual stresses that were obtained experimentally. Geometric nonlinearities were initially incorporated in the model, but the analysis failed to converge and the full shear capacity could not be reached and thus the geometric nonlinearities were excluded. Two analyses methods were used; a static pushover analysis and a cyclic analysis which included kinematic hardening to simulate the Bauschinger effect. The pushover analysis predicted the ultimate strength to be 7% higher than that of the test specimen which occurred at load cycle 22. The strength of the model kept increasing whereas the strength of the experimental SPSW decreased after cycle 22. The initial stiffness for the pushover analysis model overestimated the test specimen stiffness by approximately 15%. The cyclic analysis was performed for loading cycles 5, 11, 17, 22 and 26+. The initial stiffness and strength of the model at the early cycles were overestimated. The higher cycles were predicted well but overestimated the stiffness and ultimate strength by similar margins as the pushover analysis.

The second model of the test specimen consisted of a strip model as proposed by Thorburn *et al.* (1983) and was implemented on the software S-Frame®. Driver *et al.* (1997) modified the strip model to include inelastic behaviour by manually inserting plastic hinges to the SPSW when the plastic moment was reached in the columns and beams. When a tension strip reached its yield capacity, the strip was replaced by forces equal to the yield strength of the strip in the corresponding direction. The model

included gravity loads and P- Δ effects were considered in the analysis. The model underestimated the ultimate capacity of the SPSW by approximately 8% while the initial stiffness was underestimated by approximately 18%. It was suggested that the initial stiffness underestimation could be attributed to localized compression fields that form in the diagonally opposite corners, which are not accounted for in the strip model. The effect of the tension field inclination angle α was also studied by repeating the model with different values of the angle. The results indicated that the inclination of the tension field from 42° to 50° had minimal impact on the prediction of storey shear vs. storey drift. The number of strips selected to represent the infill plate was also investigated. It was found that increasing the number of strips from 10 to 20 did not improve the predicted results as was earlier observed by Thorburn *et al.* (1983).

2.11 Lubell (1997)

Lubell (1997) conducted experiments on a 4-storey shear wall (SPSW4) and two single-storey shear walls (SPSW1 and SPSW2). All beam-to-column connections in the test specimens were rigid connections and the tension field was anchored at the top of the specimens by a larger beam compared to the inter storey beams. Both the 4-storey and single storey specimens used 1.5 mm thick infill plates. The single storey specimens, shown in Figure 2.8, did not use gravity loading. For the 4-storey specimens, steel masses were placed at each storey as shown in Figure 2.9 to simulate gravity loading. The initial out-of-plane imperfections of the infill panel were measured for use in a finite element analysis.

The only difference between SPSW1 and SPSW2 was the top beam: SPSW2 used two fully welded S75 x 8 sections whereas SPSW1 used a single S75 x 8 section. This was done to provide better anchorage for the development of the tension field. During the fabrication of the first specimen, SPSW1, large initial out-of-plane deflections (26 mm) occurred. For the subsequent construction of SPSW2 and SPSW4 extra caution was used to limit the initial imperfections to 5 mm or less.

The specimens were subjected to a quasi static cyclic loading procedure based on ATC-24 (Applied Technology Council 1992). The initial stiffness of the single storey specimens

were significantly different, which was attributed to the smaller initial out-of-plane deformations of the infill plate and the stiffer beam in SPSW2. Both specimens exhibited excellent ductility, reaching inelastic deformations near $6 \delta_y$, where the yield deflection, δ_y , was 9 mm and 6 mm for SPSW1 and SPSW2, respectively. The 4-storey specimen, SPSW4, was less stiff than the single storey specimens due to the influence of the overturning moment. At a storey displacement of $1.5 \delta_y$, the columns of SPSW4 failed by overall out-of-plane buckling where the yield deflection, δ_y , was 9 mm measured at the first storey. Due to the low flexural stiffness of the columns, all the test specimens exhibited significant pull in during testing. All test specimens displayed an overall high initial stiffness and stable hysteretic behaviour. It was recommended that design standards require that multi-storey SPSWs be designed and analysed as complete shear walls as opposed to isolated panels since overturning moments and other interactions affect the behaviour of SPSWs.

The test specimens were modelled using a nonlinear frame analysis and subjected to two different loading methods. The first method was a cyclic loading program that used reversed cyclic loading pattern to model the hysteretic behaviour observed in the tests. The infill plate was modelled using tension only strips in both directions with the tension angle α calculated as per Timler and Kulak (1983). The second loading method was a nonlinear push-over analysis. For this loading approach, tension strips were used in only a single direction to resist the lateral loads and again calculating α as per Timler and Kulak (1983).

The results of the monotonic analysis of SPSW1 did not agree well with the test data and as such the cyclic analysis was not pursued for this model. The inconsistent results were attributed to the large initial imperfections. The monotonic and cyclic analyses of SPSW2 were in good agreement with the test results. The monotonic test accurately predicted the initial stiffness but slightly underestimated the ultimate strength while the cyclic model captured the pinching of the hysteresis loops. Two models were created for the monotonic analysis of the 4-storey specimen. Neither model was able to accurately predict both the initial stiffness and the ultimate capacity. The cyclic analysis of SPSW4

resulted in similar hysteresis behaviour as SPSW2, which suggested that the 4-storey shear wall would have resisted more loading cycles had the column not buckled.

As the analytical model of SPSW2 gave reasonable predictions of the test results, a parametric study was conducted using the monotonic loading analysis. The study indicated an increase in ultimate strength with an increase in plate thickness, t , but the initial stiffness remained unchanged. In addition, both the initial stiffness and ultimate capacity were found to decrease as the angle of the tension field, α , decreased.

2.12 Timler *et al.* (1998)

Timler *et al.* (1998) conducted an analytical study on the design and cost effectiveness of steel plate shear walls. Several medium size office buildings were designed using steel plate shear walls as the lateral load resisting system with various ductility ratings for different locations across Canada. These designs were compared with equivalent reinforced concrete shear wall designs as the lateral load resisting systems. The seismic and wind loads were established using the 1995 National Building Code of Canada (NBCC 1995) and the steel building designs were based on Appendix M procedure of CAN/CSA S16.1-94.

It was found that there were two main factors that contributed to the economic feasibility of SPSWs as compared with the reinforced concrete shear walls. The steel plate structures required less expensive super- and sub-structure work compared to the formwork required for a similar concrete design. It was also found that the speed of erection for a SPSW would result in a significantly reduced construction time, resulting in the building being turned over to the owner much sooner than a building with a concrete shear wall.

Timler *et al.* (1998) suggested several analytical modelling simplifications aimed at simplifying the design process. These include an appropriate averaging of the tension field angle for buildings of moderate height, a “cross-hatching” method to reduce the number of nodes in the strip model and a relaxation of the axial load limitations placed on the boundary columns. The cross-hatching technique, which involves the use of

common nodes for the tension strips on beam elements as seen in Figure 2.10, reduces the complexity of the strip model for numerical analysis purpose.

2.13 Schumacher *et al.* (1999)

Schumacher *et al.* (1999) examined the effect of the connection detail between the infill plate and boundary members on the cyclic performance of the corners of SPSW. Since tearing of the infill plates at the frame corners was noted in several experiments (Driver 1997; Timler and Kulak 1983) an investigation of the effect of these tears on the load capacity of the SPSW was desired. The test program consisted of four specimens with different connection types, which were also analysed using a nonlinear finite element model.

The types of connection tested consisted of the infill directly welded to the boundary members, connected on one side using a fish plate and to the boundary member on the other side, and by fish plates all around, as illustrated in Figure 2.11. The fourth method, not illustrated in Figure 2.11, used fish plates on both frame members and a chamfered cut-out at the corner in an attempt to reduce the local stresses and tearing at the corner of the infill plate. The loading of the specimen consisted of two components, the opening and closing of the beam-to-column joint that would be experienced during lateral load reversals and the diagonal tension field that develops after the plate buckles.

The results of the testing indicated that all details displayed good performance and each provided a gradual and stable reduction in load capacity. The infill plates that were directly connected to the boundary members exhibited less tearing than the connections that used fish plates. However, the formation of tears did not result in a loss of capacity. The addition of the chamfered cut out did not reduce the stress in the corner of the infill connection. The finite element model was able to predict accurately the load vs. displacement behaviour of the test specimens and gave a reliable prediction of the capacity of the corner details.

2.14 Rezai (1999)

Rezai (1999) used shake table tests to determine the dynamic behaviour of a 4-storey, single bay, steel plate shear wall as shown in Figure 2.12. The test specimen had similar dimensions to the specimen tested by Lubell (1997) and was braced in the out-of-plane direction. The beam-to-column connections were designed as rigid connections and the infill plate was 1.5 mm thick. Gravity loads were simulated by applying 1700 kg lumped masses in the form of steel plates at each floor level. The dynamic loading applied to the specimen simulated site-recorded seismic events from various locations and synthetically generated ground motions with variable intensities. The capacity of the shake table was such that the specimen remained in the elastic range, making the nonlinear performance of the steel plate shear wall impossible to observe. The specimen was also subjected to a low-amplitude vibration test to determine the natural frequency, which was determined to be 6.1 Hz in the longitudinal direction. The shake table experiment was the first test to load dynamically a steel plate shear wall.

The experimental load vs. deformation plots indicated that most of the energy dissipation occurred in the first storey where shear deformations dominated the behaviour of the storey. The top floors acted as rigid bodies rotating about the lower storey while the flexural strains in the intermediate beams could be considered negligible.

A sensitivity analysis was conducted to determine the effect of certain structural elements on the value of the inclination angle of the tension field, α , with respect to the equation proposed by Timler and Kulak (1983). The five specimens used in the analysis were the SPSWs constructed by Timler and Kulak (1983), Tromposch and Kulak (1983), Caccese *et al.* (1993), Driver *et al.* (1997) and Lubell (1997). The study illustrated that there was no significant change to α in equation 2.3 for any variation in either the beam or column cross sectional area, or for increases in plate thickness above 6 mm. The study indicated that for Equation 2.4, the values of α varied significantly with the variation of the thickness of the infill panel.

A “simplified” strip model was proposed as shown in Figure 2.13 to analyze the behaviour of SPSWs using tension only strips. The orientation of the strips, using five per storey, attempted to model the non-uniformity of the tension field angle α as well as reproduce the stiffness of the panel corners. The model was compared to several tests as well as other analytical models and it was shown to be not as accurate as the strip model proposed by Thorburn *et al.* (1983).

Rezai (1999) conducted an analytical study of the shake table specimen as well as the test specimens from Lubell (1997). It was demonstrated that though the column sections were small, they contributed to the development of the tension field. Any premature yielding and plastic hinge formation in the columns were found to reduce the ductility of the system, thus it was recommended that a lower yield strength steel be used for the infill plate compared to the boundary members to ensure that the infill plate yielded first.

2.15 Kulak *et al.* (2001)

Kulak *et al.* (2001) presented a summary of the experimental and analytical research conducted on SPSWs to date. They also provided a design example of a hypothetical 8-storey building, as seen in Figure 2.14, adapted from Chien (1987). The building was located in Vancouver, Canada, and used two SPSWs as the lateral load resisting system. The preliminary and final designs were done using the equivalent brace model and the strip model, respectively.

The initial strip model was constructed with an average tension field inclination of 42° , 10 strips and a 4.8 mm infill plate. A free vibration analysis of the model and a response spectrum analysis were conducted to estimate the effect that higher modes of vibration would have on the distribution of lateral forces over the building height. The model was then refined and modified to a tension-compression strip model to resist lateral loads in either direction. The tension strips were allowed to yield in tension while the compression capacity was limited to 8% of their tensile capacity to simulate the elastic buckling of the strips. The compressive capacity was determined by comparing the strip model with the sustained load and energy absorbed from the experimental hysteresis

loops obtained from the tests of Driver *et al.* (1997). The model used lumped masses to simulate gravity loads, 5% Rayleigh damping for the first and eighth vibration modes and included P- Δ effects.

The model proposed by Kulak *et al.* was subjected to nonlinear dynamic time history analyses of 20 scaled seismic records to investigate the behaviour of the wall under seismic loading. The results of the analysis indicated that even under the most severe earthquake, which resulted in 2.45 times the NBCC base shears, the inelastic straining was limited and the wall was found to have an over-strength factor of approximately 2.0 with respect to the NBCC 1995 design. The peak interstorey drifts were also well within the NBCC 1995 seismic limits, indicating that both non-structural and structural elements would be protected from damage. The over-strength of the wall resulted from the thickness of the infill plate which was considerably larger than what was required as determined by the detailed analysis. The optimal panel thickness was found to range from 3.3 mm for the bottom floor to 0.026 mm for the top floor, however, the initial 4.8 mm thickness was retained due to handling and fabrication requirements. By changing the thickness of the infill panel as well as some of the column sizes, it was found that the inelastic action could be contained to the first storey.

2.16 Astaneh-Asl (2001)

Astaneh-Asl (2001) examined both stiffened and unstiffened steel plate shear walls in an attempt to compile a review on the behaviour and design of the system. The failure mechanisms of steel plate shear walls were organised into a hierarchy system as shown in Figure 2.15. The chart format was used to give designers an effective tool for checking each member in a SPSW system. The system places emphasis on ductile failure as opposed to brittle failure since it is the more desirable mode of the two.

It was recommended that the plate girder equations described by AISC (1999) be used for the design of unstiffened steel plate shear walls. Although this approach would be conservative, it would lead to unnecessarily conservative design of SPSWs compared to the design methods developed specifically for steel plate shear walls

2.17 Behbahanifard *et al.* (2003)

Behbahanifard *et al.* (2003) tested the undamaged top three stories of the shear wall tested by Driver *et al.* (1997) shown in Figure 2.7. The 3-storey SPSW was loaded cyclically in a quasi static manner based on ATC-24 (Applied Technology Council 1992). The ultimate capacity of the specimen was reached at the first storey drift of $7\delta_y$, where the yield displacement, δ_y , was 7 mm. Before the ultimate capacity was reached, the beam at the first level fractured at the beam-to-column connection, however, the loss in capacity and stiffness was insignificant. Fracture of the connection initiated at a backing bar used to perform full penetration groove welds between the beam and column flanges. This detail is no longer accepted for structures in high seismic areas. As the purpose of the test was to observe the behaviour of the beams and columns under extreme loading, the fractured connection was repaired and the testing was resumed. Once the ultimate capacity was reached, there was a gradual reduction in strength due to tears that formed in the lower storey infill plate over the duration of the test. The specimen exhibited high initial stiffness as well as excellent ductility and energy absorption.

A finite element model of the specimen was developed using ABAQUS, which was able to accurately predict the cyclic behaviour of both the Behbahanifard *et al.* (2003) and Driver *et al.* (1997) specimens. The initial stiffness predicted by the model was within 5% of the measured values and the ultimate strength was 12% and 7.8% lower than the tested capacities for the specimens tested by Behbahanifard *et al.* (2003) and Driver *et al.* (1997), respectively. The model incorporated material and geometric nonlinearities, initial imperfection in the infill panels and a kinematic hardening subroutine to simulate the Bauschinger effect. Using the validated model, a parametric study was conducted to determine the effects of several non-dimensional parameters on the performance of a single storey steel plate shear wall. Of the parameters selected, several of the key ones and their effects are listed here. A decrease in the aspect ratio (L/h) was generally found to increase the capacity of the steel plate shear wall. The stiffness of the steel plate shear wall would increase as the ratio of infill plate axial stiffness to the column axial stiffness ($tL/2A_c$) increased. A decrease in the column flexibility parameter ω_n ,

defined in CSA S16-09, would result in an increase in the column lateral stiffness to the panel stiffness. Finally, a parameter relating the magnitude of initial infill imperfections to \sqrt{Lh} was studied. It was observed that imperfections could result in a noticeable reduction in stiffness and thus it was suggested that the imperfections be limited to 1% of \sqrt{Lh} . From the parametric study, a method was proposed to extrapolate the results of the single storey specimens to multi-storey specimens.

2.18 Berman and Bruneau (2003)

Berman and Bruneau (2003) used the concepts of plastic analysis and the strip model to derive equations to calculate the ultimate strength of both single- and multi-storey SPSWs. The equations were developed for frames with either simple or rigid beam-to-column connections. Using the assumed collapse mechanism shown in Figure 2.16, the storey shear strength for a single storey steel plate shear wall with simple beam-to-column connections was found to be V , which is identical to the probable storey shear strength given by CSA S16-01:

$$V = 0.5F_y t L \sin 2\alpha \quad 2.5$$

where F_y is the yield strength of the infill plate and the other variables as previously defined. In the case of rigid beam-to-column connections, Equation 2.5 was modified using components of internal work.

To calculate the ultimate strength of multi storey SPSWs, the two failure modes illustrated in Figure 2.17 were assumed. Failure mode (a) shows a soft storey mechanism and mode (b) shows yielding of all the infill plates, in addition to the formation of plastic hinges at the beams ends and at the columns for the top and bottom storeys. The ultimate strength of both single and multi-storey SPSWs can be estimated using these assumed mechanisms to predict soft storey collapse.

Berman and Bruneau (2003) also examined the CSA S16-01 provisions for calculating the infill plate thickness t . The equation used the storey shear, V , obtained from the equivalent lateral force method, and recommended that the equation be multiplied by a system over-strength factor, Ω_s , which ranged from 1.1 to 1.5. Based on this

recommendation, the minimum infill plate thickness required to resist the storey shear is calculated as:

$$t = \frac{2V\Omega_s}{F_y L \sin 2\alpha} \quad 2.6$$

2.19 Kharrazi *et al.* (2004)

Kharrazi *et al.* (2004) proposed a Modified Plate-Frame Interaction (M-PFI) model to predict the yield and ultimate resistance of a steel plate shear wall. The M-PFI model considers the displacement of a SPSW as the combination of two separate deformations, namely, shear and bending deformations. For each deformation, the elastic buckling, post-buckling and yielding behaviour were examined. The first part of the M-PFI model consists of a pure shear analysis to determine the load vs. displacement relationship from the infill plate and frame separately. The results of the analysis are superimposed to give the deformations of the steel plate shear wall in shear. The second part of the model considers the SPSW as a single unit under bending from which the stresses and displacements are obtained. Finally, the model considers the interaction between the shear and bending displacements and a shear vs. lateral displacement plot is used to predict the behaviour of the SPSW.

Kharrazi *et al.* (2004) attempted to validate the M-PFI model by examining the results of the tests by Driver *et al.* (1997) and Behbahanifard *et al.* (2003). These tests were selected for study as they were the tallest structures tested to date. For both specimens, an assumed tension field angle of 45° was used in the model. While the M-PFI method led to satisfactory results for the Driver *et al.* (1997) and Behbahanifard *et al.* (2003) tests, the model does not describe the failure mechanism, ductility of the structure or provide a method to determine the design frame forces.

2.20 Shishkin *et al.* (2005)

Shishkin *et al.* (2005) investigated several refinements to the strip model proposed by Thorburn *et al.* (1983) in an attempt to improve the accuracy of the prediction of the response envelope for steel plate shear walls under cyclic loading. The proposed modifications were applied to a static pushover analysis using the commercially

available software SAP2000®. The first model proposed, named the “detailed model”, included several complex modifications that were later simplified in the “simplified model” in an attempt to reduce the modelling effort without significant loss in accuracy. The detailed model incorporated features such as stiff elements at the rigid joints panel zones to approximate the finite size of the members at the connections, a compression strut to model the post-buckling compression contribution of the infill plate, “deterioration hinges” to try to model the effect of tears on the load carrying capacity, and detailed multi-linear axial load vs. moment interaction definitions for all the plastic hinges.

The simplified model gave results similar to the detailed model for the test results from Driver *et al.* (1997) and was thus renamed the “modified strip model”. The modified strip model was further validated using several other SPSW test specimens (Timler and Kulak, 1983; Lubell, 1997). Finally, a parametric study was conducted using the modified strip model to determine the sensitivity of the inelastic behaviour to variations in the tension field angle α used for the tension strips.

As for the original strip model proposed by Thorburn *et al.* (1983), the stiffness associated with the panel zone stiffness was ignored and was modeled by a simple beam-to-column node and a simple elastic-plastic hinge definition was used. The strip pattern originally proposed by Thorburn *et al.* (1983) was simplified to the “crosshatching” technique suggested by Timler *et al.* (1998). This was done to simplify the modelling procedure. A comparison between the results of the simplified model and the detailed model indicated that very little accuracy was lost as the simplified model was within 4% of the ultimate capacity prediction of the detailed model and gave the same result for the initial stiffness. The simplified model was renamed the modified strip model and used in a subsequent parametric study.

The modified strip model was used to determine the sensitivity of the inelastic behaviour to variations in the tension field angle α used for the tension strips. The tension field angle α was varied from 38° to 50° and it was found that the model was insensitive to the variations. It was suggested that a value of 40° could be used throughout the structure.

2.21 Berman and Bruneau (2008)

Berman and Bruneau (2008) proposed a capacity design method to predict the design axial forces and bending moments in the boundary columns of SPSWs. Lateral forces causing full infill plate yielding and plastic hinging at the beam ends were derived from the earlier plastic collapse mechanism of Berman and Bruneau (2003). These forces were used on the free body diagrams of a 4- storey SPSW shown in Figure 2.18. The free body diagram includes web plate yielding at storey i , ω_{xci} and ω_{yci} , the lateral forces consistent with the plastic collapse mechanism, F_i , plastic hinging beam moments, M_{prli} and M_{prri} , beam axial forces, P_{bli} and P_{bri} , and base reactions, R_{yl} , R_{xl} , R_{yr} , and R_{xr} .

The proposed design method was used to design two 4-storey SPSWs; one with constant and one with variable infill plate thickness. The design column axial forces and bending moments were then compared to two methods; the Indirect Capacity Design and combined Linear Elastic and Capacity Design, described in the AISC 2005 seismic design provisions for structural steel buildings (AISC 2005). The results from each design method were compared with the results from a nonlinear static pushover analysis for both SPSW specimens. The method proposed by Berman and Bruneau (2008) was shown to give results that were considerably closer to the pushover analysis results, and was able to capture the moment-axial interaction in beams.

The researchers noted that while the proposed design procedure could predict accurate design forces, it was assumed that the SPSW has fully yielded infill panels on all floors. This would restrict the procedure to shorter SPSWs as it would be improbable that taller structures would experience simultaneous yielding of the infill panels over the entire height. Thus it was suggested that for taller SPSWs, the column forces be reduced to account for various infill plates remaining elastic. This reduction follows a similar procedure proposed earlier by Redwood and Channagiri (1991).

2.22 Bhowmick *et al.* (2009)

Bhowmick *et al.* (2009) investigated the behaviour of SPSWs using a finite element model that incorporated geometric and material nonlinearities as well as damping, P- Δ and loading rate effects. The model was implemented using ABAQUS/Standard (Hibbitt

et al. 2007) using four-node doubly-curved shell elements with reduced integration and an implicit time integration method for seismic analysis. The model was validated by replicating the results from previous quasi-static and dynamic cyclic tests.

The validated model was then used to study the performance of Type D and Type LD steel plate shear walls in two major Canadian cities. Several theoretical designs were carried out according to CSA S16-01 and NBCC 2005 for buildings with 4, 8 and 15 storeys for the cities of Vancouver and Montreal. The short and tall buildings used similar dimensions for ease of storey scaling, shown in Figure 2.19. The designs were implemented in the FE model and subjected to spectrum compatible earthquake records. Frequency analyses were also performed on the 4- and 15-storey buildings.

The results of the analyses indicated that the capacity design approach in CSA S16-01 underestimated both the probable shear strength of the SPSW and the flexural seismic demand at the base. It was suggested that the underestimated probable base shear results from neglecting the shear strength contributions from the boundary columns. The underestimated probable base shear leads to a reduced value of bending moment from the capacity design equations. Similar reasoning suggests that axial forces and bending moment demands in the boundary columns were also underestimated. It was recommended that during the design stage, the shear strength contributions from the columns be included. It was also noted that there was no significant increase in ductility from the use of over-strength infill plates and it was recommended that the infill plate thickness be adjusted to reduce over-strength variations throughout the building height.

The analysis also showed the absence of yielding in the top storey infill plate. Thus the top storey infill plate does not require tension field anchoring by a significantly stiffer beam compared to the inner storey beams. This is especially significant when the thickness of the top storey infill plate is limited by the use of a minimum practical infill plate thickness.

Bhowmick *et al.* (2009) proposed a capacity design procedure that does not require any nonlinear analysis for the boundary column members. The method locates the infill plates that are expected to yield during a design earthquake using the indirect capacity

design principles of CSA S16-01. The forces from the identified infill plates are then applied to the boundary columns for each storey to determine the axial load. The associated column moments are estimated for each individual storey based on the individual conditions for that storey.

The proposed approach was used to design two 4-storey and one 8-storey SPSWs subjected to four distinct nonlinear seismic analyses using the FE modelling software. The design forces were shown to be slightly conservative and agreed well with the analysis results. A comparison of the proposed design forces was made with the capacity design procedures from CSA S16-01 (CSA 2001), AISC (2005) and the procedure proposed by Berman and Bruneau (2008). The proposed design method was found to provide the most reliable and consistent column axial forces and bending moments when compared with the current capacity design methods which tend to either overestimate or underestimate boundary column forces. Bhowmick *et al.* (2009) extended their proposed analysis approach to SPSWs with infill plate openings.

2.23 Bing and Bruneau (2009)

Bing and Bruneau (2009) noted that North American design codes (AISC 2005, CSA 2001) neglect lateral resistance contributions provided by the moment resisting boundary frame. The researchers investigated the relative contributions of the bounding elements and their contribution to the overall strength of the SPSW. A method was proposed to account for the boundary frame contribution to the lateral resistance of the SPSW as well as to optimize the design of SPSWs based on those contributions. The proposed method was used to design an eight storey building which is compared to the results of a nonlinear time history analysis to a similar building designed according to the AISC 2005 specifications.

As noted by other researchers before, the contribution of the frame to the shear capacity of the SPSW was found to be significant. Therefore the shear resistance used in AISC (2005) to determine the required infill plate thickness was modified by a factor κ as follows.

$$w = \frac{\kappa V_n}{0.42 F_y \sin(2\alpha)} \quad 2.7$$

where w is the storey infill panel thickness, V_n is the nominal lateral storey shear, F_y is the yield strength of the infill panel, and α as previously defined. The factor κ , proposed by Bing and Bruneau assigns a percentage of the design shear to the infill panel. With this design equation the system overstrength factor, Ω_κ , is expressed in terms of κ , the panel aspect ratio, L/h , and the tension field angle, α , as:

$$\Omega_\kappa = \kappa \left[1 + \frac{1}{2} \tan^{-1}(\alpha) \left(\frac{L}{h} \right) \frac{\eta}{1 + \sqrt{1 - \eta^2}} \right] \quad 2.8$$

where η is a reduction ratio for reduced beam sections, and all other terms as previously defined. A parametric study was conducted using this equation to determine the impact of variations of the percentage of lateral shear attributed to the infill panel κ on the resulting system overstrength, Ω_κ . For the study, the tension field angle was held at 45° , and no reduced beam sections were used. Equation 2.8 was also examined for various aspect ratios allowed by the AISC design approach. The results of the study are illustrated in Figure 2.20. The balanced case corresponds to a system overstrength of 1.00. From this definition, it was shown that using the current AISC design, the system overstrength varies from 1.4 to 2.25 for a given aspect ratio due to the additional capacity of the boundary frame. In the balanced case, it can be seen that the percentage of shear resisted by the infill panel is reduced from 1.0 from the AISC design specifications, to values between 0.45 to 0.70 percent, depending on the aspect ratio.

Using a hypothetical 8-storey building, a SPSW was designed using several different philosophies: the AISC specifications where $\kappa=1.00$, the balanced condition where $\Omega_\kappa=1.00$, and low strength infill panels where the selected value for κ resulted in an overstrength below the balanced condition ($\Omega_\kappa < 1.00$). These SPSWs were modelled using a bi-directional, tension only strip model and subjected to a nonlinear time history analysis with three different ground acceleration histories. The results of the analysis indicated that the balanced method of design gave results that were similar to the AISC design specification while the low strength infill panel models had larger interstorey

drifts. The models were also compared using the required weight of steel used and it was seen that the balanced case used significantly less steel than the AISC design specification for SPSW.

It was suggested that more work be done in this area to determine the amount of storey shear that could be safely attributed to the boundary frame in order to properly utilize the amount of available shear resistance from the bounding elements.

2.24 Neilson *et al.* (2010)

Neilson *et al.* (2010) tested a single storey SPSW 1900 mm high by 2440 mm wide using a thin gauge, cold rolled infill panel. The infill panel was comprised of two 20 Gauge A1008 CS (0.91 mm) cold rolled panels welded together in a lap splice. The research program examined methods of welding the thin infill to the thick boundary members as well as the lap splice between two thin sheets. The wall was subjected to cyclic loading in accordance to the seismic testing guideline ATC-24 (ATC, 1992). A push-over analysis of the test specimen was also conducted using the strip model proposed by Thorburn *et al.* (1983) and the analysis software SAP 2000®.

Thin panels (about 1 mm) were selected for the study as thicker-than-required sections is not desirable when designing according to capacity design. The use of thicker-than-required plates in capacity design results in an overstrength problem leading to excessively large boundary elements. As fabricators do not typically handle thin plates, a procedure was developed for handling and welding thin infill panels. The parameters investigated in developing the procedure included material properties, joint geometry, welding process, and electrode and shielding gas selection. ASTM A1008 CS 20 gauge plate was selected based on the low measured yield and ultimate strength of 173 MPa and 288 MPa, respectively. The low strength characteristic was desirable to ensure that the boundary elements designed according to capacity design principles remained small. As the plates selected were cold rolled, their width is usually too small to fit the bay using a single piece. Thus two plates were used and it was found that a lap splice, welded on both sides gave the best performance. A welding procedure was developed for the lap to minimize distortion and burn through of the thin plates. The lap was tack

welded at regular intervals, and then stitch welds were placed between the tacks. This was done on both sides of the splice. A chill strip was used to reduce burn through and weights were placed on the infill panel to minimize welding distortions. A similar procedure was used to connect the infill panel to the fish plates using a weld at the cut edge of the infill panel only. Short-circuiting gas metal arc welding was selected for the weld process to minimize heat input coupled with an ER70S-6 electrode, which provided the desired strength, toughness and deoxidizer content. The shielding gas selected was CO_2 as the trial results indicated that it provided the desired weld penetration and arc stability.

The SPSW was subject to a cyclic loading protocol based on ATC-24, which resulted in a peak load of 630 kN reached at cycle 16. In the following cycle, a fracture occurred near the base of the SPSW column, near a column base stiffener, at a storey drift of 3.5%. Local buckling and lateral buckling of the beam near the loaded column occurred at about the same time. The loading was continued for a final cycle in the opposite direction where a storey drift of 6.9% was reached at 86% of the peak capacity of the frame. Several small imperfections were noted during the test including a 10 mm tear in the fish plate to infill panel connection which was a result of a poor quality weld. Also noted was the local buckling of the fish plate in the corners of the specimen resulting in a 15 mm tear. Despite some noted imperfections, there was no detectable loss of performance or integrity noted for the duration of the test.

The test specimen was modelled using the strip model (Thorburn *et al.*, 1983) in SAP2000® and subjected to a static nonlinear pushover analysis. The model was created using 10 tension strips with an angle of inclination, α , of 40°. Material properties for the infill panel and the beam and columns were similar to those measured from tension coupon tests. The model gave good agreement with the envelope of the hysteresis plot, underestimating the ultimate strength by 7.5% while the initial stiffness was predicted to within 8%. The moment frame, without the infill panel, was analysed separately and it was seen that with the addition of the infill panel, the model demonstrated an increase in the initial elastic stiffness of 280% and an increase in the ultimate load capacity of 48%.

2.25 Infill Panel with Circular and Cut Out Sections

Several researchers (Roberts and Sabouri-Ghomi, 1992; Vian, 2005; Purba, 2006; Bhowmick 2009; and others) have investigated reducing the strength of the infill panel by adding holes or corner cut-out sections. In addition to limiting overstrength issues by reducing the strength of thick infill panels, perforations and cut-outs provide designers the ability to run utilities through the infill panels. S16-09 provides provision for the use of infill panels with circular holes and corner cut-outs in Clauses 27.9.2.3 and 27.9.2.4, respectively, as well as additional details in the commentary section.

Vian (2005) tested SPSWs with infill panels using both circular and corner cut-out sections using a quasi-static cyclic loading procedure. The SPSW frames were single storey, single bay specimens with rigid connections and used reduced beam sections on the beams. The infill with the perforations used circular cut-outs with a diameter, D , of 200 mm staggered at 300 mm centre-to-centre along both vertical and horizontal directions and arranged at a 45 ° angle as shown in Figure 2.21. The infill with the cut-out corner sections used quarter-circle cut-outs with a 500 mm radius at the upper corners of the plate as shown in Figure 2.22. Under the loading routine, the frame with the perforated infill reached an interstorey drift of 3% and the frame with the cut-outs reached an interstorey drift of 4%. All specimens exhibited stable, ductile performance and plastic hinging occurred in the beam sections. It was suggested that infill panels with cut-outs and perforations be used when the available plate thickness is larger than what is required to resist the predicted lateral loads.

Purba (2006) developed a series of finite shell element models to predict the behaviour of the perforated and cut-out SPSW specimens tested by Vian (2005). It was found that provided that the hole diameter was less than 60% of the strip width, the performance of the SPSW can be accurately predicted by the finite element analysis. Additionally, Purba (2006) examined the work proposed by Roberts and Sabouri-Ghomi (1992) which approximates the strength of a perforated infill panel. Using this research, and based on the analysis results, Purba (2006) found that the shear strength of a perforated infill panel with multiple and regularly spaced perforations could be calculated by multiplying the shear strength of a SPSW with a continuous infill panel by a factor of:

$$1 - 0.7 \frac{D}{S_{diag}} \quad 2.9$$

where D is the diameter of the perforations; and S_{diag} is the shortest distance between perforations.

The provisions outlined by S16-09 for infill plates with perforations are based on the work done by Purba (2006), Vian (2005), Roberts and Sabouri-Ghomi (1992), and others. The perforations are required to be of constant diameter and regularly spaced in both the vertical and horizontal planes. S16-09 incorporates the recommendation by Purba (2006) to limit the hole diameter to 60% of the strip width. Also included is Equation 2.9 in the determination of the factored shear resistance of the infill panel which is calculated as:

$$V_r = 0.4 \left(1 - 0.7D / S_{diag} \right) \phi F_y w L_i \sin 2\alpha \quad 2.10$$

where L_i is the width of the bay under consideration and all other terms as previously defined. S16-09 allows for corner cut-outs provided that the edges of the cut-outs are reinforced, the radius of the cut-outs is less than one-third of the height of the infill panel, and the beams and columns are able to resist the compression and axial tension introduced by the reinforcing segments of the cut-outs.

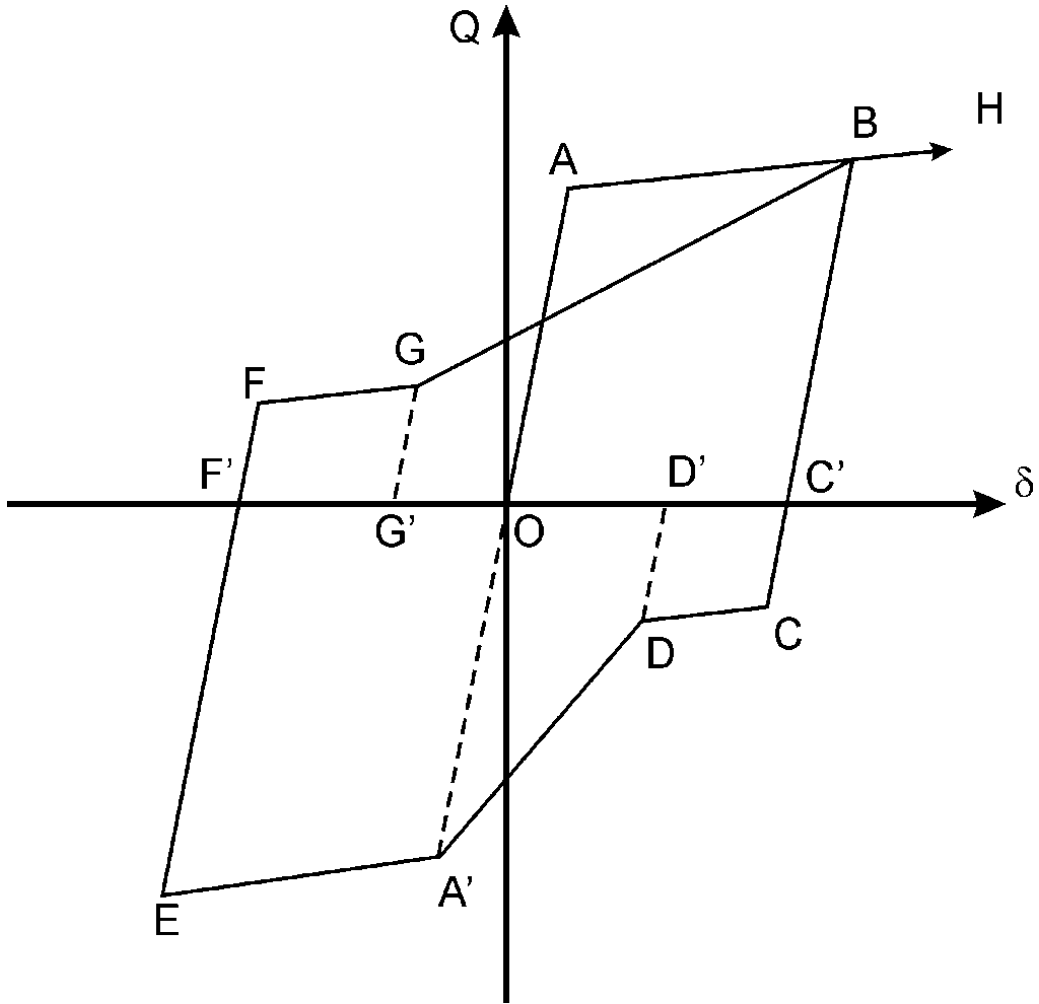


Figure 2.1 - Hysteresis Model Proposed by Mimura and Akiyama (1977)

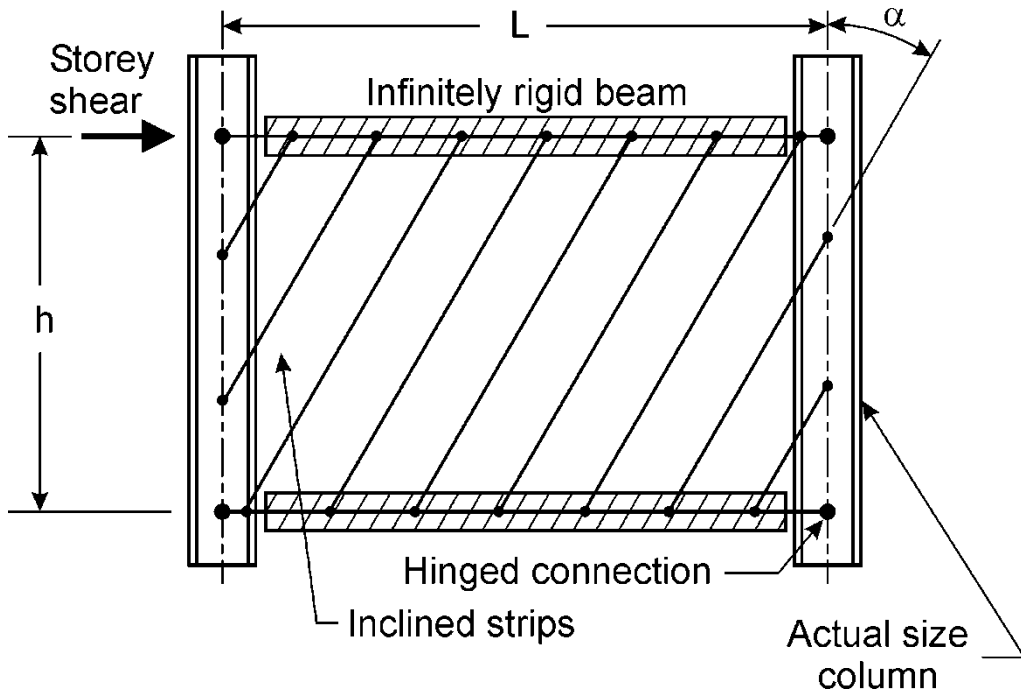


Figure 2.2 - Strip Model proposed by Thorburn et al. (1983)

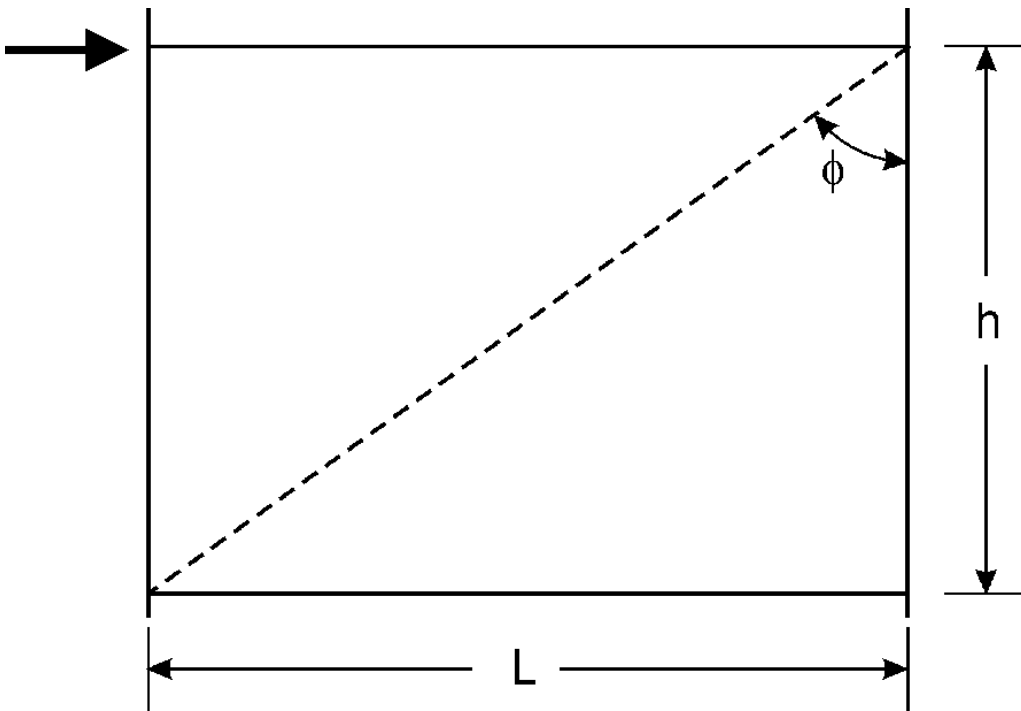
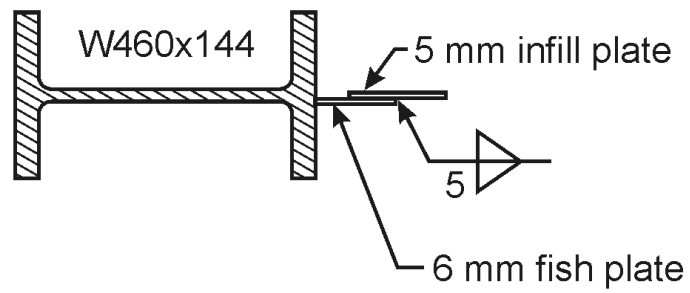
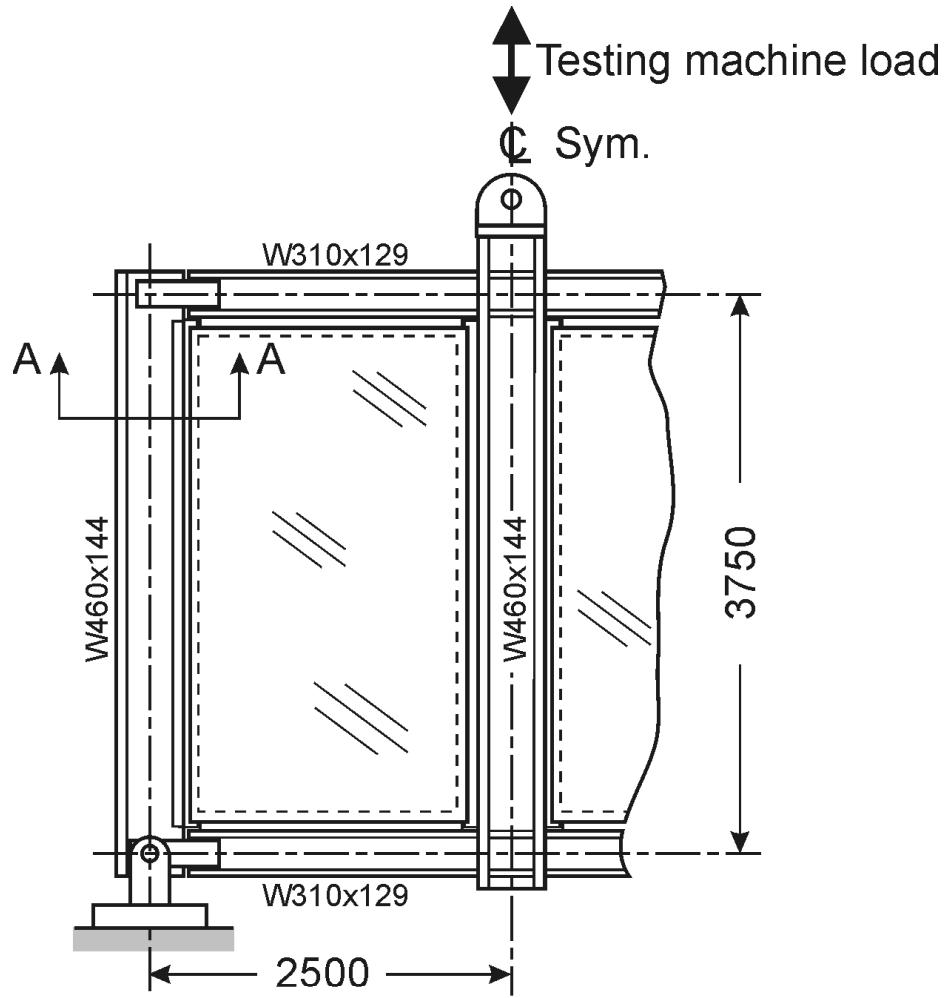


Figure 2.3 - Equivalent Brace Model proposed by Thorburn et al. (1983)



Section A-A

Figure 2.4 - Single Storey Test Specimen from Timler and Kulak (1983)

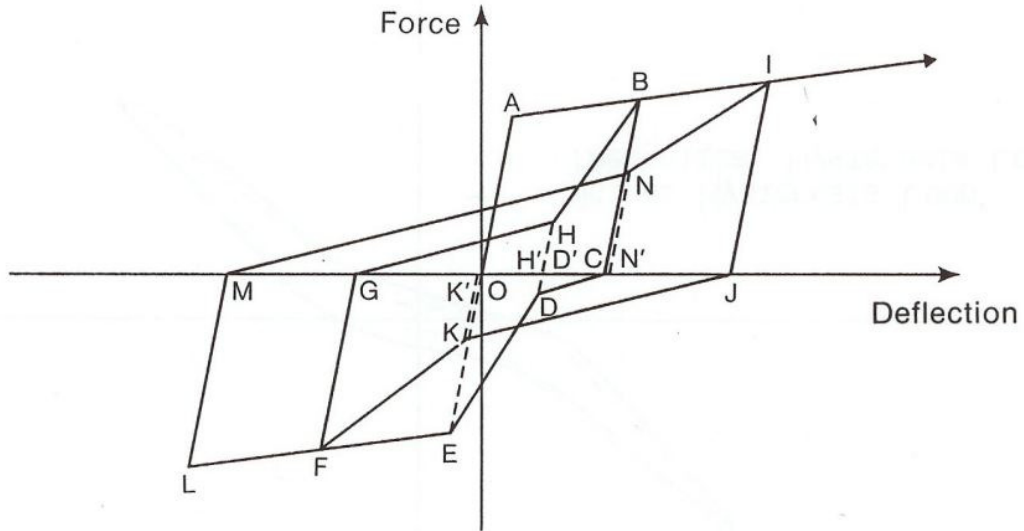


Figure 2.5 - Hysteresis Model Proposed by Tromposch and Kulak (1987)

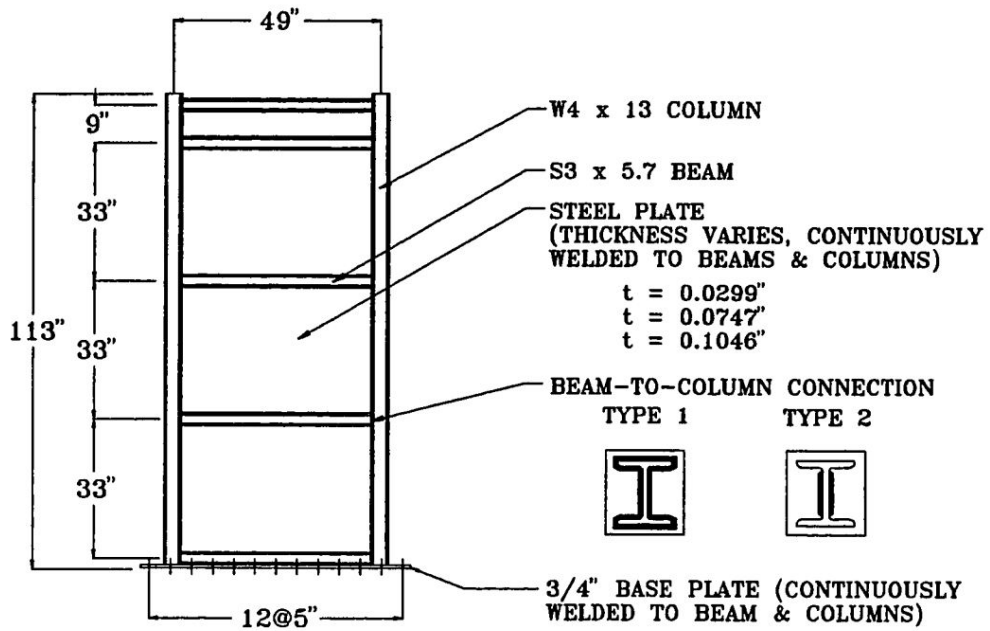


Figure 2.6 – 3-Storey Model used by Chen (1991)

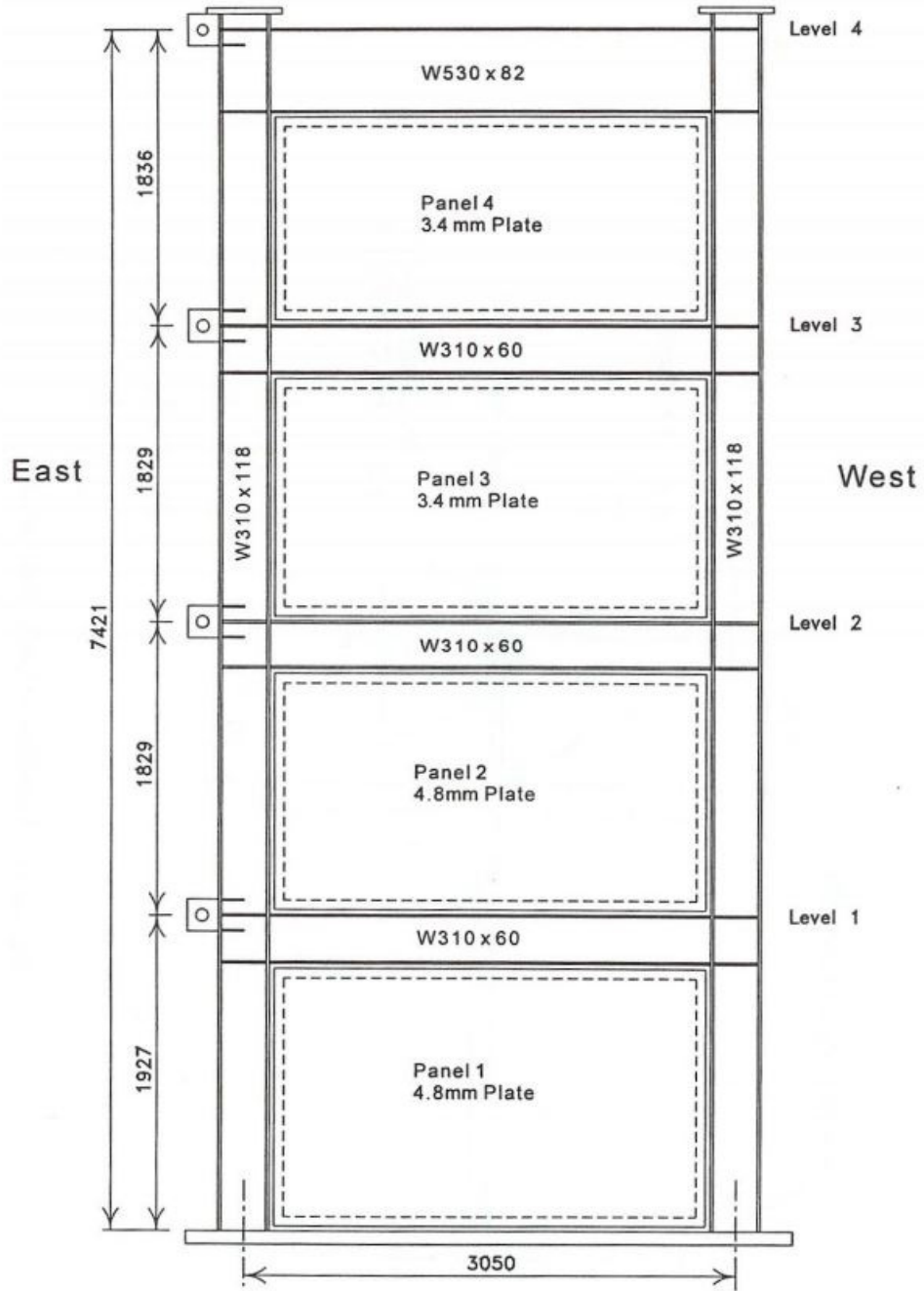


Figure 2.7 – 4-Storey Specimen (Driver et al. 1997; 1998a)

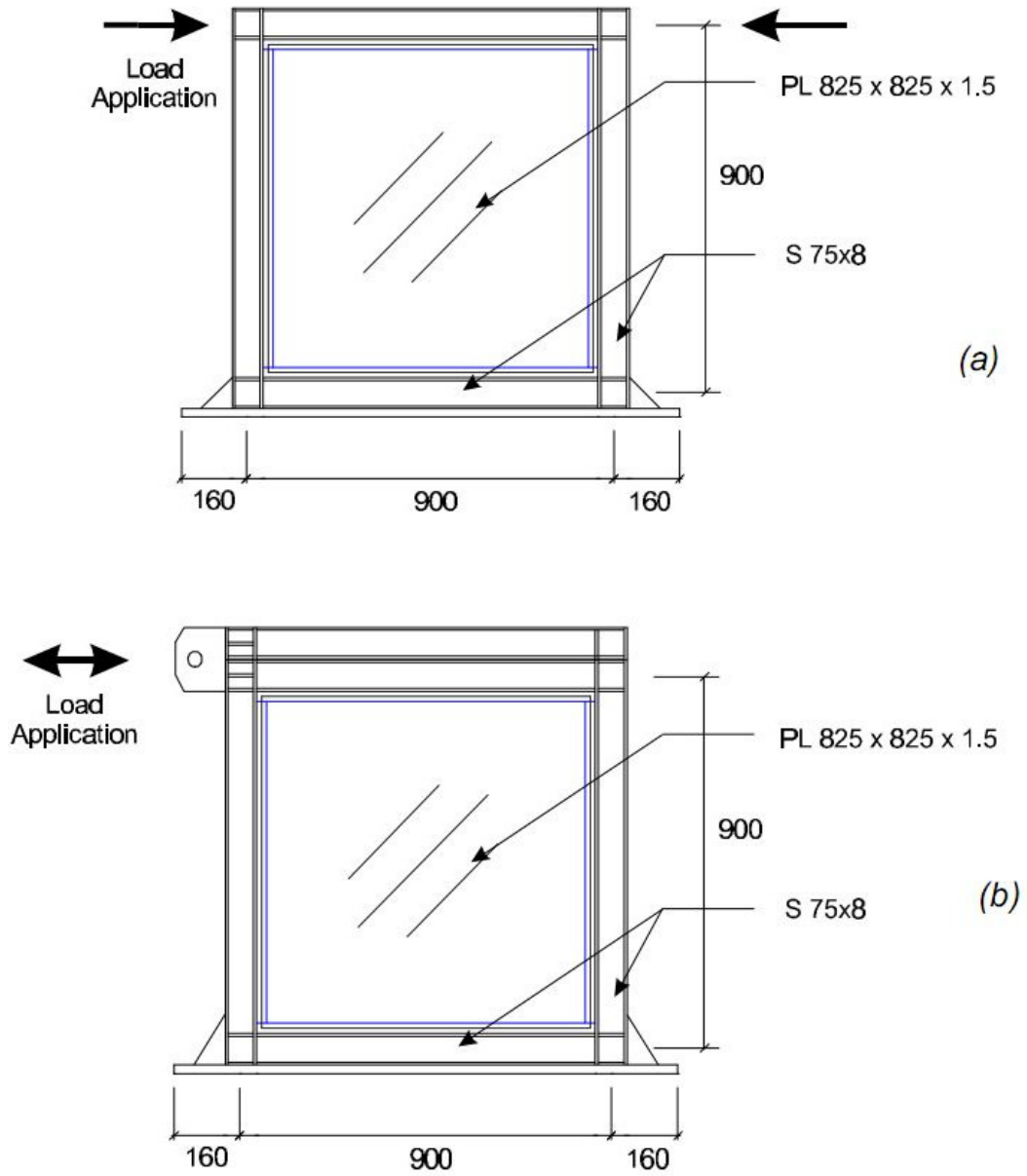


Figure 2.8 - Single Storey Test Specimens (Lubell 1997): (a) SPSW1; and (b) SPSW2

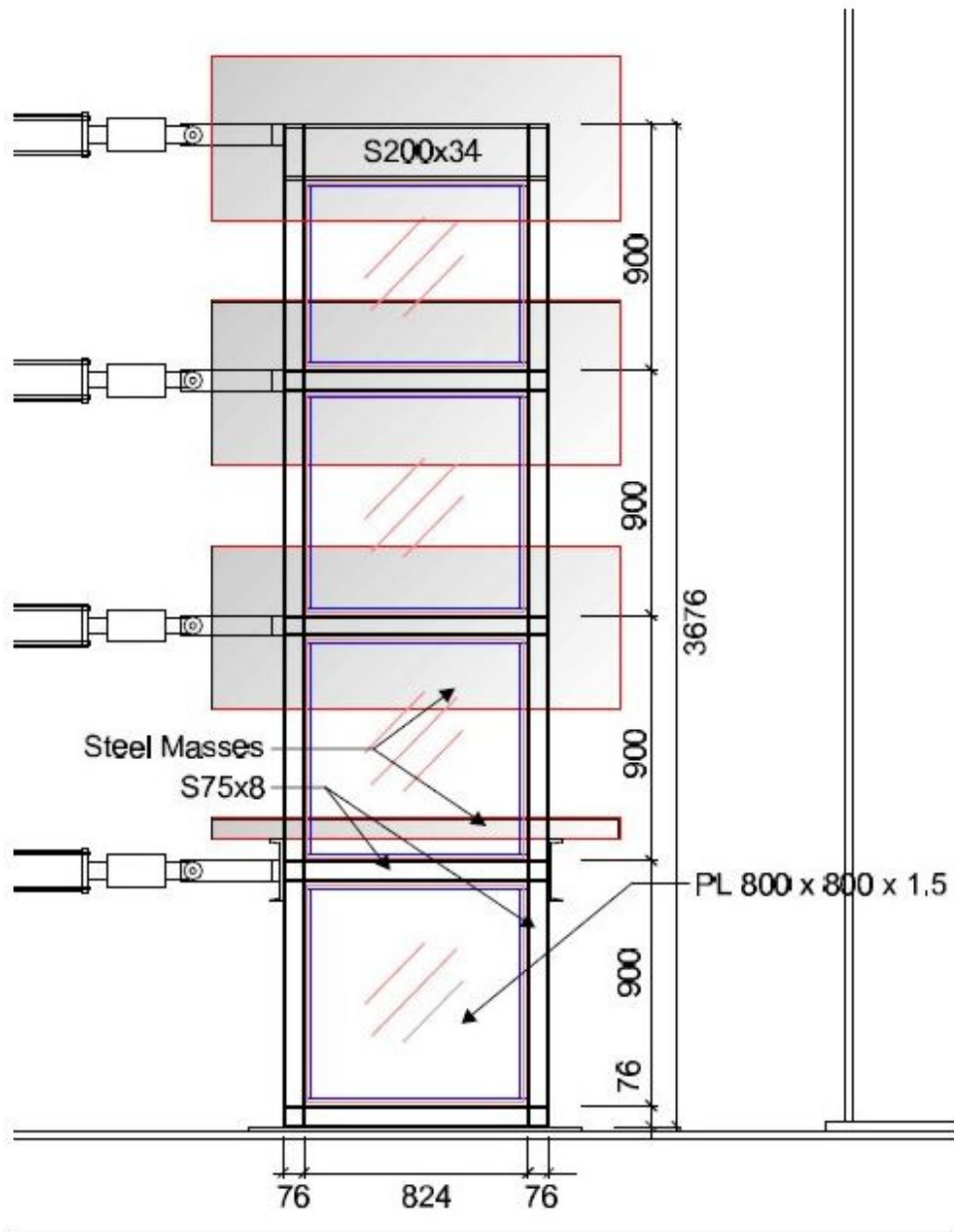


Figure 2.9 – 4-Storey Test Specimen (Lubell 1997)

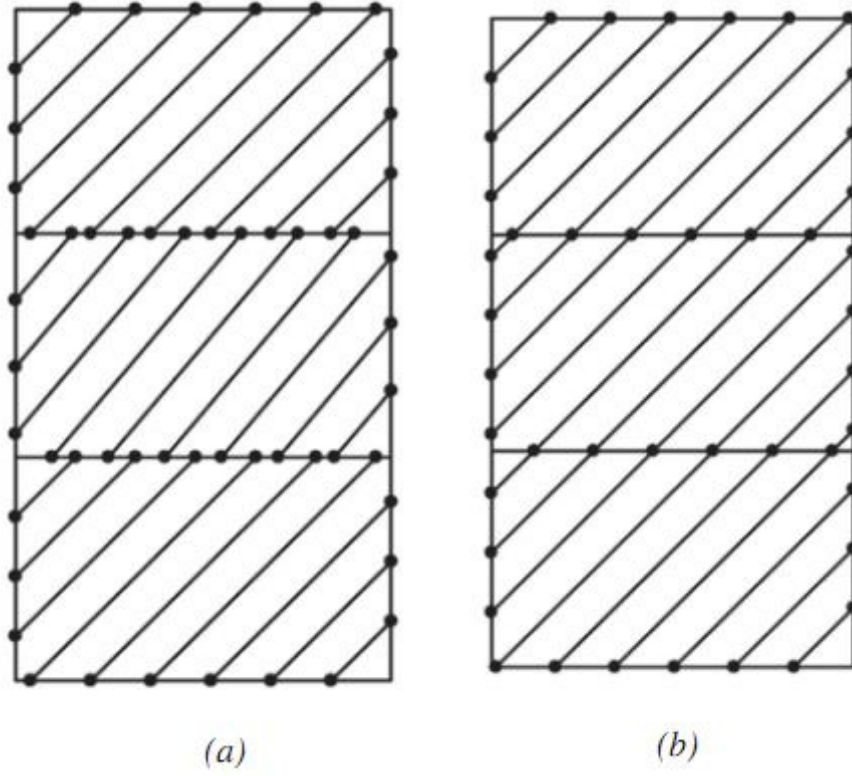


Figure 2.10 - Staggered Strip (a) and Cross Hatching Method (b)

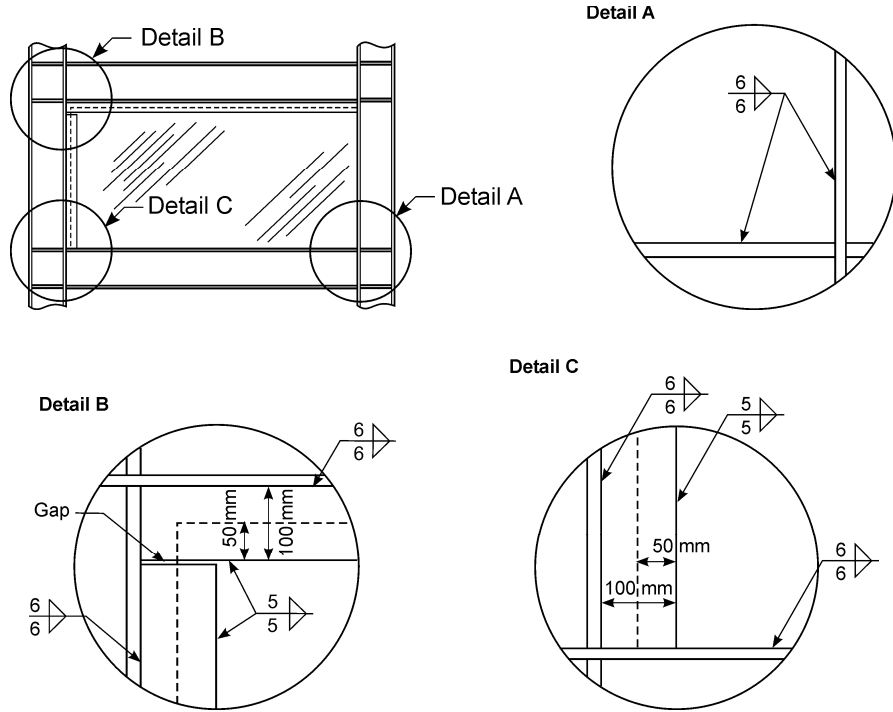


Figure 2.11 - Corner Details Tested by Schumacher et al. (1999)

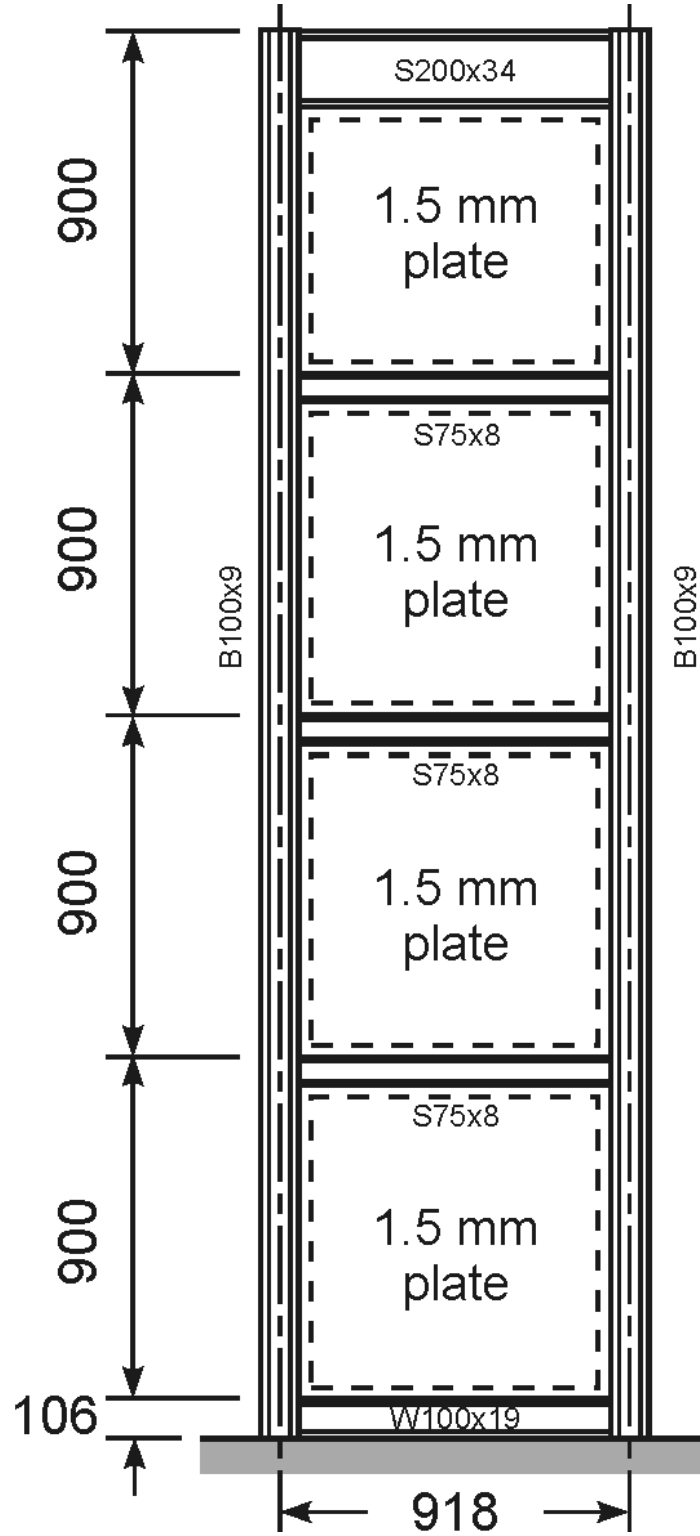


Figure 2.12 – 4-Storey Shake Table Specimen (Rezai 1999)

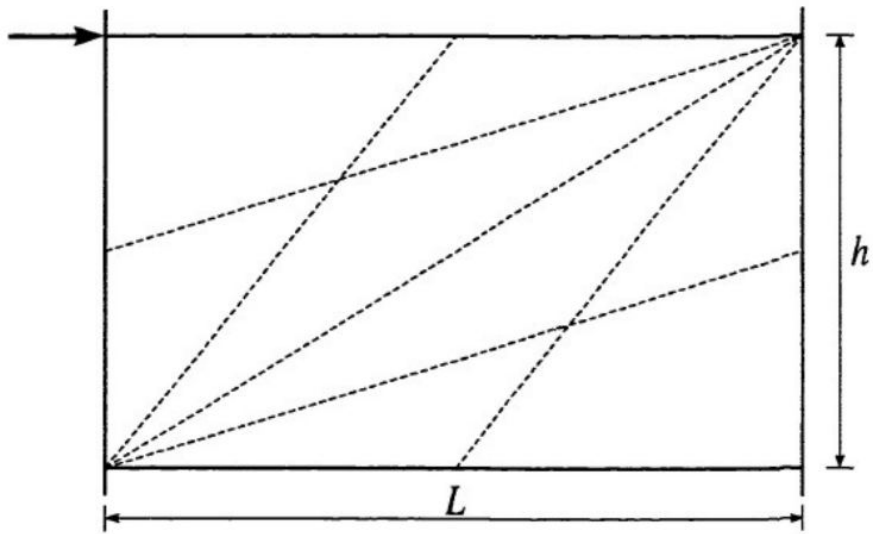


Figure 2.13 - Simplified Strip Model (Rezai 1999)

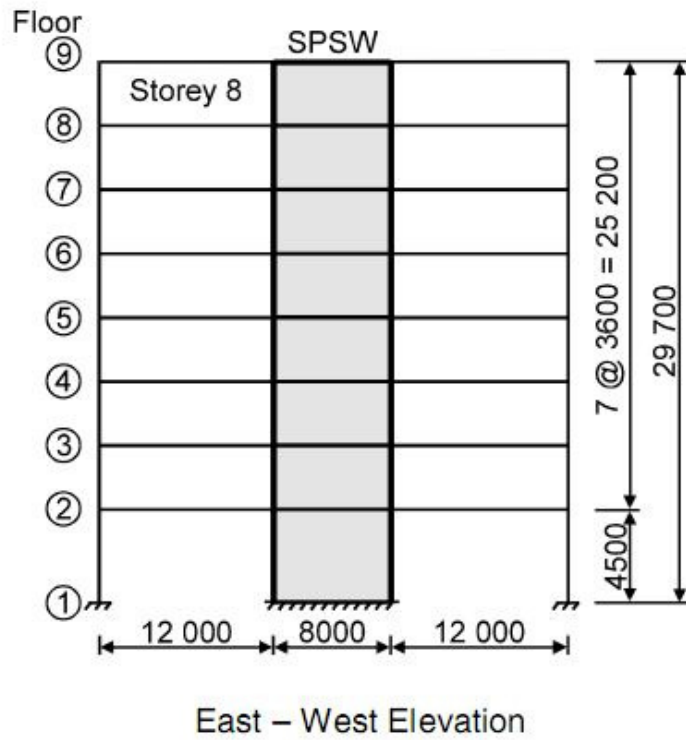
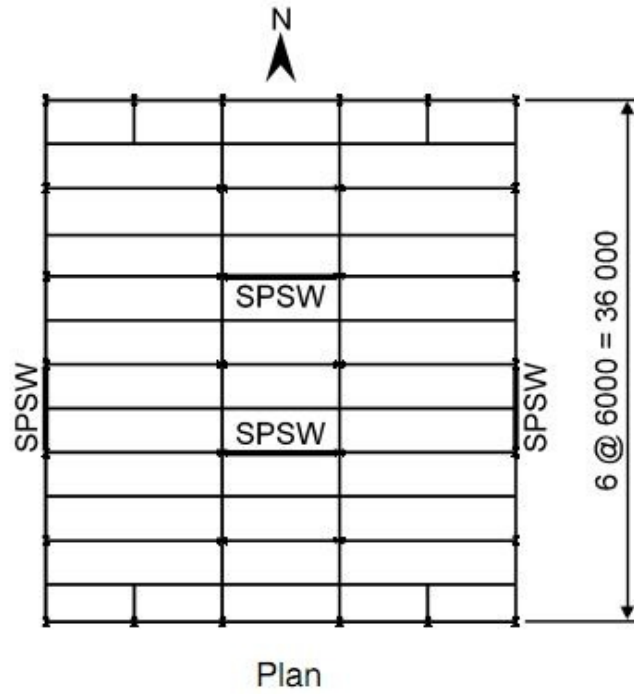


Figure 2.14 - Hypothetical Vancouver Building Layout (Kulak et al. 2001)

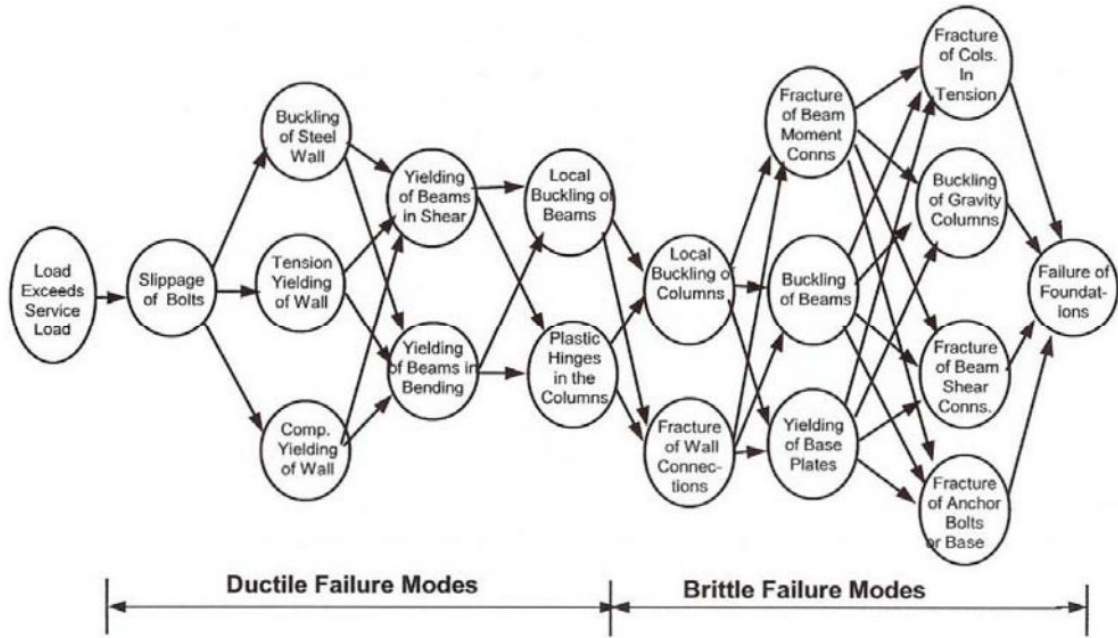


Figure 2.15 - SPSW Failure Mechanism Hierarchy (Astaneh-Asl 2001)

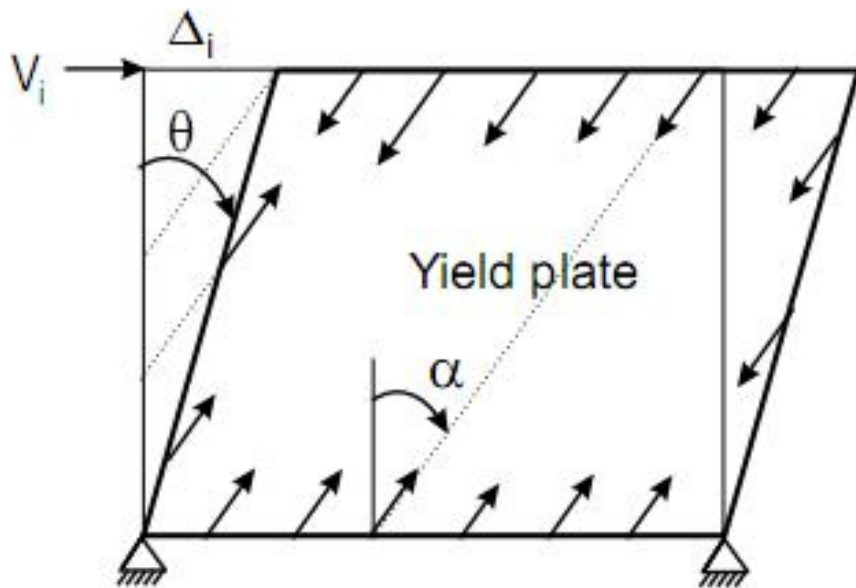


Figure 2.16 - Single Storey Collapse Mechanism (Berman and Bruneau 2003)

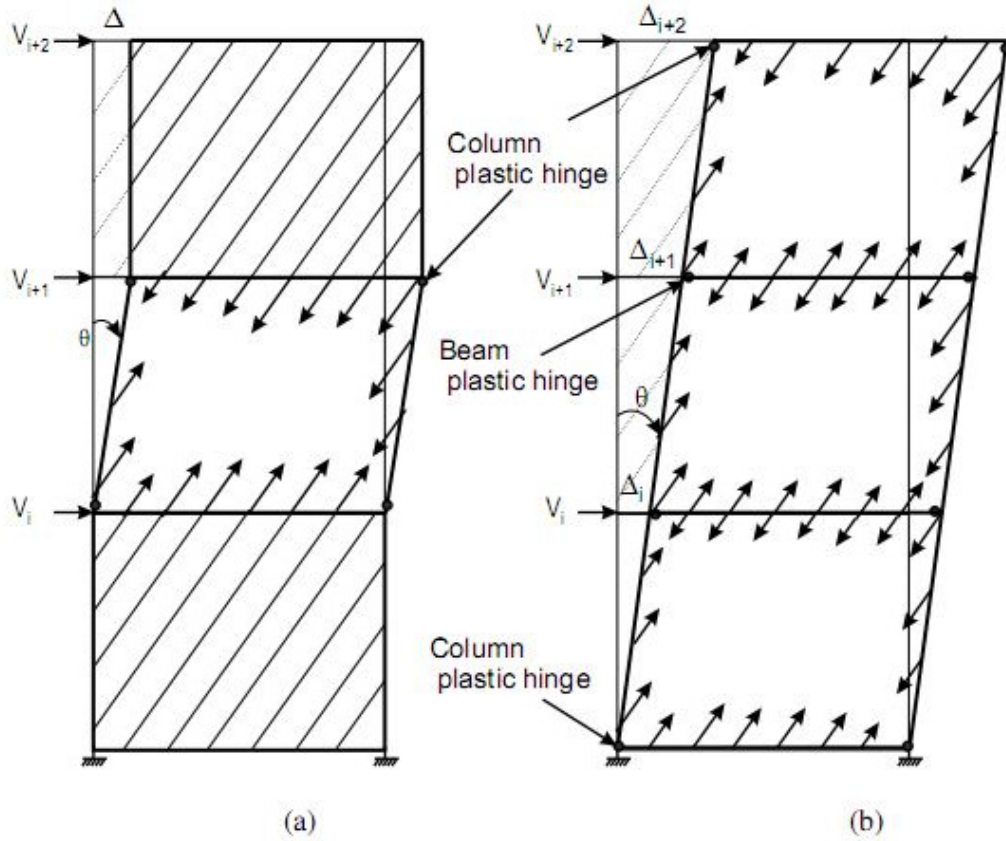


Figure 2.17 - Multi-Storey Collapse Mechanisms Proposed by Berman and Bruneau (2003): (a) Soft Storey Mechanism; and (b) Unified Collapse Mechanism

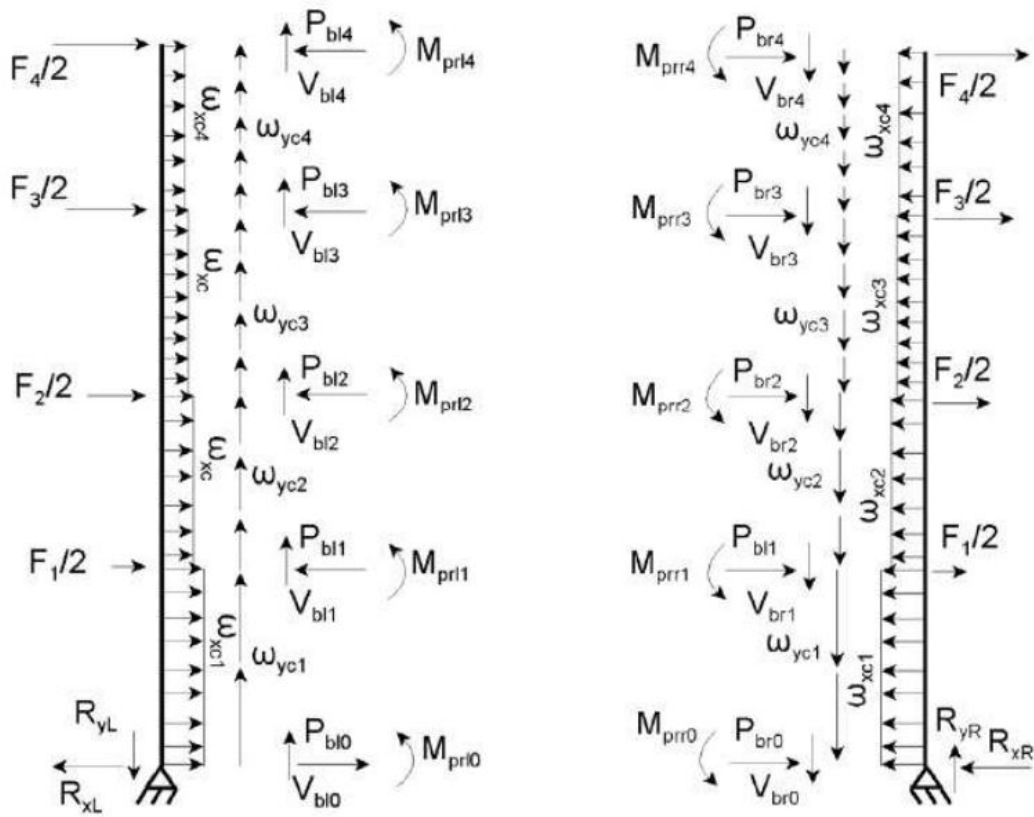


Figure 2.18 - Column Free Body Diagrams (Berman and Bruneau 2008)

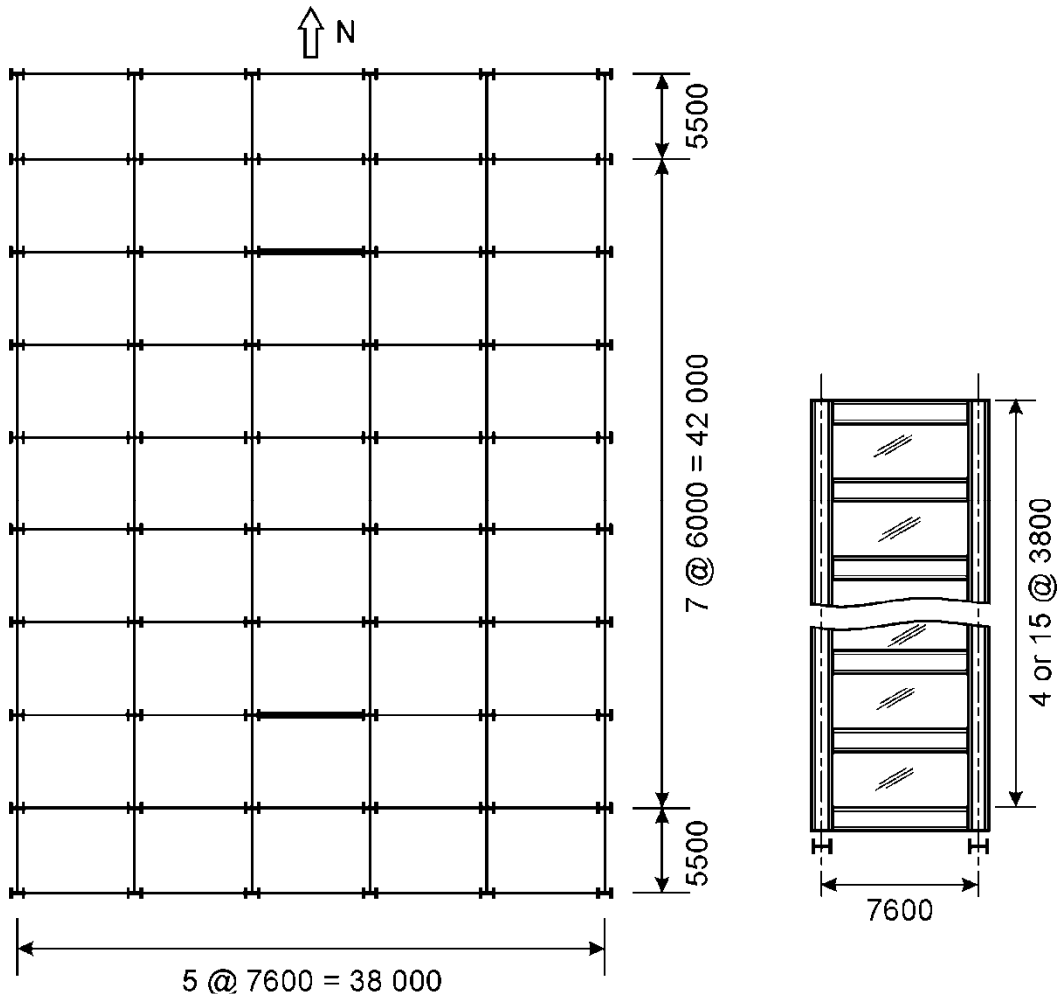


Figure 2.19 - Office Floor Plan and Elevation of 4-storey and 15-storey SPSW analysed by Bhowmick et al. (2009)

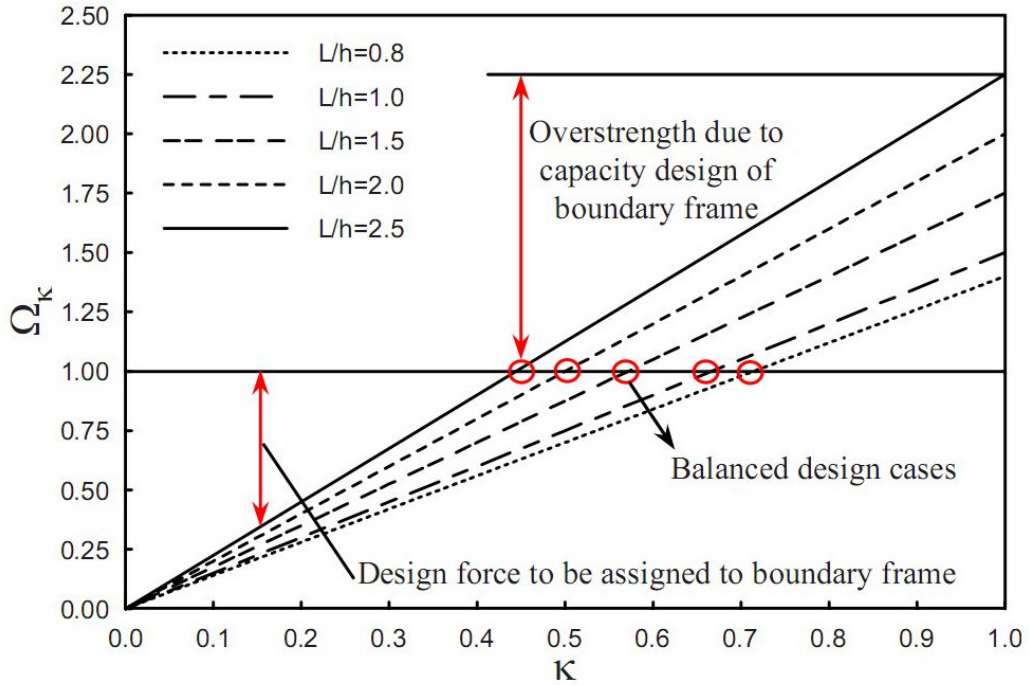


Figure 2.20 - Relationship Between system overstrength Ω_{κ} and percentage of shear in infill panel κ (Bing and Bruneau 2009)

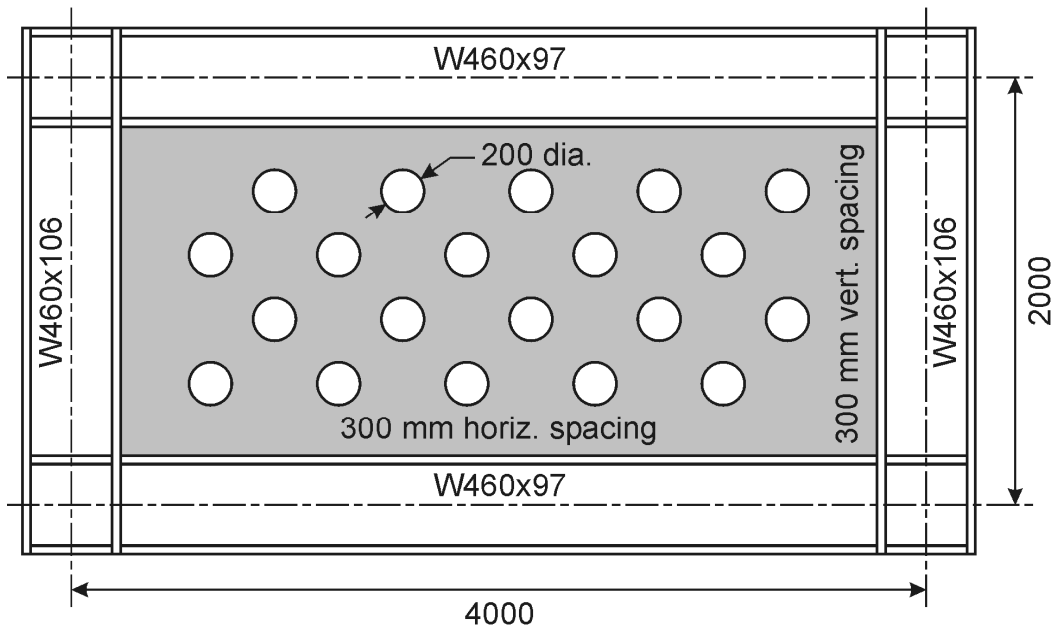


Figure 2.21 - SPSW with Perforated Infill Panel (Vian 2005)

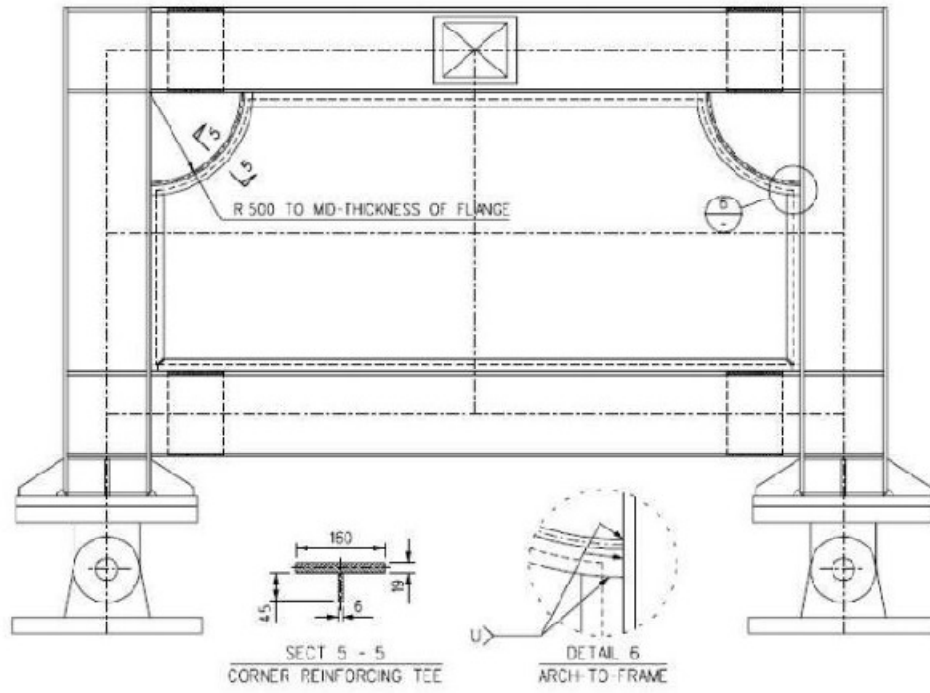


Figure 2.22 - SPSW with Corner Cut-Outs (Vian 2005)

3. DESIGN PROCEDURE

3.1 Introduction

The design procedure for steel plate shear walls (SPSW) has been addressed in a number of design guides and design standards (AISC 341-05, AISC 2007, CSA S16-09). This chapter presents a description of the current Canadian standard CSA-S16-09 (CSA 2009), as well as the current AISC design specifications (AISC 2005) for the design and analysis of SPSWs. The general and seismic design loads procedure presented in this section will be in accordance to the National Building Code of Canada, Division B Section 4 (NBCC 2005). The following sections describe specific aspects of design, construction and analysis of SPSWs while referencing general sections that are applicable to any building design.

3.2 Design Forces

The 2005 edition of the National Building Code of Canada (NBCC 2005) provides guidelines to determine the appropriate live, wind, and seismic loading for building design in Canada. Using the calculated loads, the various limit states can be checked for the structure under consideration.

3.2.1 General Loading

General loading covered in NBCC 2005 includes forces generated by local effects, such as wind and snow loading as well as dead and live loads caused by the self weight of the building and the proposed occupancy. The limit states and calculations for dead and live loads are covered in Section 4.1 of the NBCC. The loads resulting from snow, wind and rain include location specific variables to account for the climate variability across Canada. Snow and rain accumulations are calculated as follows:

$$S = I_s [S_s (C_b C_w C_s C_o) + S_r] \quad 3.1$$

where I_s is the importance factor for the snow load; S_s is the 1-in-50-year ground snow load; C_b is the basic roof snow load factor; C_w is the wind exposure factor; C_s is the slope factor; C_o is the shape factor; and S_r is the 1-in-50-year associated rain load.

Wind load is calculated as a static pressure on either exterior and interior walls, or suction acting in a normal direction on part or the entire surface of the structure. The wind pressure is calculated as:

$$p = I_w q C_e C_g C_p \quad 3.2$$

where I_w is the importance factor for wind; q is the reference velocity pressure; C_e is the exposure factor; C_g is the gust factor; and C_p is the averaged external pressure coefficient acting on the surface under consideration. These factors are explained in detail in the NBCC 2005. Dynamic effects due to wind loading are also included for buildings that meet certain requirements as outlined in Section 4.1.7.2 of the NBCC.

3.2.2 Seismic Loading

In seismic design according to the NBCC, the lateral load path must be clearly defined and shown on structural drawings. In the case of SPSW, the infill panel plate and bounding elements comprise the load path and must be clearly identified as the seismic force resisting system and is designed to resist 100% of the seismic loads (DeVall 2002).

NBCC 2005 classifies SPSWs designed for seismic loads into two distinct types: Type D (ductile), and Type MD (moderately ductile). The difference between the two types is reflected in the values of the ductility-related force modification factor, R_d , and the overstrength-related force modification factor, R_o . The value of R_d , is higher for Type D walls than for Type MD walls, 5.0 vs. 2.0, respectively, to account for the ability of the structure to dissipate energy. The overstrength related force modification factor, R_o , is also higher for Type D walls as opposed to Type MD walls, 1.6 vs. 1.5, respectively, to account for a dependable portion of reserve strength beyond the nominal material strength normally used for design.

NBCC 2005 specifies two types of procedures to determine the seismic forces on a structure. The first procedure is the dynamic analysis procedure and the second is the equivalent static force procedure. In general, the dynamic analysis procedure is used to determine the deformations and member forces that are required for design. Although the dynamic analysis procedure is preferred for obtaining the design forces, it can be

simplified provided the structure satisfies certain criteria. This simplified approach is the basis for the equivalent static force procedure for which the seismic design forces are approximated by equivalent static forces. In the equivalent static force procedure, the design member forces and deformations are obtained from a static analysis. Both methods are described in detail in the following sections.

3.2.2.1 Equivalent Static Force Procedure

The equivalent static force procedure is an attempt to approximate the dynamic effects of an earthquake on a structure by static loads. Several assumptions are made in the model, such as the vibrational modes of the building. It is assumed that the response of the building, which is modelled as a single degree of freedom structure, is primarily in the fundamental mode. The higher modes are later accounted for by the use of a modifier that attempts to incorporate the participation of higher modes into the response. These and other assumptions are discussed by Humar and Mahgoub (2002). Cases where there is a high modal participation ratio, such as in tall flexible long period buildings, require dynamic analysis. To use the equivalent static force procedure, the designer must ensure that the structure meets the requirements outlined by the NBCC 2005 to ensure that the assumptions are valid.

The equivalent static force procedure may be used on a structure if the structure meets any of the following criteria:

1. Structures in low seismicity zones where $I_E F_a S_a(0.2) < 0.35$.
2. Structures under 60 m in height with fundamental lateral periods in both orthogonal directions, defined by Clause 4.1.8.8, less than 2 s.
3. Irregular structures, except torsionally sensitive irregularities as defined by table 4.1.8.6 of NBCC, with a height less than 20 m and fundamental lateral periods in both orthogonal directions, defined by Clause 4.1.8.8, less than 0.5 s.

For the seismic design of SPSWs using the equivalent static force procedure, the NBCC specifies the minimum design base shear force as:

$$V = \frac{S(T_a)M_v I_E W}{R_d R_o} \geq \frac{S(2.0)M_v I_E W}{R_d R_o} \quad 3.3$$

where I_E is the importance factor of the structure; M_v is an adjustment factor to account for participation of higher vibrational modes in multi-storey buildings; and W is the weight of the structure and is calculated as follows:

$$W = \sum_{i=1}^n W_i \quad 3.4$$

where W_i consists of the individual floor dead loads; 25% of the design snow load for the roof level; 60% of the storage load and the full contents of any tanks or permanent masses. The term $S(T_a)$ is the damped spectral response acceleration for the fundamental lateral period, T_a , of the structure. This can be either calculated as (Saatcioglu and Humar, 2003):

$$T_a = 0.05(h_n)^{3/4} \quad 3.5$$

where h_n is the height of the structure in meters, or by the use of a structural model but limited to $2.0T_a$ as calculated by Equation 3.5. However, Equation 3.5 was developed using reinforced concrete shear walls (Saatcioglu and Humar, 2003) and it has been shown (Bhowmick *et al.*, 2009; Topkaya and Kurban, 2009) that Equation 3.5 provides low estimates of the period for SPSWs. Bhowmick *et al.*, (2009) proposed a new equation to better predict the natural period of a structure with SPSWs as:

$$T_a = 0.03h_n \quad 3.6$$

with the terms as defined previously.

Previous engineering experience places a maximum limit on the base shear value (Heidebrecht, 2003), which is calculated as:

$$V_{max} = \frac{2}{3} \frac{S(0.2)I_E W}{R_d R_o} \quad 3.7$$

with the terms defined previously. As the maximum base shear calculation assumes a period of 0.2 s, the higher mode factor, M_v , is 1.0 and omitted in the equation. The base shear is reduced by the factors R_d and R_o defined previously which are determined by the type of SPSW under analysis.

The term $I_E S(T_o)$ represents the importance modified design spectral response acceleration, and when multiplied by the weight, W , becomes the maximum base shear for an elastic single degree of freedom system (Humar and Mahgoub, 2003). This is then modified by M_v to account for higher modal participation and divided by R_d and R_o to account for the effect of structure ductility and material overstrength on the reduction of the elastic base shear. The seismic base shear, V , is distributed throughout the structure with an additional load placed at the top floor if the fundamental lateral period, T_o , is greater than 0.7 s. This additional shear at the top floor accounts for the effect of higher modes, which tend to increase the shear in the upper storeys. The additional top floor load is defined as:

$$F_t = 0.07T_o V \leq 0.25V \quad 3.8$$

With the terms as defined previously. The remaining portion of the lateral force is distributed to all the floors, including the top floor, as follows:

$$F_x = (V - F_t) W_x h_x / \left(\sum_{i=1}^n W_i h_i \right) \quad 3.9$$

where W_x and W_i are the portions of W assigned to level x and i , respectively; h_x and h_i are the height above the base to level x and i , respectively; and all other terms as previously defined. For stiffer structures with $T_o < 0.7s$, $F_t = 0$. The overturning moment caused by the lateral seismic forces at any given storey is calculated as:

$$M_x = J_x \sum_{i=x}^n F_i (h_i - h_x) \quad 3.10$$

where J_x is the numerical reduction coefficient for the storey-level overturning moment at level x and all other terms as previously defined. The numerical reduction coefficient

term is included to balance the overestimation of the higher mode effects on the overturning moment and is defined as:

$$J_x = 1.0 \text{ for } h_x \geq 0.6h_n \quad 3.11$$

$$J_x = J + (1 - J)(h_x / 0.6h_n) \text{ for } h_x < 0.6h_n \quad 3.12$$

where J is the base overturning moment reduction factor given by NBCC 2005 in Table 4.1.8.11 and all other terms as previously defined. The basis for the overturning moment reduction factors was presented by Humar and Mahgoub (2003).

It has been observed that severe damage can occur in structures subjected to torsional oscillations (Humar *et al.* 2003). Torsion occurs in buildings when the center of rigidity and center of mass are not coincident. In addition to structural asymmetry, accidental torsion may occur from rotational ground motions and any uncertainties in the evaluation of the building stiffness or mass. Torsional effects are taken into consideration by examining any eccentricities between the centre of mass and the centre of rigidity, or shear centre, as well as dynamic amplification effects. The NBCC 2005 also takes into account any torsional moments due to accidental eccentricities. To determine the severity of torsional effects, a torsional sensitivity parameter, B , is calculated as the maximum value of (Humar *et al.*, 2003):

$$B_x = \delta_{max} / \delta_{ave} \quad 3.13$$

The values are calculated for both orthogonal directions where δ_{max} is the maximum storey displacement at the extreme point of the structure at level x in the direction of the equivalent static forces applied at $\pm 0.10D_{nx}$ from the centre of mass at each floor. δ_{ave} is the average of the displacements of the extreme points of the structure at level x . The variable D_{nx} is the plan dimension of the building at floor level x , measured perpendicular to the direction of the seismic loading. The requirement of B_x values with the corresponding δ_{max} and δ_{ave} values in both orthogonal directions requires a three-dimensional analysis of the structure. Depending on the value of the torsional sensitivity parameter, B , two torsional moments are applied separately about a vertical axis at each level. They are calculated as:

$$T_x = F_x (e_x + 0.10D_{nx}) \text{ for } B \leq 1.7 \quad 3.14$$

$$T_x = F_x (e_x - 0.10D_{nx}) \text{ for } B \leq 1.7 \quad 3.15$$

where e_x is the distance between the centre of mass and the centre of rigidity, measured perpendicular to the applied seismic force at level x , and all other terms were defined previously. De La Llera and Chopra (1994) demonstrated that in Equations 3.14 and 3.15, $\pm 0.05D_{nx}$ accounts for accidental torsion introduced by the structure. The remainder of the term accounts dynamic amplification effects introduced by natural torsion not captured by static analysis. When the torsional sensitivity parameter $B > 1.7$ and $I_E F_a S_a(0.2) \geq 0.35$, a dynamic analysis is required. A detailed discussion is presented by Humar *et al.*, (2003) regarding the forces introduced by seismic torsion.

3.2.2.2 Dynamic Analysis Procedure

The NBCC lists two methods for dynamic analysis; linear dynamic analysis and nonlinear dynamic analysis. The use of the strip model (Thorburn *et al.* 1983) for SPSWs prevents a linear analysis as the tension strips must be defined as nonlinear elements (tension only elements or elements with a limited compressive capability corresponding to the dynamic buckling capacity of the strips). The nonlinear analysis accounts for the yielding of members in flexure, changes in strength and stiffness, as well as any associated period lengthening that may occur with the inelastic phenomenon (Saatcioglu and Humar, 2003).

When a nonlinear dynamic analysis is used to justify a structural design, NBCC 2005 requires a special study to be performed, which consists of a complete design review by a qualified independent engineering team (Saatcioglu and Humar, 2003). Items of particular importance to the study discussed here include ground motion accelerations, inelastic properties of elements and global and local response parameters and their impact on the performance on the entire structure.

The use of ground motions for time history analysis are required to be representative of the seismotectonic environment of the location of the building, or spectrum compatible with the location. This is possible by scaling or modifying actual seismic records or by

creating synthetic time histories. To make existing seismic records spectrum compatible, the ground acceleration records are modified such that their response spectra are similar to existing response spectra for a specific Canadian city. Various programs exist to modify such records such as SYNTH (Naumoski 2001).

To ensure that certain elements are deformed plastically, the duration and waveform of the time history records are to be sufficient to cause the model to behave inelastically. The inelastic behaviour allows for elements to experience yielding by either flexural or other inelastic motion. The hysteretic behaviour of the elements, as well as any softening behaviour is also taken into account. In addition to the required inelastic behaviour, the time history records must be sufficient to cause the structure to pass through several cycles of load reversal.

Finally, both global and local effects must be considered in the design of elements. Global parameters include lateral displacements and interstorey drift from lateral displacements. Local phenomena include member curvature and rotations. The effect of the global and local parameters on the structure in its entirety must also be considered. All general aspects of seismic design outlined by the NBCC 2005 apply for a nonlinear dynamic analysis.

3.2.2.3 *Deflections and Drift Limits*

The NBCC imposes limits on the building deflections and interstorey drifts associated with both the equivalent static force and dynamic analysis methods. It is recommended that only the stiffness of the lateral load resisting system be used in calculating the lateral deflections as it is assumed that non-structural elements are to crack during a seismic event, thus not contributing to the overall stiffness.

Lateral deflections obtained from either the Dynamic Analysis Procedure or Equivalent Static Force Procedure using linear elastic analysis must incorporate torsional and accidental torsional effects. When torsional effects are included, the largest deflection is taken from one of the two extreme edges of the structure. In addition, the lateral deflections are to be multiplied by $R_d R_o / I_E$ to achieve realistic values that may be achieved from inelastic behaviour (Mitchell *et al.* 2003). Lateral deflections obtained

from a nonlinear analysis must take into account both global (lateral displacement and interstorey drift) and local (member end curvatures/rotations) response parameters. The lateral deflections calculated are to be used to account for the sway effects that occur from gravity loads acting on a displaced structure (P–Δ effects).

The maximum interstorey drift at any level is based on the importance level of the structure and the total lateral drift calculated above. The limits imposed are $0.01h_s$, $0.02h_s$, and $0.025h_s$ for post-disaster, schools, and all other buildings respectively, where h_s is the interstorey height.

3.3 CSA-S16-09 Design Requirements

The Canadian Standards Association Design of Steel Structures covers the design of SPSWs in conjunction with the NBCC 2005. The general design procedure is covered in Section 20 with seismic design considerations covered by Section 27. The following covers the main design aspects while referring to more common or minor clauses with respect to structural and SPSW design.

3.3.1 General Design

The lateral resistance of the SPSW is obtained from a combination of frame action and the development of a tension field in the infill plate. As a result, axial forces and moments are developed in the members which can be determined using plane frame analysis. The procedure S16-09 recommends for the design and analysis of the tension field is the strip model proposed by Thorburn et al. (1983). The structure is modelled with the infill plate discretized as a series of inclined, pin-ended, tension only strips. The angle of inclination for the strips, α , can be determined by using the following equation:

$$\tan^4 \alpha = \frac{1 + \frac{wl}{2A_c}}{1 + wh \left(\frac{1}{A_b} + \frac{h^3}{360I_c L} \right)} \quad 3.16$$

which is the angle of inclination from the vertical and with the limits of $38^\circ \leq \alpha \leq 45^\circ$. Alternatively, if the aspect ratio of the frame, L/h , is between 0.6 and 2.5, the angle of inclination may be taken as 40° . S16-09 allows an analysis to be performed on an entire plate wall using a single angle of inclination which is an average of all the panels.

3.3.1.1 Member design

S16-09 places limits on the flexibility of columns and beams in order to properly develop the tension field and prevent beam and column buckling. If the boundary elements do not provide the required stiffness, the elements may develop local or global instabilities. The column flexibility parameter provided is calculated as:

$$\omega_h = 0.7h \left(\frac{w}{2Ll_c} \right)^{0.25} \leq 2.5 \quad 3.17$$

where w is the infill panel thickness; h is the height of the column; L is the width of the bay; and l_c is the moment of inertia of the column. The flexibility parameter for the upper and lower bounding elements are determined by:

$$\omega_l = 0.7 \left(\left(\frac{h^4}{l_c} + \frac{L^4}{l_b} \right) \frac{w}{4L} \right)^{0.25} > 0.84\omega_h \quad 3.18$$

where l_b is the moment of inertia for the beam. The value calculated for ω_l is not to exceed 2.5 and 2.0 for the members at the top and bottom panel of the SPSW, respectively (Dastfan and Driver, 2008).

The infill plate is designed using the tension strip model where the tension strips are to be designed to resist forces according to Clause 13.2. The beams are required to resist bending and compressive axial stresses introduced by the tension field according to Clause 13.8. The beams are to be a minimum of Class 2 sections except for seismic design of Type D SPSWs where Class 1 sections are required. Columns are to be designed according to Clause 13.8 or 13.9 and must be Class 1 sections. The infill plate is assumed to provide negligible in-plane and out-of-plane support to the boundary beams and columns.

3.3.1.2 *Infill Plate Anchorage and Connection*

S16-09 requires that the infill plates at the top and bottom storeys be properly anchored to beams that meet the requirement of Equation 3.18. The horizontal component of the bottom panel tension field must be transferred to the substructure. The infill plate must be connected to both the surrounding beams and columns and it has been shown (Schumacher *et al.*, 1999) that the specifics and eccentricities of the infill plate connection do not have a significant effect on the capacity and performance of the SPSW. These connections, and any infill plate splicing connections if required, are to be done according to Clauses 13.12 or 13.13. In addition, these connections are to be designed to reach the factored tensile strength of the infill plate strips.

3.3.2 *Seismic Design*

The design provisions for steel structures subjected to seismic loading are outlined in Section 27 of S16-09, beginning with general clauses covering several types of seismic load resisting frames.

3.3.2.1 *General*

The seismic design using Clause 27 is to be applied with the requirements of the NBCC, however, S16-09 allows for the maximum seismic loads to be determined using a nonlinear time history analysis. The time history analysis must be done using an appropriate structural model and ground motions. When a nonlinear time history analysis is done, or the building has a short period spectral acceleration ratio less than 0.35, the height restrictions on the structure are waived.

S16-09 requires that SPSWs be designed according to capacity design principles. The main objective of capacity design is to provide the structure with specific elements that act as ductile “fuses”, designed and detailed to dissipate energy by inelastic deformation. Other members and components are designed to resist the forces developed from the fuse element deforming while maintaining structural integrity. The structure must be able to withstand the maximum anticipated seismic loads but not exceeding the values corresponding to $R_d R_o = 1.3$.

Members and connections that are not part of the seismic force resisting system must be, under seismic induced deformations, capable of supporting gravity loads. As such, column splices that are not part of the seismic force resisting system are to be designed to resist a factored shear in both orthogonal directions equal to the sum of $0.2ZF_y / h_s$ of the columns above and below the splice.

The material requirements outlined in Clause 27.1.5 requires F_y not to exceed 350 MPa for the energy-dissipating elements in addition to the requirements of Clauses 5.1.3 and 8.3.2(a). For the columns that are not energy-dissipating elements the allowed material yield strength is not to exceed 450 MPa. Additional requirements for members with thick flanges and buildings with period spectral accelerations greater than 0.55 and welding limitations are outline in Clauses 27.1.5.2 and 27.1.5.3. The probable yield strength of the material is to be calculated as $R_y F_y$ where R_y is taken as 1.1 as well as other restrictions noted in Clause 27.1.7.

When designing the energy dissipating element of the SPSW, notional load and P- Δ effects are to be taken into account. However, these stability effects do not need to be considered in determining the member forces introduced by yielding of the energy-dissipating elements and mechanisms of the seismic force resisting system. When calculating the P-delta effects according to S16-09, the value of U_2 maybe taken as:

$$U_2 = 1 + \left(\frac{\sum C_f R_d \Delta_f}{\sum V_f h} \right) \leq 1.4 \quad 3.19$$

where C_f is the factored compressive force in the member; Δ_f is the relative first order lateral displacement of the storey under the factored shear force V_f in the storey; and h is the storey height.

The protected zones refer to the ductile “fuses” or areas in the structure where energy dissipation is to occur according to capacity design principles. These areas are to be free from sudden changes in hardness or stress concentrations such as those introduced by welded studs and/or attachments unless the details form part of the design system. Attachments are permitted provided that the requirements of Clause 27.2.5.1 are

satisfied. The protected zones must be indicated on the structural design documents and shop details. Further details about the requirements for protected zones are given in the following sections.

3.3.2.2 Ductile Plate Walls

Ductile plate walls, or Type D plate walls, have the highest ductility and overstrength allowance for a seismic force resisting system of 5.0 and 1.6, respectively. Type D walls require rigid beam-to-column connections for the framing elements, which act together with the infill panel to form a stiff lateral force resisting system capable of developing significant inelastic deformations. The deformations occur from yielding of the infill panels and plastic hinges forming in the columns and in the beams near the column faces. S16-09 restricts plastic hinging in columns to the base level only.

Current design provisions require that the infill plate be designed to resist 100% of the factored storey shear. The infill plate shear resistance is given in Clause 27.9.2.1 as:

$$V_r = 0.4\phi F_y w L \sin 2\alpha \quad 3.20$$

where ϕ is the resistance factor; w is the infill plate thickness and all other terms are as previously defined. As the infill plate yields, the forces imparted to the rest of the structure can be calculated as R_y multiplied by the tension yield resistance of the infill plates. This force is referred to as the probable yield force; however these forces need not exceed the value corresponding to $R_d R_o = 1.3$.

Perforated infill plates are allowed, and if the requirements of Clause 27.9.2.3 are met, the factored shear resistance of SPSWs with circular perforations can be calculated as:

$$V_r = 0.4 \left(1 - 0.7D / S_{diag} \right) \phi F_y w L_i \sin 2\alpha \quad 3.21$$

where D is the diameter of the perforations; S_{diag} is the shortest centre to centre distance between the perforations and all other terms as previously defined. S16-09 also specifies an allowance for corner cut-outs with certain restrictions.

Beams for each storey of the SPSW must meet the slenderness limitations of Class 1 section and be properly braced according to Clause 13.7(b). Plastic hinging is allowed in the beams during cyclic loading provided the beam-to-column connection maintains a strength at the column face of at least M_{pb} , the nominal plastic moment resistance of the beam, and 80% of the nominal plastic moment if a reduced beam section is used. This capacity must be maintained through a minimum interstorey drift of 0.02 radian. Beam-to-column connections capable of this capacity are listed in Annex J, or if another connection type is desired, must be verified by physical testing. The factored resistance of the beam web-to-column connection must be equal to or greater than the sum of the gravity loads, tension forces from the infill plates above and below the beam, and the shears introduced by the moments of $1.1R_y M_{pb}$ acting at the plastic hinge location. The reduced moments acting in the beam plastic hinges may be taken as:

$$M_{rpb} = 1.18(1.1R_y M_{pb})(1 - C_f / \phi C_y) \quad 3.22$$

where C_f is the factored axial force in the beam resulting from the tension field in the infill plate; and C_y is the axial yield resistance of the beam. The beams at each storey must have sufficient strength such that the moment-resisting frame resists at least 25% of the applied factored storey shear force. Finally, the beams must meet all requirements of Clause 13.8, incorporating all axial loads, bending moments from gravity loads, lateral loads and the tension force from the infill plate. The tension force from the infill plate is calculated as the probable yield force as previously described.

The provisions for columns of SPSWs are outlined in Clause 27.9.4. The columns must be Class 1 sections and braced in accordance with Clause 13.7 (b) and shall be designed to resist the effects of gravity loads as well as axial and shear forces and bending moments introduced by yielding of the infill plate. Forces induced from the beams must also be accounted for in the design of the columns. Column splices must be designed to resist the shear force consistent with plastic hinging at each ends of the columns bending in double curvature in addition to the full flexural resistance of the smaller column section at the splice, which is to be located as close as possible to the quarter point of the column above the floor. Any plastic hinging to occur in the column must form above the base plate or foundation beam.

At the column joint panel zones, the horizontal shear resistance is taken as either:

$$V_r = 0.55\phi d_c w' F_{yc} \left[1 + \frac{3b_c t_c^2}{d_c d_b w'} \right] \leq 0.66\phi d_c w' F_{yc} \quad 3.23$$

where beam and column variables are denoted by subscripts b and c , respectively, or

$$V_r = 0.55\phi d_c w' F_{yc} \quad 3.24$$

Doubler plates are to be groove- or fillet-welded to develop their full shear resistance. Joint panels designed using Equation 3.23 must be detailed such that the sum of the panel zone depth and width divided by the panel zone thickness must be less than 90 for short period spectral acceleration ratios equal to or greater than 0.55. When designed using Equation 3.24, joint panels must meet the width-to-thickness requirement of Clause 13.4.1.1(a)(i). The beam-to-column connections shall meet the requirements outlined in the previous paragraph. An alternative beam-to-column connection design is provided by Clause 27.9.6.

The protected zone of a Type D SPSW includes the infill plates, and the regions of the beams and column bases where inelastic deformations and straining are expected. The protected zone of the beam extends from the column face to $0.5d_b$ past the theoretical plastic hinge location.

3.3.2.3 Limited-Ductility Plate Walls

Limited-ductility plate walls, or Type LD plate walls, have similar design requirements to Type D plate walls, except that several design requirements have been relaxed, resulting in a limited amount of energy dissipation and, consequently, lower ductility and overstrength factors of 1.5 and 1.3 respectively. Type LD plate walls are limited to 60 m in height and the beam sections are allowed to be either Class 1 or Class 2 sections. In addition, the beam-to-column connections are allowed to be of the shear type, which allows for other simplifications outlined in Clause 27.10(e) of S16-09.

3.4 AISC 2005

The American Institute of Steel Construction (AISC) refers to lateral load resisting frames with thin steel infill plates as special plate shear walls (SPSW). The term shall be used interchangeably with steel plate shear walls for the remainder of this report. The governing specifications for design forces and design requirements are obtained from the American Society of Civil Engineers (ASCE) specification ASCE 7-05 and AISC specifications 341 and 360, respectively. As AISC 360 and ASCE 7 are general requirements and do not refer directly to the design of SPSWs, they will not be discussed in this report. AISC 341 covers high-seismic design and will be the focus of this section. As the AISC design requirements for SPSWs are similar to the S16-09 requirements, only the significant differences will be outlined.

AISC recognizes several methods for the analysis of SPSWs. These methods include nonlinear push-over analysis, combined linear elastic computer programs and capacity design concept, and indirect capacity design approach, with the latter being adopted from CAN/CSA S16-01 (CSA 2001). Only the indirect capacity design approach will be discussed in the following. AISC also recognizes the use of both the strip model (Thorburn *et al.* 1983) and the orthotropic membrane model for member sizing and force distribution, of which only the former will be reported.

The design criteria for SPSWs are separated into two categories, namely, low seismic design using $R=3$ and high seismic design using $R > 3$ where R is the seismic response modification coefficient. The low seismic design criteria are similar to the criteria used in S16-09 for Type LD SPSW. Beam to column rigid connections are not required, and the design is based on limited tension yielding, which results in nominally ductile performance. For low seismic design, SPSWs do not rely on the inelastic distribution of stress to achieve strength, thus a web plate of sufficient thickness is required such that full infill panel yielding does not occur. The design of the elements can be done assuming a uniform distribution of the average stress in the panel.

Similar to Type D plate walls in S16-09; high seismic SPSWs use capacity design principles for the analysis and design procedure. The infill panel is assumed to yield while the columns and beams, referred to as vertical and horizontal boundary elements

by AISC, must be designed to resist the forces generated by full infill panel yielding. The system is expected to undergo multiple cycles of inelastic straining in addition to several load reversals. Plastic hinging is expected and is to be confined to specific areas. The lateral bracing requirements for high seismic SPSWs are more stringent compared with low seismic bracing. The beam-to-column connections are required to be moment resisting throughout the lateral load resisting structure.

3.4.1 General Design

As SPSWs are only covered in the seismic provisions of AISC 341, the general requirements for a high-seismic design will be outlined. Low seismic design structures have less stringent requirements. Similar to S16-09, AISC 2005 recognizes the use of the strip model for analysis. The angle of inclination α for the strips is determined from Equation 3.16. The aspect ratio, L/h , is limited to $0.8 \leq L/h \leq 2.5$, however, AISC allows the limits to be exceeded in certain cases. When the beams and columns are not identical in a particular storey, the average value of the vertical and horizontal member areas and vertical member inertias can be used to calculate A_b , A_c , and I_c , to determine α . To assist in preliminary design, AISC recommends the following equation, which approximates the infill plate tension field with a single diagonal strut. The area of the strut is calculated as:

$$A = \frac{Lw \sin 2\alpha}{2\Omega_s \sin \theta} \quad 3.25$$

where θ is the angle between the vertical members and the longitudinal axis of the proposed strut, Ω_s is the proposed system overstrength factor of 1.2 for SPSWs (Berman and Bruneau, 2003b), and all other terms as previously defined.

The yield strength is limited to a maximum of 345 MPa for all structural members and special provisions are made for high ductility–low yield steel in the range of 80-230 MPa. Webs with openings are permitted, but are required to have horizontal and vertical members that extend to the full height and width of the infill plate to bound the openings on all sides.

The infill panel design shear strength, ϕV_n , can be determined according to LRFD as:

$$V_n = 0.42F_y w L_{cf} \sin 2\alpha \quad 3.26$$

where F_y is the specified minimum yield strength, and L_{cf} is the clear distance between the vertical members flanges. The resistance factor, ϕ , is taken as 0.9.

The required connection strength for the infill panel to the boundary elements is to be based on the expected yield strength of the infill panel in tension.

In addition to the general strength requirements for beam and column elements, the required strength of the vertical members must be sufficient to resist the expected yield strength of the infill panel in tension, calculated at an angle α . The required strength of the horizontal members is to be the greater of the forces introduced by yielding of the infill plate in tension calculated at the angle α , or the forces from the load combinations, assuming that the infill panel does not carry any gravity loads.

In addition to the general requirements for the shear strength of the beam-to-column connections, AISC 2005 poses several other requirements for SPSWs. The connections are required to resist, in addition to the shear resulting from yielding of the infill plate, the shear generated from the columns and beams end moments, taken as $1.1R_y M_p$ for LRFD design.

High seismic SPSWs have more stringent lateral bracing requirements compared to ordinary moment frames. AISC specifies that the beams be braced at both flanges at the columns and at a minimum spacing of $0.086r_y E / F_y$, where r_y is the radius of gyration with respect to the weak axis, and E is the modulus of elasticity. The strength of the brace is to be greater than $0.02F_y b_b t_b$, where b_b and t_b are the width and thickness of the beam flange respectively.

To ensure that the stiffness of the columns is sufficient to enable the development of the yield strength of the infill panel, the minimum column stiffness is taken as:

$$I_c = 0.00307w \frac{h^4}{L} \quad 3.27$$

where h is the storey height under consideration and all other terms as previously defined. AISC does not present an explicit stiffness requirement for the beams;

however, the SPSW design guide published by AISC (AISC 2007) recommends a minimum stiffness of:

$$I_b \geq 0.003 \frac{(\Delta t_w) L^4}{h} \quad 3.28$$

where Δt_w is the difference in the infill panel thickness bounding the horizontal member in question.

3.4.2 Seismic Design

For seismic design of SPSWs, AISC, in conjunction with ASCE 7, uses coefficients similar to S16-09 to determine the effectiveness of a system to resist lateral loads. The effectiveness is measured in terms of the seismic response modification coefficient, R , a system overstrength factor, Ω_o , and a deflection amplification factor, C_d . Two parameters, C_r and x , are also used to determine the approximate fundamental period. The values of these coefficients are determined based on the type of SPSW construction.

For areas that require low seismic design, AISC specifies a system similar to S16-09 type LD SPSWs, with $R=3$. This system is not specifically covered although many of the high seismic design requirements described in AISC 341 also apply to this system. For areas of high seismic activity requiring $R > 3$, AISC describes a SPSW system similar to type D plate walls in S16-09. The design coefficients and factors for this type of SPSW are $R=7$, $\Omega_o=2$, and $C_d=6$. Height restrictions are imposed based on location, soil conditions, and anticipated occupancy. AISC allows for an increase in the design coefficients and factors provided that the SPSW is constructed using a moment frame designed to resist at least 25% of the prescribed seismic forces. In this case, the design coefficients and factors are increased to $R=8$, $\Omega_o=2.5$, and $C_d=6.5$. In addition, all height restrictions imposed on general high seismic SPSWs are removed by incorporating a special moment frame.

For high seismic design locations, the expected shear strength at the base of the wall according to indirect capacity design is calculated as:

$$V = 0.5R_y F_y w L \sin 2\alpha \quad 3.29$$

with the terms as previously defined. Using the principles of indirect capacity design (CSA 2002), the loads in the columns can be determined from the gravity loads combined with the seismic loads using the amplification factor:

$$B = \frac{V}{V_u} \quad 3.30$$

where V_u is the factored seismic base shear.

The factor B need not be greater than R when calculating the loads in the columns. The design axial forces in the columns can be determined from the overturning moment for several locations as follows:

1. Using the factored seismic base shear, the moment at the base is calculated as BM_u , where M_u is the factored seismic overturning moment at the base corresponding to V_u ;
2. The base moment, BM_u , extends to a height H above the base or a minimum of two stories from base; and
3. The moment decreases linearly above H to the lesser of: B multiplied by the overturning moment one storey below the top of the wall or R multiplied by the current storey factored seismic overturning moment corresponding to the force V_u .

Bending moments introduced from the development of the tension field are to be included and multiplied by the amplification factor B .

Details of the AISC design procedures for low- and high-seismic SPSWs can be found in the AISC steel design guide for SPSWs (AISC Design Guide 20-2007).

4. ANALYSIS

4.1 Introduction

Lateral loads on buildings above ground include wind loads and seismic loads, which are defined in NBCC (2005). The following sections describe the lateral loads that must be included in the design. The analysis model and methods implemented using structural analysis software commonly available to practicing engineers are also described. The design of the structural members to resist the force effects outlined in this chapter is presented in Chapter 5.

4.2 Lateral Loading

Several principal load combinations are described in NBCC (2005) and are defined as follows:

$1.4D$	4.1
$(1.25D \text{ or } 0.9D)+1.5L$	4.2
$(1.25D \text{ or } 0.9D)+1.5S$	4.3
$(1.25D \text{ or } 0.9D)+1.5W$	4.4
$1.0D+1.0E$	4.5

where D is the dead load, L is the live load due to use and occupancy, S is the snow load, W is the wind load, and E is the earthquake load. These combinations are to be used with the corresponding companion loads outlined in NBCC. As the focus of this document is the design of steel plate walls, the design example will only deal with the lateral loads as defined by the NBCC. Wind loading is calculated according to the NBCC guidelines with the equations presented in Section 3.2.1 and the calculations are illustrated in Chapter 5. These loads are applied as static forces to the structure and in the case of a statically indeterminate lateral load resisting system (four or more lateral load resisting components¹) their distribution to the lateral load resisting system is dependent on the stiffness of the individual elements of the lateral load resisting system. Once the design forces are established, the elements can be sized using an

¹ For the design example presented here, two steel plate walls are used in each direction. The system is therefore statically indeterminate.

iterative procedure to determine the deflections. For earthquake loading, the NBCC default analysis method is a dynamic analysis, with a static analysis option available for structures that meet the criteria presented in Chapter 3.

The use of capacity design principles is required by CSA S16-09 for the seismic design of SPSWs. Capacity design involves the use of local “fuses” designed to dissipate energy while other structural and non-structural components must be designed to remain elastic. The nonlinear behaviour of SPSWs has been well documented in previous research (Caccese and Elgaaly, 1993; Driver *et al.*, 1997; Lubell *et al.*, 1997; Shishkin *et al.*, 2005; Berman and Bruneau, 2008; Bhowmick *et al.*, 2009), and it has been shown that a SPSW typically exhibits high initial stiffness followed by yielding of the infill plates, which act as the ductile “fuse” for the system to dissipate energy. Upon further loading, properly designed frames develop plastic hinges at the beam ends and column bases. Analysis methods traditionally use pushover analysis or complex FEA models to predict the hysteresis curve envelope or cyclic and dynamic behaviour. While the pushover analysis method has been able to predict reliably the hysteresis envelope (Driver *et al.* 1997, Shishkin *et al.* 2005, Bhowmick *et al.* 2009) this type of monotonic behaviour depicted is not what is seen during earthquake loading. It has been shown that pushover analysis may not capture certain behaviours exhibited by a structure from dynamic loading which a time history or dynamic analysis would capture (Krawinkler and Seneviratna, 1997; Fragiaco *et al.*, 2006). Furthermore, since cyclic material properties can be significantly different from the better known monotonic material properties (Bhowmick *et al.*, 2009; Seal *et al.* 2007), the fact that a pushover, monotonic, analysis model is able to predict the envelope of the cyclic behaviour does not guarantee that the model is suitable for cyclic analysis. In addition, the pushover analysis, while an approved method for analysis by AISC (AISC 2006), is not an approved analysis method by the NBCC. The default analysis method required by the NBCC is a dynamic analysis.

The following sections will use a specific commercially available software package to perform an analysis of a SPSW as outlined by the NBCC; however, the principles and reasoning used with the software used for the design example presented in this document apply to any structural analysis software. For the structural modeling, this

chapter describes the model required for seismic analysis of SPSWs; however, the same model can be used for wind loading and other loading conditions. The two methods of analysis for seismic design outlined by NBCC are an equivalent static force procedure and a dynamic analysis, with the latter being the preferred method of analysis. The dynamic analysis will be implemented using a nonlinear analysis due to the nature of the model discussed later. The model will also be used with the equivalent static force procedure as the dimensions of the sample building satisfy the requirements set in NBCC for the simplified analysis method. The results of both analyses will be compared.

4.3 Description of Software and Analysis Method

While most structural analysis programs can perform static or dynamic linear elastic analysis, the analysis of SPSWs under dynamic seismic loading using the strip model requires various additional capabilities. The capabilities specifically required for seismic loading in this study include nonlinear material and geometric analysis, time history analysis, and a tension only element to model tension strips under cyclic reversed loading. In addition, the software should be readily available to design engineers. SAP 2000® V14.0.0 (CSI 2009) was selected as it satisfies all these criteria. However, the methods outlined in this chapter can be implemented in any type of commercial package with similar capabilities.

Although several models have been proposed for SPSWs, the strip model (Thorburn *et al.* 1983) is recommended in CSA-S16-09 and it will be used in the following. In the strip model, the infill plate is discretized into a series of equally spaced tension only elements anchored to the beams and columns bounding the individual infill plates. The tension elements are pinned and inclined at an angle α to represent the angle of inclination of the tension field. A nonlinear analysis is used to account for yielding of the tension strips and the flexural members, their strength and stiffness changes, and the associated period lengthening that may occur because of the softening that takes place when the strips yield. Additionally, a nonlinear analysis provides a good estimate of the maximum ductility demand in members, the deflections experienced, and can account for system overstrength and the reduction in elastic forces due to inelasticity, thus removing the requirements for the results to be modified by $R_d R_o$ (Saatcioglu and Humar, 2002). Another type of nonlinear behaviour option available in SAP2000® is the ability to insert

and define plastic hinging in the beams and columns which is a requirement of the capacity design approach.

4.3.1 Direct Integration Analysis

While several methods exist for dynamic analysis, due to the nonlinearity of the problem, plastic hinging in the frame elements and compression limits for the tension strips, SAP2000® uses a direct integration analysis with time history records for ground motions. Direct integration techniques attempt to solve the following dynamic equilibrium equation (Chopra 1995):

$$Ku(t) + C\dot{u}(t) + M\ddot{u}(t) = F(t) \quad 4.6$$

where K is the stiffness matrix; C is the damping matrix; M is the diagonal mass matrix; u , \dot{u} , and \ddot{u} are the displacements, velocities and accelerations of the structure, respectively; and $F(t)$ is the time-dependent applied load or acceleration. The structure begins initially at rest, and using a time history record, either loads, displacements or accelerations are applied at small equal time increments, Δt . For each time increment, Δt , the dynamic equilibrium equations are to be satisfied within a specified tolerance. Since direct integration results are sensitive to the time step size, increasingly smaller step sizes are used until convergence is reached.

Several methods to solve the equations of dynamic equilibrium are available in SAP2000®, including Newmark's, Wilson's, Hilber-Hughes-Taylor's and Collocation methods. The method selected for this analysis was the Hilber-Hughes-Taylor method as it is a method used in many current software and is unconditionally stable. The Hilber-Hughes-Taylor method uses a modified version of the Newmark method to solve the following equation of motion (Chopra 1995):

$$M\ddot{u}_t + (1 + \alpha)C\dot{u}_t + (1 + \alpha)Ku_t = (1 + \alpha)F_t - \alpha F_t + \alpha C\dot{u}_{t-\Delta t} + \alpha Ku_{t-\Delta t} \quad 4.7$$

where α is a constant that takes a value between 0 and -1/3. When $\alpha = 0$ the Hilber-Hughes-Taylor method reduces to the Newmark method. With α set close to zero, the solution has the best accuracy. However, excessive higher mode frequencies may be introduced as the value of α approaches zero. As α approaches -1/3, nonlinear

solutions converge more rapidly at the expense of higher modes of vibration being suppressed from the solution. The value of α used for the direct integration scheme was -1/3.

The direct integration method uses a full damping matrix constructed using a form of Rayleigh damping (Chopra 1995) defined as:

$$[C] = a_0[M] + a_1[K] \quad 4.8$$

where a_0 and a_1 are proportionally scaled coefficients for the mass and stiffness matrices, respectively. These coefficients can either be specified directly, or computed by specifying two different periods obtained by a modal analysis of the structure. The stiffness coefficient, a_1 , is linearly proportional to the frequency and is related to the deformations of the structure. As the coefficient increases, high frequency components may be excessively damped out. The mass coefficient, a_0 , is linearly proportional to the period of the structure and related to the motion of the structure. As the coefficient increases, the long period components may be excessively damped.

SAP2000 uses a method of least squares fit to determine the two coefficients based on frequency values submitted by the user and determined from a modal analysis. The damping coefficients are calculated using the following equation:

$$\xi_n = \frac{a_0}{2\omega_n} + \frac{a_1\omega_n}{2} \quad 4.9$$

where ξ is the damping desired for the structure; and ω_n is the angular frequency of the structure. The angular frequency is defined as:

$$\omega_n = 2\pi f_n \quad 4.10$$

where f_n is the frequency of the n^{th} mode. It can be reasonably assumed (Chopra 1995) that the damping ratio, ξ_i and ξ_j , between the i^{th} and j^{th} modes, respectively, are the same. From this assumption, we can solve for a_0 and a_1 using Equation 4.9:

$$a_0 = \xi \frac{2\omega_i\omega_j}{\omega_i + \omega_j} \quad 4.11$$

$$a_1 = \xi \frac{2}{\omega_i + \omega_j} \quad 4.12$$

The determination of the coefficients with equation 4.9 is illustrated in Figure 4.1.

4.3.2 Time History Records

A time history analysis requires earthquake time history records as input to generate the required ground motions. NBCC allows the use of both recorded data and synthetic records for time history analysis. However, due to the uncertainty and variability of earthquakes, it is not possible to elicit all possible building responses from a single record. Thus the NBCC suggests the use of multiple ground motion time histories when performing seismic analyses. While the NBCC does not specify how many ground motion histories should be used, NEHRP (2000) guidelines suggest a minimum of three seismic records, while seven is the recommended number for a time history analysis. The NBCC indicates that the records that are used must be scaled to match the local design spectrum (Saatcioglu and Humar, 2002) such that the records response spectrum meets or exceeds the spectrum of the desired location throughout the period range of interest. SAP2000® and other analysis programs allow for the input and scaling of earthquake records in several formats, with tabular ground accelerations being the most common. The spectrum compatible records, in addition to the original records, used in this report are identical to the records used by Bhowmick *et al.* (2009) and can be seen in Figure 4.2 and Figure 4.3. These records were made to be spectrum compatible using the SYNTH program (Naumoski 2001) for buildings located in Vancouver but can be used to modify existing records to match the conditions for any location.

4.3.3 Geometric and Material Nonlinearities

According to capacity design principles, SPSWs are designed with specific “fuses” capable of dissipating the energy from seismic events while the remaining elements of the structure remain elastic. These so-called “fuses” are designated as protected zones in S16-09. The protected zones in a SPSW include the infill plate(s), the beam ends and column bases. The infill plates are modeled as tension-only strips while the beams and

columns are modeled with beams elements. To incorporate the inelastic behaviour of these elements into the model, a definition of the material nonlinearities is required. Material nonlinearities are introduced into these elements by inserting axial, moment, and moment-axial force interaction plastic hinges in the model elements. SAP2000® allows the user to either define plastic hinge behaviour or to use pre-defined hinge behaviour. The pre-defined hinge properties provided in SAP2000® are the FEMA 356 (FEMA 2000) and Caltrans definitions. The hinges are inserted at discrete points along the element.

Previous research (Shishkin *et al.*, 2005) has shown that increasing the complexity of the hinge definition based on material testing data does not have a significant effect on the overall behaviour of the model, thus the provided hinge definitions are adequate for modeling purposes while remaining simple for users to implement. The selected hinge definition for this model is the FEMA 356 hinge. The FEMA 356 hinge is deformation controlled for axial hinge types and rotation controlled for moment and moment-axial interaction hinges. The user is allowed to change various parameters upon defining the hinge including labelling the element as primary or secondary member based on acceptable damage, as well as including a load deterioration model beyond a certain deformation or rotation. The load deterioration can vary from a sudden drop of capacity to zero, a linear deterioration, or the continuation of the current load capacity.

The FEMA 356 hinge definitions in SAP2000® include reference points *A* through *E* and “performance range” indicators (*IO*, *LS*, *CP*) as shown in Figure 4.4. The reference points indicate the level of deformation or rotation in the hinge and can be modified by the user. The indicators are assigned to a discrete damaged state chosen from the infinite damaged states that a building may experience during a severe earthquake (FEMA 2000). Point *A* represents the origin while point *B* represents the yield point of the element. Point *C* represents the ultimate capacity of the hinge, i.e. the onset of degradation. The slope of the degradation line, *CD*, is defined by the position of point *D* and point *E* defines the length of the residual strength plateau. Beyond point *E* the user may specify the load to drop to zero, be maintained, or implement a linear deterioration to zero. The performance ranges of the hinges are defined as immediate occupancy

structural performance (*IO*), life safety structural performance (*LS*) and collapse prevention structural performance (*CP*).

The performance ranges, *IO*, *LS*, and *CP*, have different criteria and locations along the hinge definition graph depending on whether an element is defined using a primary or secondary hinge type, and are an attempt to determine the level of performance and safety of the structure following a seismic event. The acceptance criteria for these performance values can be found in Table 5-6 of FEMA 356. The locations of these points may be changed and do not have an effect on the behaviour of the analysis model. The immediate occupancy performance level for both primary and secondary members indicate minor local yielding or buckling may have occurred but fractures are not expected. The life safety performance level indicates that plastic hinges have formed with severe distortion, and with isolated moment connection fractures for primary members and many fractures for secondary members. Both primary and secondary member shear connections remain intact. Collapse prevention performance level for both primary and secondary elements indicate excessive distortion of beams and columns as well as multiple fractures at moment connections, however, shear connections remain intact. Further details can be found in the pre-standard and commentary for the seismic rehabilitation of buildings provided by FEMA (FEMA 2000).

The axial hinge selected for the strips uses two scale factors to determine the reference points and performance range indicators. These scale factors are dependent on the properties of the element selected (in this case the tension strip) and are as follows:

1. Load scale factor, $L_{SF} = 1.1A_s F_y$
2. Deformation scale factor, $d_{SF} = \frac{L_{SF}L}{A_s E}$

where A_s is the area of the strip; and L is the length of the strip. The hinge definition and performance range indicators for the axial hinge of a strip can be seen in Figure 4.5. The load and deformation values for the reference points *A* through *E* are determined using the normalized load and deformation. The applied load is normalized using the load scale factor, L_{SF} , of the element and the element deformation is normalized using the deformation scale factor, d_{SF} . The numerical values for the hinge path are

presented in Table 4.1. The values used to define the axial hinge are the default values according to FEMA (2000) and can be adjusted by the user. The default values for the performance range indicators, IO , LS , and CP , are specific deformations normalized by the deformation scale factor and have values of 0.25, 7, and 9, respectively.

In the case of the axial moment interaction hinge, the reference points and performance range indicators are determined using the interaction between the applied moment and load, and a scale factor. The interaction and scale factors are determined as follows:

1. Axial force – moment interaction, $M_{rpb} = 1.18Z_x F_y \left(1 - \frac{P}{A_c F_y} \right) \leq Z_x F_y$
2. Rotation scale factor, $r_{SF} = \frac{Z_x F_y L}{6EI_c} \left(1 - \frac{P}{A_g F_y} \right)$

where P is the axial force; L is the length of the element; and Z_x is the plastic section modulus. The axial force-moment interaction for a column is presented in Figure 4.6. The interaction equation is consistent with the cross-section strength interaction equation used in CSA-S16-09 for bending of Class 1 and Class 2 I-shape sections about the strong axis (Kulak and Grondin, 2009). Class 3 sections are not allowed for Type D SPSWs and Type LD SPSWs.

The hinge definition and performance range indicators for the axial force-moment interaction hinge can be seen in Figure 4.7. The ordinate and abscissa for the reference points A through E are determined using the normalized moment and rotation, respectively. The applied moment is normalized using the reduced plastic moment obtained from the interaction equation, which is valid for Class 1 and Class 2 sections, and the rotation is normalized using the rotation scale factor. The numerical values are presented in Table 4.2. These values are the default values according to FEMA (2000) and can be adjusted by the user. The default values for the performance range indicators, IO , LS , and CP , and are rotations normalized by the rotation scale factor and have values of 0.20, 4.30, and 5.90, respectively.

Alternatively, the user may define a simple perfectly plastic hinge definition which has been shown to give accurate results (Shishkin *et al.* 2005).

In addition to material nonlinearities, SAP2000 has the capability to include geometric nonlinearities. The NBCC covers $P-\Delta$ effects in the non-mandatory commentary and suggests the method by Paulay and Priestly (1992), which is based on a stability approach. In this method, the $P-\Delta$ effects are accounted for by amplifying the storey shear and overturning moment at each level. The design storey shear suggested by the NBCC commentary is defined as:

$$V_x^* = V_x (1 + \theta_x) \quad 4.13$$

where the stability factor, θ_x , is defined as:

$$\theta_x = \frac{P_x \Delta_{mx}}{R_o V_x h_{sx}} \quad 4.14$$

where P_x is the total gravity load on the structure above and including the level x under consideration, Δ_{mx} is the maximum inelastic storey drift of the storey below the level x under consideration, and h_{sx} is the storey height immediately below level x . If the stability factor is less than 0.10, the NBCC suggests that the $P-\Delta$ effects can be neglected. However, if θ_x is calculated to be above 0.40, the NBCC recommends that the structure be stiffened. Two methods of $P-\Delta$ analysis are discussed in S16-09, as well as the notional load which accounts for initial out of plumb of the structure and inelastic behaviour. The preferred method to account for $P-\Delta$ effects by S16-09 is a second order analysis using structural analysis software. The second method is to multiply the first order moments obtained from the lateral loads and natural sway of the structure by the amplification factor, U_2 , calculated as:

$$U_2 = 1 + \left(\frac{\sum C_f R_d \Delta_f}{\sum V_f h} \right) \quad 4.15$$

where C_f is the factored column axial load, Δ_f is the relative first order storey displacement from translational loads, V_f is the factored column shear and h is the storey height.

Recent work by Bhowmick *et al.* (2009) indicated that for structures that met the interstorey drift limits set by the NBCC, the $P-\Delta$ effects were small and did not

significantly contribute to the behaviour of the SPSWs. In the FEA study, the researchers analyzed a 15-storey SPSW and upon inclusion of $P-\Delta$ effects, the top storey displacement and flexural demand at the base of the structure increased by 3.7% and 1.7%, respectively.

4.4 Model Generation and Analysis

The building to be modeled is a hypothetical office building with a height of 57.0 m shown in Figure 4.8, which is adapted from Bhowmick *et al.* (2009). This building was selected because of the opportunity to compare the results of the analysis presented in this report with a full nonlinear analysis of the same structure modeled with three dimensional shell elements conducted by Bhowmick *et al.* (2009). The length and height of the SPSWs are 7.6 m and 3.8 m, respectively, resulting in a L/h ratio of 2.0. The hypothetical building is located in Vancouver, Canada, and has an importance factor of 1.0. The lateral load resisting system consists of two SPSWs in each direction and has a 2014 m² rectangular footprint with no structural irregularities.

The torsional effects are neglected in this study so that the response of the building can be studied by analysing a single SPSW. This was done so that this study could focus on the design of SPSWs only. Clause 4.1.8.11 of NBCC (2005) provides guidance to account for torsional effects under seismic loads. For a building such as the one selected here where the centre of mass and the shear centre coincide, NBCC requires that the effect of accidental torsion (due to unavoidable eccentricity of the centre of mass with respect to the shear centre and torsional movement of the ground) be accounted for in the design. For torsionally non-sensitive structures ($B \leq 1.7$ where B is defined in Clause 4.1.8.11(9) of NBCC) NBCC offers three options to account for the torsional effect:

- 1) The torsion is taken as the sum of the natural torsion and accidental torsion as $F_x (e_x \pm 0.1D_{nx})$ where F_x is the static seismic force at level x , e_x is the distance between the centre of mass and the shear centre and $0.1D_{nx}$, 10% of the plane dimension of the building perpendicular to the direction of the earthquake, which accounts for both accidental and natural torsion effects. The plus or minus sign deals with the stiff side of the building (side of the shear centre where the centre of mass is located) and the soft side of the building which is located on

the opposite side of the shear centre. For the building selected for this design example, e_x is zero at all levels and the torsion can therefore be taken as $(F_x \times (\pm 0.1D_{nx}))$. The lateral force, including the torsional effect, can be calculated using a rigid diaphragm assumption and accounting for the stiffness of all lateral load resisting elements in the building.

- 2) The second approach consists of conducting a dynamic analysis to determine the lateral forces, F_x , on a SPSW and incorporate the torsional effect in the manner described in option 1.
- 3) The third approach consists of conducting a three-dimensional analysis of the building with the floor masses shifted by $0.05D_{nx}$ from the theoretical centre of mass.

For torsionally sensitive buildings ($B > 1.7$) NBCC requires that a dynamic analysis be used and the torsional effects can be added as $F_x \times 0.1D_{nx}$ where F_x for the torsion component can be taken as either the equivalent static force or the value obtained from the dynamic analysis. It is noted, however, that for buildings for which the equivalent static load method of design is permitted, the building is torsionally stiff and the condition $B \leq 1.7$ is satisfied (Humar *et al.* 2003).

The building dead loads were calculated in accordance with the NBCC guidelines as presented in Chapter 5. The storey self weight was multiplied by 0.25 (due to two SPSWs in each direction and two columns in each SPSW) and imposed directly on each of the columns in the SPSW as lumped masses in order to perform a modal and time history analysis. The lumped masses act in the horizontal direction (for horizontal earthquake accelerations) and do not contribute to the gravity loads. The local dead loads were applied directly to the beam and column elements according to their tributary areas.

The 15-storey frame was modeled using beam elements for both the beams and columns to provide rigid beam-to-column connections and the columns were fixed at their base. The material selected for the beam elements and the tension strips from SAP2000® was ASTM A992 grade 50 steel which has material properties equivalent to CSA-G40.21 350W steel.

In order to model the infill panel, the steel plate was represented by a series of discrete pin ended tension only strips according to the strip model. Due to the load reversals initiated by the dynamic loading, the original strip model was modified to use bi-directional strips. This has been used successfully in earlier research to analyze the SPSW behaviour during seismic events (Lubell *et al.* 1997, Kulak *et al.* 2001). Once the tension field angle α is selected (discussed below), the preliminary design of individual strips can proceed. The strip design and spacing is based on the thickness of the infill plate, as well as the bay height and width. The spacing of the strip can be calculated as:

$$\Delta_x = \frac{1}{n} [L + h \sin \alpha] \quad 4.16$$

where n is the number of strips in a single bay. Using the calculated strip spacing, the area of the individual strip can be calculated as:

$$A_s = \Delta_x w \cos \alpha \quad 4.17$$

with all the terms as previously defined. Once the dimensions of the strips are determined, a section is defined using the required cross-sectional properties and assigned to behave as a tension only member.

During the modeling procedure, several simplification methods were used for the strip arrangement to allow for multi-storey buildings to be generated quickly and easily. The cross hatching method suggested by Timler *et al.* (1998) was used, which utilizes common beam nodes for strip elements of adjacent storeys, thus reducing the number of nodes as well as simplifying the geometry of the model. Additionally, a single tension field angle α was used for the entire SPSW as S16-09 allows for the use of an averaged single angle of inclination for analysis purposes. Furthermore, research has shown that the behaviour of the SPSW model is relatively insensitive to strip angle changes between 38° and 50°. Selecting 45° as the strip angle further reduces the geometric complexity of the model while remaining in the allowable range provided by S16-09. Finally, as the storey heights remained the same throughout the structure, the strip spacing was adjusted, as well as the corresponding strip area, such that the upper and lower strip nodes of a single storey were co-incident. This allowed an individual floor to be scaled to the desired height of the structure by replication.

With these simplifications, the first storey of a SPSW was modeled and then replicated as shown in Figure 4.9 until the desired height was reached. Once the structure had been created, the plastic hinges were inserted as previously described. Axial hinges were inserted at the midpoint of all tension strips, moment hinges were inserted at both beam ends and axial-moment interaction hinges were inserted at each end of individual storey columns. Once the model was constructed, a modal analysis using Ritz vectors was performed to determine the natural frequencies of the structure. The first two modal frequencies were used to generate the Rayleigh damping matrix for dynamic analysis as explained in Section 4.3.1. However, four modes were generated to compare with the 15-storey results from Bhowmick *et al.* (2009).

The loading phase of the analyses consisted of the dynamic analysis, which is the favoured method of analysis by the NBCC. A static analysis as outlined by the NBCC in the equivalent static force procedure was also conducted. The differences in the results are discussed in Chapter 6.

Nonlinear time history analyses were conducted for four different spectrum compatible time history records. The results from the modal analysis were used to set the Rayleigh damping matrix for the structure and the time step was decreased until the analysis results converged. In addition to the base moments and shears, the element forces were obtained from each of the four time histories. SAP2000® records the element forces from the analysis for each time step of the time history analysis. The records are exported to a spreadsheet from which the peak forces are determined for the individual members. The peak forces are then compared to the forces determined using the capacity design equations.

The static analysis follows the NBCC requirements for determining seismic loading using equivalent static forces. The static forces required for this analysis are calculated in Chapter 5. The forces are applied to the SPSW model at each of the story floors as point loads and a nonlinear static analysis is conducted to determine the base moment and shear, and beam and column axial forces and moments. The static analysis is used to verify that the member sizes determined from the capacity design are adequate to develop the full yield capacity of the infill plates. The nonlinear static analysis is also used to obtain deflections and interstorey drift values.

The results of the static and dynamic analyses, as well as comparisons with the shell element model of the same structure by Bhowmick *et al.* (2009) are presented in Chapter 6.

Table 4.1 - Reference Point Coordinates for Axial Hinge

Reference Point	Load/ L_{SF}	Deformation/ d_{SF}
A	0.00	0.0
B	1.00	0.0
C	1.33	11.0
D	0.80	11.0
E	0.80	14.0

Table 4.2 - Reference Point Coordinates for Moment Axial Interaction Hinge

Reference Point	Moment/Yield Moment	Rotation/SF
A	0.00	0.00
B	1.00	0.00
C	1.22	5.92
D	0.20	5.92
E	0.20	9.15

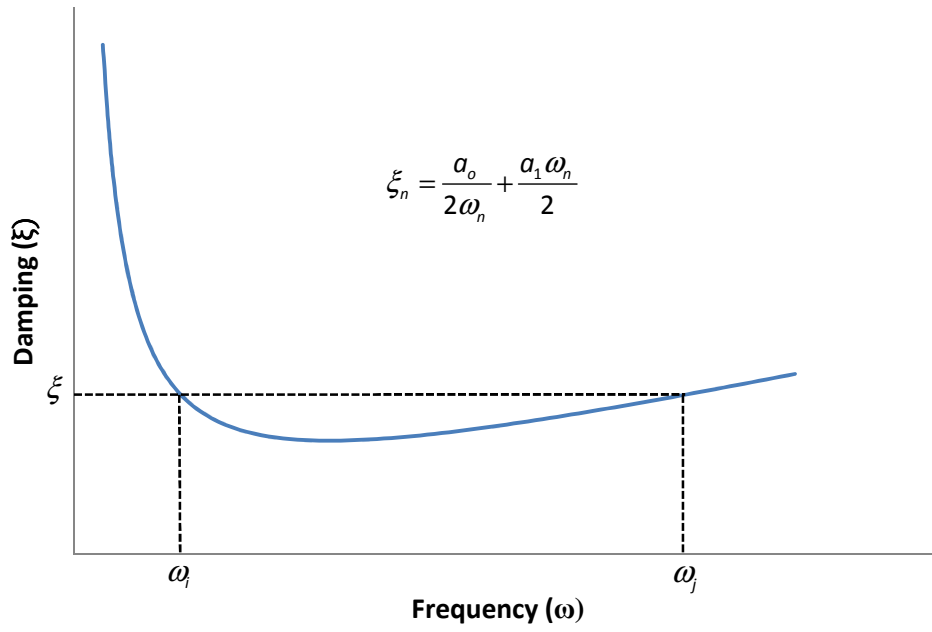


Figure 4.1 - Damping Ratio as a Function of Frequency

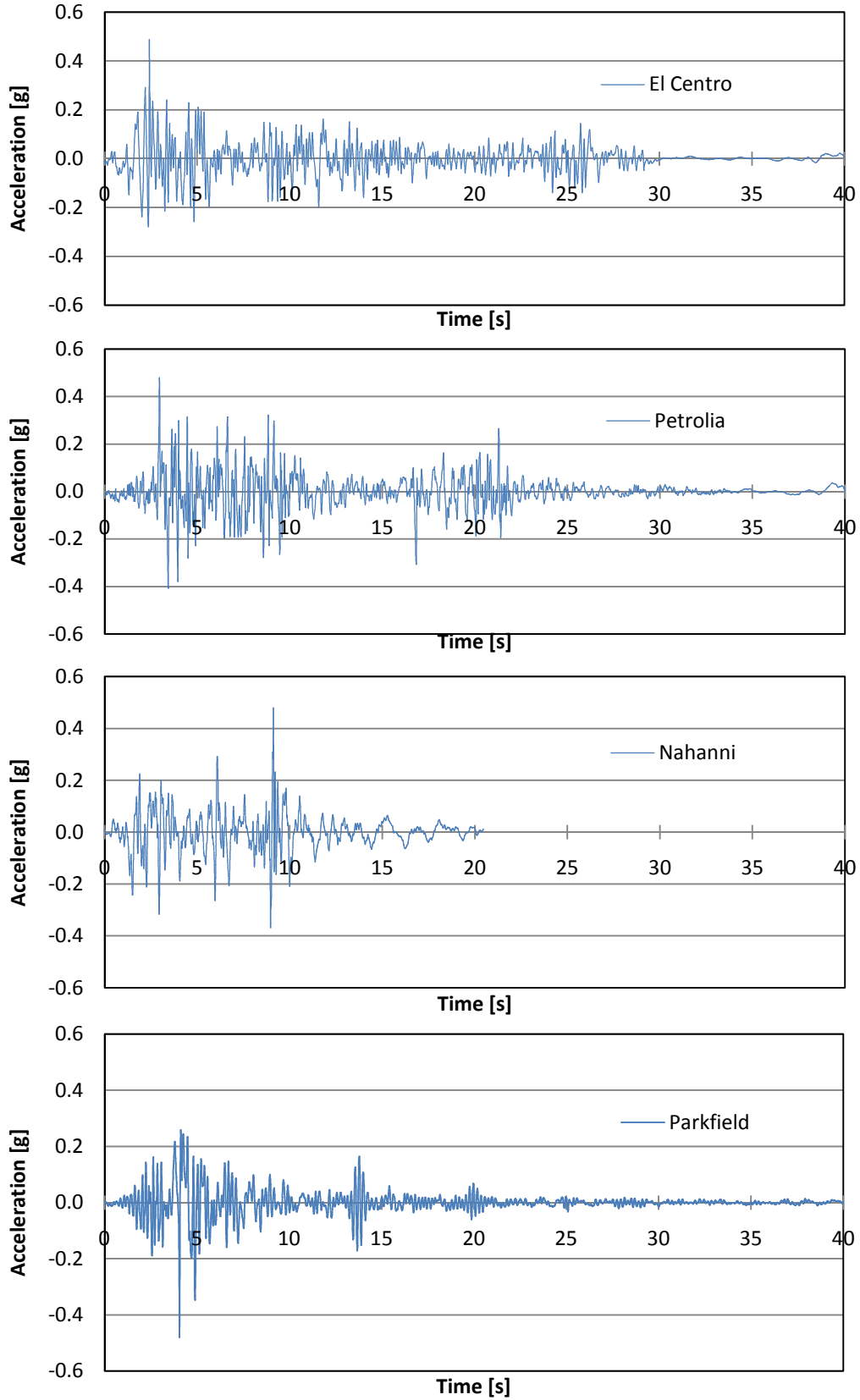


Figure 4.2 - Vancouver Spectrum Compatible Ground Motion Histories

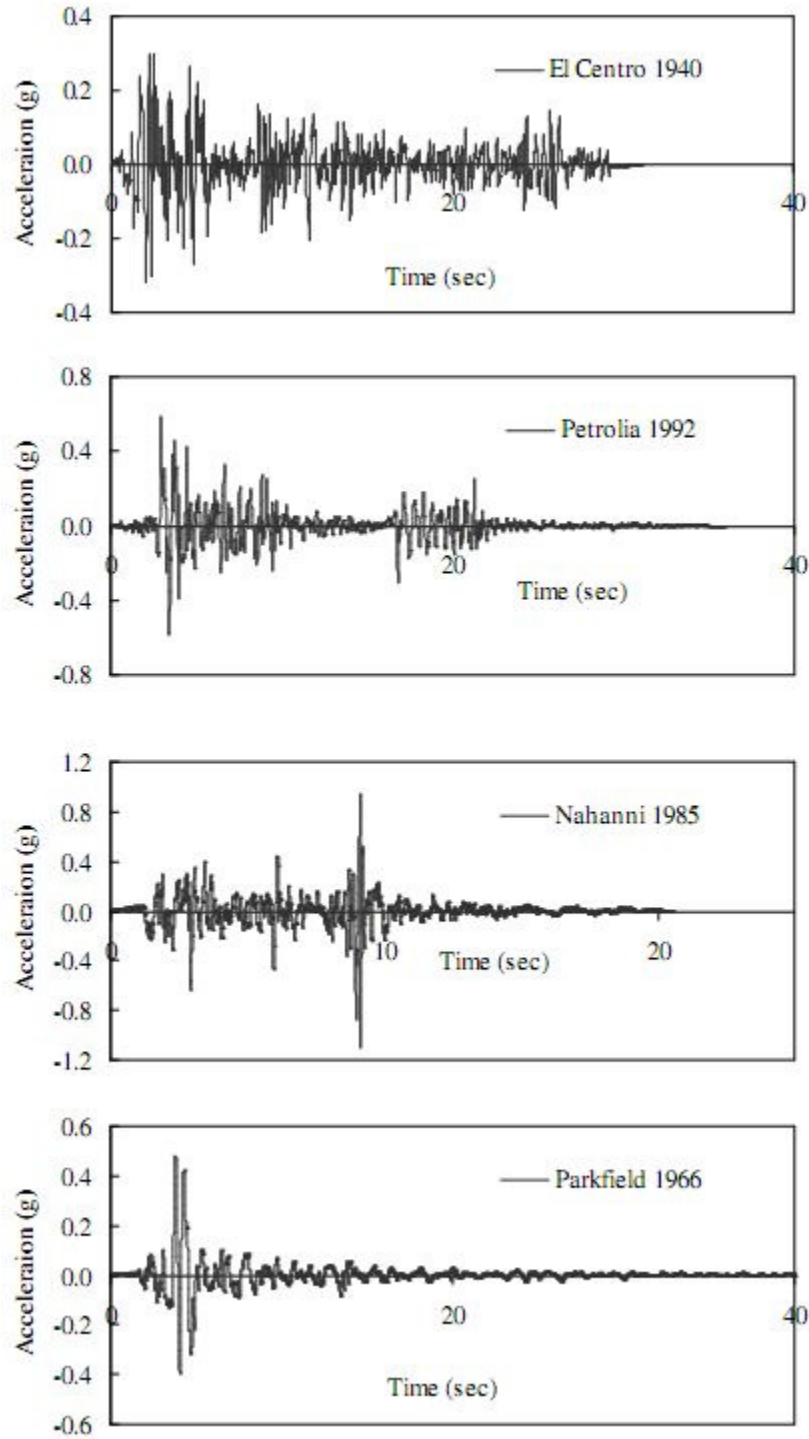


Figure 4.3 - Original Ground Motion Histories (Bhowmick 2009)

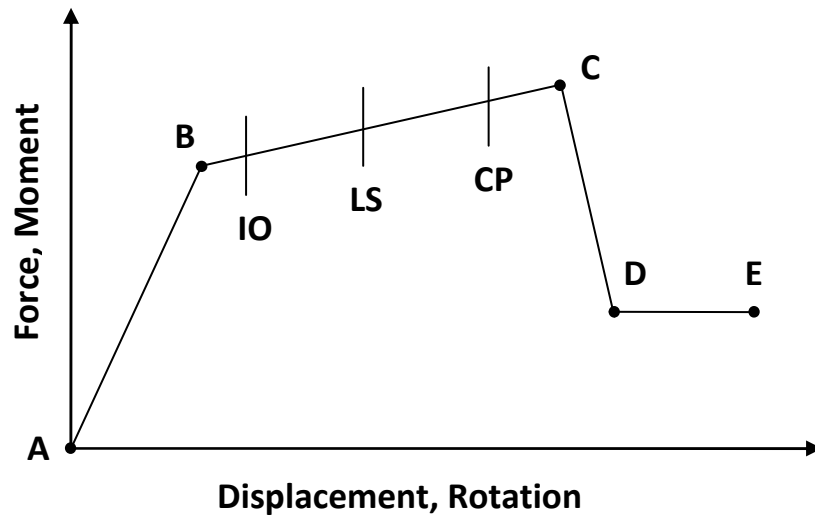


Figure 4.4 - FEMA Axial Hinge definition (FEMA 356, 2000)

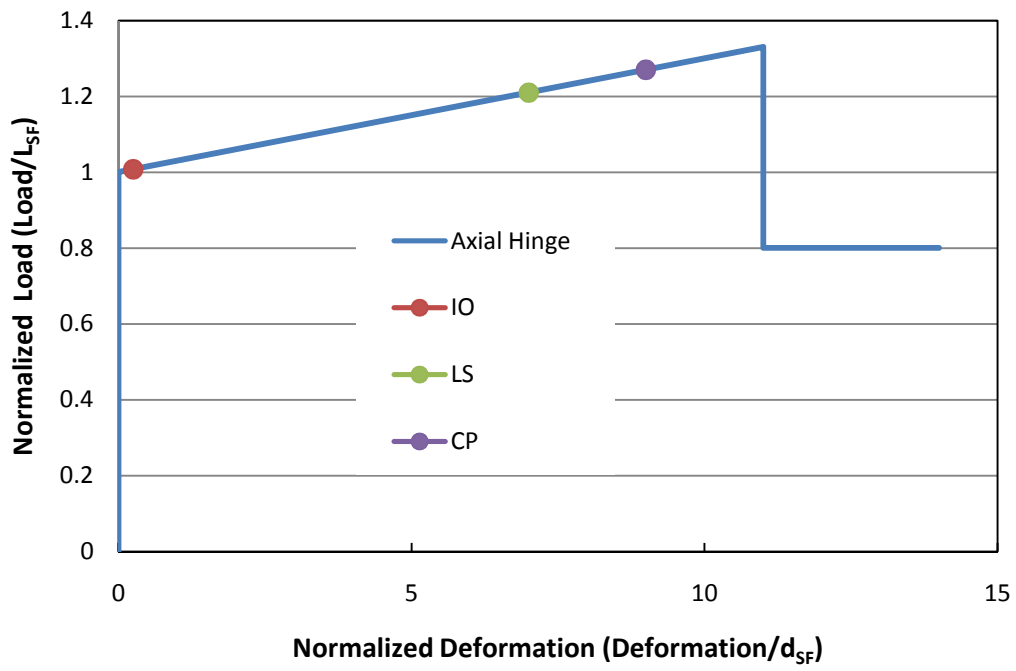


Figure 4.5 - Axial Hinge Definition

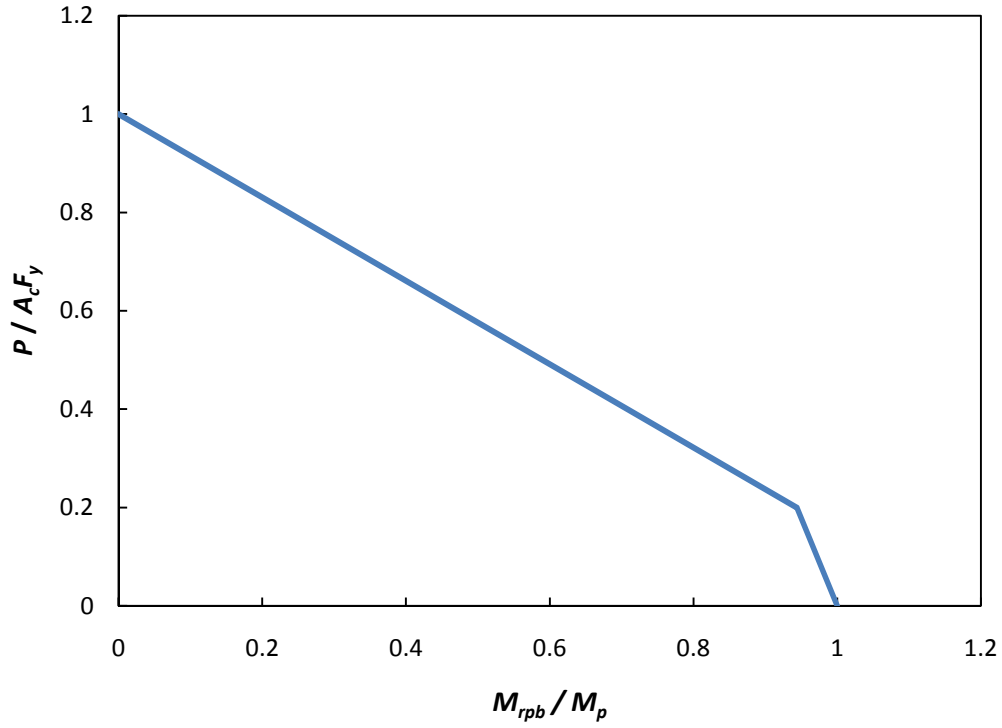


Figure 4.6 – Axial-Moment Interaction

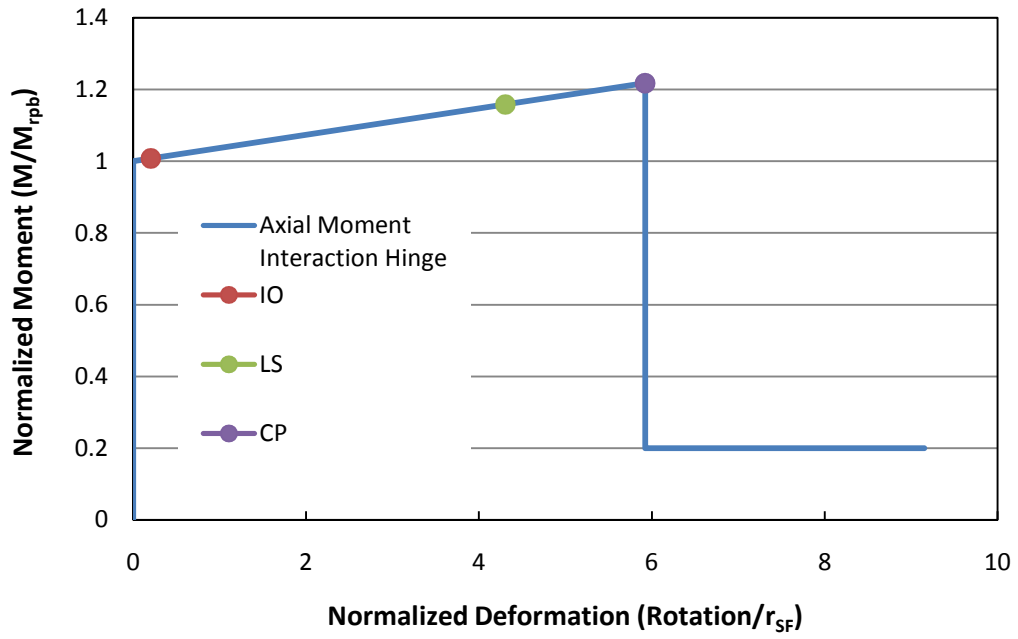


Figure 4.7 – Axial-Moment Interaction Hinge Definition

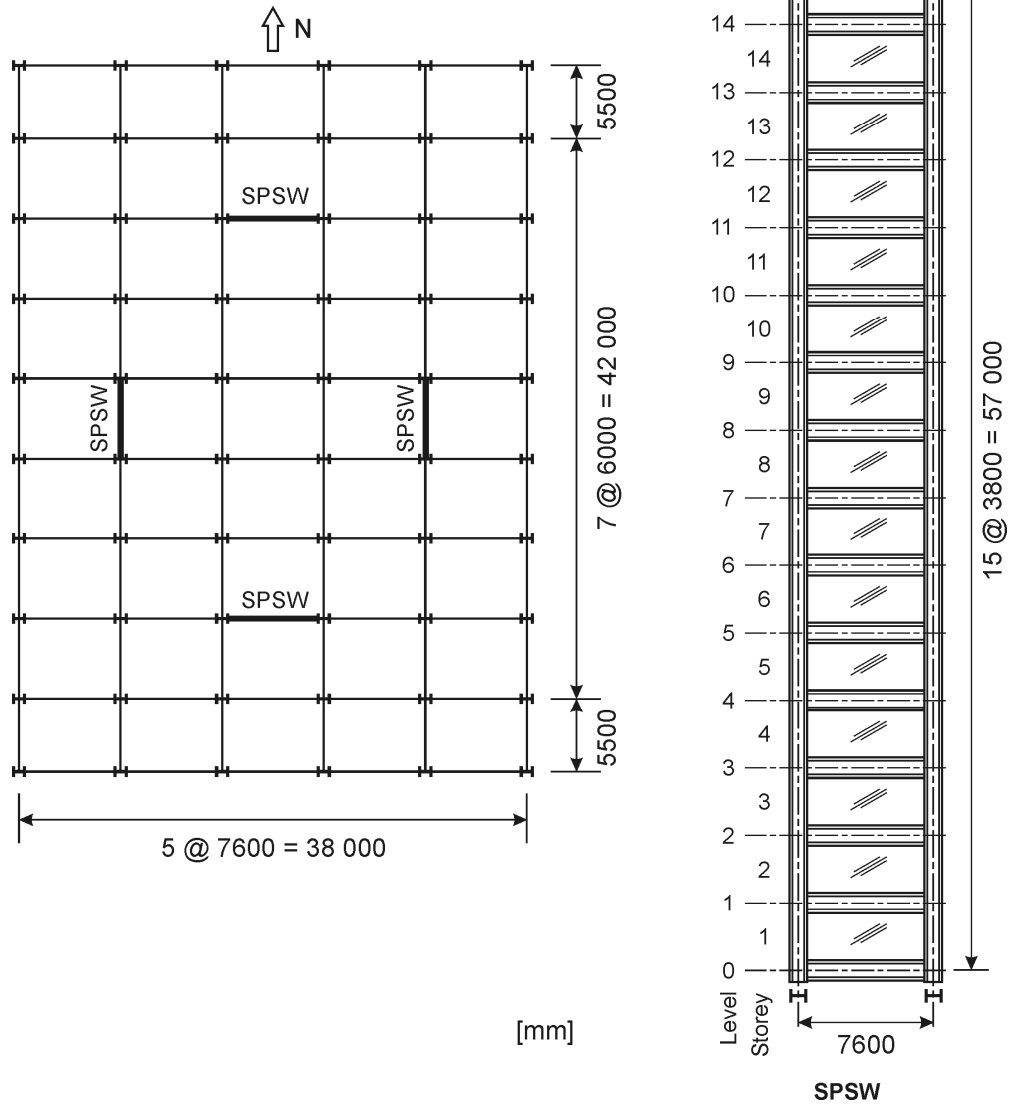


Figure 4.8 - Hypothetical Office Building Adapted from Bhowmick et al. (2009)

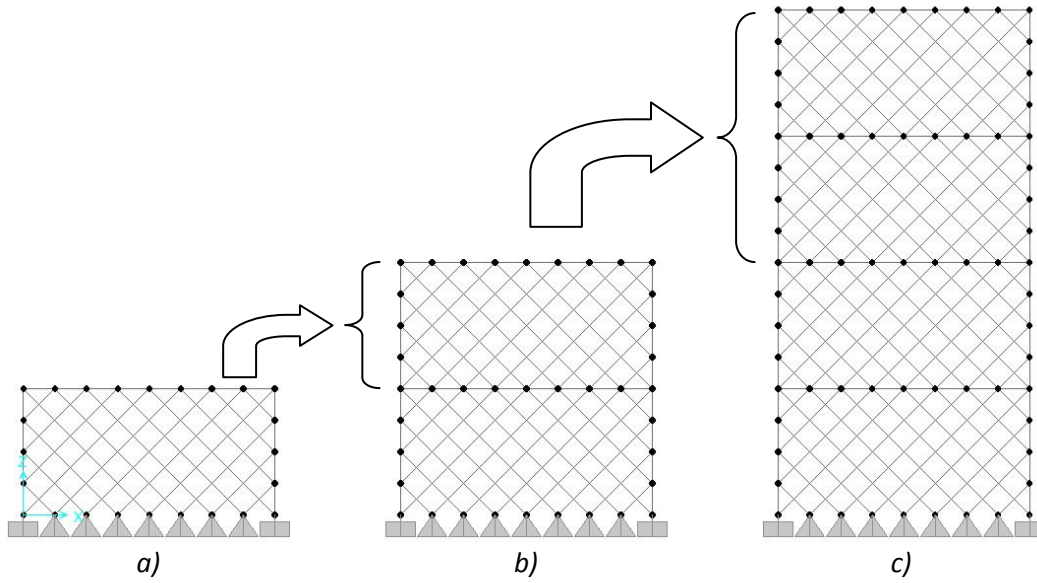


Figure 4.9 - 4-Storey Scaling Example: a) initial single storey; b) single storey replicated above initial storey; c) 4-storey created using 2-storey replication

5. DESIGN EXAMPLE

5.1 General

This chapter presents the design of a steel plate shear wall (SPSW) for a 15-storey office building located in Vancouver. The structure is designed according to NBCC (2005) and S16-09, then analyzed using SAP2000® V14.0.0. Based on the results of the analysis, the beam and column sections are re-designed to satisfy all the design requirements.

5.2 Building Information

The building under consideration is adapted from Bhowmick *et al.* (2009) with the floor plan and SPSW elevation shown in Figure 5.1. The beams and columns are referenced according to their corresponding level or storey respectively. The foot print of the building is 2014 m² and with a storey height of 3.8 m throughout the structure. The total height of the building is 57 m. The width of the SPSW bay is 7.6 m. To resist the lateral loads, two SPSWs are oriented in each the North-South and East-West directions. The SPSW used for this application is classified as a Type D, or ductile, plate wall with a R_dR_o value of 8.0, which is the highest ductility and overstrength modification ratios of any seismic force resisting system. It is noted that S16-09 also allows for Type LD SPSW, which has a R_dR_o value of 3.0. A Type D wall was selected as large interstorey drifts are expected from the seismic loading. Type LD walls can be used where interstorey drifts are not a concern. As the main difference between the two types is the fact that Type LD would use simple beam to column connections whereas Type D requires rigid beam to column connections, this example serves for the design of either type. The weight of the building, W , is calculated to be 122000 kN. The dead loads and the individual floor weights are listed in Table 5.1 and Table 5.2, respectively.

The infill plates and the beams and columns for the SPSW are made of CSA G40.21 350W steel. The lateral load resisting system of the building consists of two SPSWs in each orthogonal direction. This configuration was selected to minimize torsional effects. The seismic loads are obtained from Appendix C in Division B of the NBCC 2005. The soil conditions at the site are assumed to be class B and the importance factor, I_E , used for the building is 1.0 since it is an office building.

5.3 Design Procedure

Although the SPSW will be designed to resist live, dead, wind, and seismic loads as the principal loads, its main function is to resist the earthquake and wind loading. The wind load calculations are done according to NBCC 2005 and the analysis is carried out using a static loading procedure. The analysis for the seismic loading is conducted using two methods: the equivalent static force procedure and a dynamic procedure as the preferred method of NBCC 2005. The SPSW will be designed according to capacity design principles and other requirements as outlined by S16-09. The calculations presented in this section illustrate the design of the 10th level beam and 10th storey column and infill panel of the SPSW. A spreadsheet was setup for the calculations for the other storeys.

5.4 Static Design

The static design of the SPSW consists of wind and seismic loading based on the equivalent static force procedure, both outlined in NBCC 2005. The preliminary member and infill panel sizes are selected to resist the wind loads while capacity design principles are used for the seismic load design. Using the preliminary sizes, a model is constructed in SAP2000® using the strip model proposed by Thorburn *et al.* (1983) for analysis. The model is then used to check that the members selected are adequate for resisting the loads according to S16-09 and the NBCC 2005.

5.4.1 Wind Loading

The values for the reference wind velocity and coefficients are obtained from Appendix C, Division B, of the NBCC which are used in Equation 3.2 to determine the global wind loading for the windward surface of the building in the East-West direction:

$$p = I_w q C_e C_g C_p$$

$$p = (1.0)(0.48)(1.12)(2.0)(0.8)$$

$$p = 0.86 \text{ kPa}$$

and the global suction for the leeward surface in the East-West direction:

$$p = (1.0)(0.48)(1.12)(2.0)(-0.5)$$

$$p = -0.54 \text{ kPa}$$

The wind pressure is then converted into point loads applied to the SPSW model as static loads at the floor levels, with each SPSW to resist half the load. Each static load is 140 kN. The NBCC requires dynamic effects of the wind to be taken into account for structures taller than 120 m or 4 times their minimum effective width, which is defined as:

$$W = \sum_{i=1}^n w_i \quad 5.1$$

where the summation is over the height of the building, h_i is the height above grade to level i ; and w_i is the corresponding width of the building orthogonal to the wind direction. Since the building under consideration is of constant width over the full height, the effective width for the east west wind direction is 53 m. Since $4 \times 53 \text{ m} = 212 \text{ m}$ is greater than 120 m, the governing reference height is 120 m. The actual building height (57 m) is less than the reference height and, as such, the dynamic effects of the wind can be ignored for this building.

The wind loading effects will be compared with the seismic loading effects in Section 6.3.

5.4.2 Seismic Loading-Equivalent Static Force Procedure

Using the criteria established in Chapter 3, the building under consideration qualifies for the use of the equivalent static force procedure as the structure is below 60 m in height and has a fundamental lateral period below 2 s as calculated by the following equation from the NBCC:

$$T_g = 0.05(57.0)^{3/4} = 1.04 \text{ s}$$

From the tables of climatic data of NBCC, the 5% damped spectral response acceleration, $S_a(T)$, for periods of 0.2 s, 0.5 s, 1.0 s and 2.0 s is 0.94, 0.64, 0.33 and 0.17, respectively. To determine the minimum design base shear, V , as well as the maximum

base shear, V_{max} , Equation 3.3 and Equation 3.7 are used, with the variables required from the NBCC, and are calculated as:

$$V = \frac{S(T_a)M_v I_E W}{R_d R_o} \geq \frac{S(2.0)M_v I_E W}{R_d R_o}$$

where the design spectral acceleration, $S(T_a)$, is obtained from clause 4.1.8.4 of NBCC by interpolating linearly between:

$$S(T) = F_v S_o(1.0) \text{ for } T = 1.0 \text{ s}$$

and

$$S(T) = F_v S_o(2.0) \text{ for } T = 2.0 \text{ s}$$

The value of F_v is obtained from Table 4.1.8.4.C of NBCC for site class B by interpolating between a value of 0.7 for $S_o(1.0) = 0.3$ and 0.8 for $S_o(1.0) = 0.4$. For $S_o(1.0) = 0.33$, the value of F_v is 0.73. Therefore, $S(T = 1.0 \text{ s}) = 0.73 \times 0.33 = 0.241$ and $S(T = 2.0 \text{ s}) = 0.73 \times 0.17 = 0.124$ and linear interpolation for $S(T = 1.04 \text{ s})$ results in a value of $S(T_a = 1.04 \text{ s}) = 0.236$. The factor M_v , used to account for the higher modes on the base shear is obtained from Table 4.1.8.11 of NBCC as follows:

The value of $S_o(0.2)/S_o(2.0) = 0.94/0.17 = 5.53$ is less than 8.0 and, according to the first row of Table 4.1.8.11, we interpolate between a value of $M_v = 1.0$ for $T_a = 1.0$ and a value of $M_v = 1.2$ for $T_a = 2.0$. From a linear interpolation, $M_v = 1.01$.

Recalling that the importance factor for this building is 1.0, W on a plate wall is half the building weight (61 000 kN) and $R_d R_o$ for Type D plate walls is 5.0×1.6 , the minimum design base shear, V , can now be calculated as:

$$V = \frac{0.236 \times 1.01 \times 1.0 \times 61000 \text{ kN}}{5.0 \times 1.6} \geq \frac{0.17 \times 1.0 \times 1.0 \times 61000 \text{ kN}}{5.0 \times 1.6}$$

$$V = 1820 \text{ kN} \geq 1300 \text{ kN}$$

The minimum design base shear is thus 1820 kN.

The maximum base shear, calculated according to Clause 4.1.8.11(2), is

$$V_{max} = \frac{2 S(0.2) I_E W}{3 R_d R_o}$$

$$V_{max} = \frac{2 \times 0.94 \times 1.0 \times 61000 \text{ kN}}{3 \times 5.0 \times 1.6}$$

$$V_{max} = 4780 \text{ kN}$$

The concentrated force at the top of the SPSW is determined using Equation 3.8 as:

$$F_t = 0.07 T_o V \leq 0.25 V$$

$$F_t = 0.07 \times 1.04 \times 1820 \text{ kN} \leq 0.25 \times 1820 \text{ kN}$$

$$F_t = 130 \text{ kN} \leq 460 \text{ kN}$$

The remaining portion of the lateral load to be distributed to all the floor levels is calculated using Equation 3.9:

$$F_x = \frac{(V - F_t) W_x h_x}{\sum_{i=1}^n W_i h_i}$$

The storey forces, F_x , are presented in Table 5.2 and will be applied to the SPSW model as static loads at the appropriate floor levels.

The overturning moment calculation requires the numerical reduction coefficient for the storey-level overturning moment, J_x , calculated using Equations 3.11 and 3.12 as:

$$J_x = 1.0 \text{ for } h_x \geq 0.6 h_n$$

$$J_x = J + (1 - J)(h_x / 0.6 h_n) \text{ for } h_x < 0.6 h_n$$

The values of J_x for each storey are presented in Table 5.2. The base overturning moment reduction factor, J , was determined to be 0.893 by linear interpolation between 1.0 for $T_o = 0.5$ and 0.7 for $T_o = 2.0$ obtained from Table 4.1.8.11 of the NBCC.

The overturning moment, M_x , at the base of each storey is calculated using Equation 3.10 as:

$$M_x = J_x \sum_{i=x}^n F_i (h_i - h_x)$$

The results for the overturning moment are presented in Table 5.2.

The NBCC restricts the use of the equivalent static force procedure to buildings that are relatively stiff in torsion as flexible buildings can experience large displacements due to dynamic amplification (Humar *et al.*, 2003). The NBCC requires the calculation of a torsional sensitivity parameter, B , to determine the type of seismic analysis that is acceptable. If $B > 1.7$, a dynamic analysis is required. Further details are provided in Section 3.2.2.1, the NBCC 2005, and the report by Humar *et al.*, (2003). For this building, the center of mass and center of rigidity are coincident, and thus the eccentricity, e_x , is zero. The equation from the NBCC regarding torsion (for an earthquake in the east-west direction) of the 10th storey, including the seismic load (F_x) for both SPSWs, reduces to:

$$T_x = F_x (e_x \pm 0.10 D_{nx})$$

$$T_x = F_x (0 \pm 0.10 D_{nx})$$

$$T_x = 306 \text{ kN} \times (\pm 0.10 \times 53.0 \text{ m})$$

$$T_x = \pm 1620 \text{ kN} \cdot \text{m}$$

where D_{nx} is the dimension of storey x perpendicular to the direction of the earthquake. The moment is applied in combination with the seismic loads and can be applied to the SPSW model by considering the stiffness of each SPSW. The loading for the North and South SPSWs, V_1 and V_3 , and East and West SPSWs, V_2 and V_4 , can be calculated as (Kulak and Grondin, 2009):

$$V_i = F_x \frac{K_{xi}}{\sum_{i=1}^m K_{xi}} + \frac{TK_{xi}d_i}{\sum_{k=1}^{m+n} K_k d_k^2} \quad 5.2$$

where K_{xi} is the stiffness of the i^{th} SPSW in the direction of loading; K_k is the stiffness of any SPSW in their respective direction; m and n are the number of SPSWs parallel and perpendicular to the direction of loading, respectively; and d is the distance from the shear center to the SPSW. Using this equation, and assuming that the SPSWs have

equal stiffness, the static load applied to the storey is calculated as (for an earthquake in the E-W direction):

$$V_1 = 306 \text{ kN} \times \frac{1}{2} + \frac{1620 \text{ kN} \cdot \text{m} \times 15 \text{ m}}{2 \times (15 \text{ m})^2 + 2 \times (11.4 \text{ m})^2}$$

$$V_1 = 153 \text{ kN} + 34.2 \text{ kN} = 187 \text{ kN}$$

$$V_2 = 0 + \frac{1620 \text{ kN} \cdot \text{m} \times 11.4 \text{ m}}{2 \times (15 \text{ m})^2 + 2 \times (11.4 \text{ m})^2}$$

$$V_2 = 26.0 \text{ kN}$$

$$V_3 = 306 \text{ kN} \times \frac{1}{2} - \frac{1620 \text{ kN} \cdot \text{m} \times 15 \text{ m}}{2 \times (15 \text{ m})^2 + 2 \times (11.4 \text{ m})^2}$$

$$V_3 = 153 \text{ kN} - 34.2 \text{ kN} = 119 \text{ kN}$$

$$V_4 = -V_2 = -26.0 \text{ kN}$$

The loads are calculated for each storey and applied in the analysis model. The maximum and average storey deflections, δ_{max} and δ_{ave} , are determined from the static analysis and used to calculate the individual storey torsion sensitivity parameter, B_x , calculated as:

$$B_x = \frac{\delta_{max}}{\delta_{avg}}$$

with the largest value becoming the global torsional sensitivity parameter, B . For more detail and examples regarding elastic and inelastic building torsion, see Humar and Kumar (1998, 1998).

5.4.3 Preliminary Design

For the preliminary design of the SPSW using the equivalent static force procedure the strips inclination angle α can be determined using Equation 3.16. However, as stated in Section 4.4, an angle of 45° will be used throughout the structure. Using the storey shear, V , calculated in Section 5.4.2, the infill plate thickness required for the 10th storey is determined according to Clause 27.9.2.1 of S16-09 as:

$$V_r = 0.4 \phi F_y w L \sin 2\alpha$$

$$1130 \text{ kN} = 0.4 \times 0.9 \times 350 \text{ MPa} \times w \times 7600 \text{ mm} \times \sin(2 \times 45^\circ)$$

$$w = 1.12 \text{ mm} \rightarrow \text{use } 2.0 \text{ mm}$$

In previous research, the minimum infill plate thickness has generally been limited to 3 mm, mainly because of handling and welding limitations. Recent work (Berman and Bruneau, 2005; Neilson *et al.*, 2010) has shown that infill plates as thin as 0.7 mm can be used in SPSWs as an effective seismic force resisting system. Neilson *et al.* (2010) have presented a detailed welding procedure for MIG welding of a 1.0 mm infill plate to a steel frame. Based on these results, infill plates thinner than 3.0 mm have been selected in the design process. The thickness calculated and selected for the remaining storeys can be seen in Table 5.3.

The panel thickness was selected in five separate lifts for convenience. The storey shears shown in Table 5.2 include the notional load as described in Clause 8.4.1 of S16-09, which is discussed in Section 5.4.4.1.

The preliminary column sections are selected based on the minimum required moment of inertia from Clause 20.5.1 of S16-09 and calculated as:

$$I_c \geq \frac{0.0031wh^4}{L}$$

$$I_c \geq \frac{0.0031 \times 2.0 \text{ mm} \times 3800^4 \text{ mm}^4}{7600 \text{ mm}} = 170 \times 10^6 \text{ mm}^4$$

In order to prevent premature local buckling, the columns are required by S16-09 to be of Class 1 section. Table 5.3 lists wide flange sections that meet both the moment of inertia and section class requirements. The flanges of the selected sections were checked to meet the requirement of Class 1 sections ($b_{el}/t \leq 135/\sqrt{F_y}$) while the web can be checked only after the compressive force is determined. The top beam is selected by considering the minimum required moment of inertia according to Clause 20.5.2 of S16-09 calculated as:

$$I_b \geq \frac{wL^4}{650L - (wh^4 / I_c)}$$

$$I_b \geq \frac{1.0\text{mm} \times (7600\text{mm})^4}{650 \times 7600\text{mm} - (1.0\text{mm} \times (3800\text{mm})^4 / 99.2 \times 10^6 \text{mm}^4)}$$

$$I_b \geq 1180 \times 10^6 \text{mm}^4$$

The top beam is also required to be a Class 1 section for Type D plate walls since plastic hinges are expected to form at both extremities. The flanges of the selected sections are checked to be Class 1 sections while the web is checked after the axial force is determined. Class 1 sections are selected for the beams of the intermediate storeys to resist the moments resulting from the distributed factored dead and live loads, calculated assuming a simple span. The factored distributed load, w_g , due to the dead and live loads according to the NBCC (1.0D + 0.5L) and the corresponding moment on the beam, $M_{beam(gravity)}$, are calculated as:

$$w_g = b_t (1.0D + 0.5L)$$

$$w_g = 6.0\text{m} \times (1.0 \times 4.26\text{kPa} + 0.5 \times 2.4\text{kPa}) = 32.8 \text{ kN/m}$$

$$M_{beam(gravity)} = \frac{w_g L^2}{8}$$

$$M_{beam(gravity)} = \frac{32.8\text{kN/m} \times (7600\text{mm} - 407\text{mm})^2}{8} = 212 \text{ kN}\cdot\text{m}$$

where b_t is the tributary width for the beam (this is equal to 6.0 m for this sample building). The sections selected for the initial design can be seen in Table 5.3. The length, L , is adjusted to account for the depth of the columns on either side of the beam by subtracting the depth of the column from the bay width.

As outlined in Clause 27.9.2.2 of S16-09, the members that transfer forces to the infill plate must be designed for the yield capacity of the infill plate times the material factor, R_y , although the forces need not exceed the value corresponding to $R_d R_o = 1.3$. The following equations are derived from free body diagrams presented by Berman and

Bruneau (2008) (see Figure 5.2 and Figure 5.3) and can be used to calculate the force effects acting on the beams and the columns. The distributed load, w , on the beam from yielding of the infill panel identified in Figure 5.2, can be resolved into its respective horizontal and vertical components as:

$$\omega_{xb} = \pm \frac{1}{2} R_y F_y w (\sin 2\alpha) \quad 5.3$$

$$\omega_{yb} = \pm R_y F_y w (\cos^2 \alpha) \quad 5.4$$

The distributed loads ω_{xc} and ω_{yc} acting on the columns identified in Figure 5.3 are the loading components from the yielding of the infill panel and are calculated as:

$$\omega_{xc} = R_y F_y w (\sin^2 \alpha) \quad 5.5$$

$$\omega_{yc} = \frac{1}{2} R_y F_y w (\sin 2\alpha) \quad 5.6$$

These components are used in the following equations to calculate the force effects acting on the beams and columns.

The sections from the initial member selection listed in Table 5.3 do not satisfy the S16-09 requirements using capacity design approach. Using the following equations and an iterative process via spreadsheet, the boundary elements that satisfy the S16-09 requirements are chosen and the calculations will be shown below. The elements selected are presented in Table 5.4 and the sections are labelled as the preliminary design elements.

The design force effects for the beam at level 10 are calculated using a W460x193 section as presented in Table 5.4. The design axial force effects consists of two components, $P_{beam(infill)}$, and $P_{beam(column)}$ which are the axial forces in the beam from yielding of the infill panel above and below the beam, and from the tension field acting on the columns, respectively. These components are calculated using the following equations:

$$P_{beam(infill)} = \frac{1}{4} R_y F_y [w_i \sin 2\alpha_i - w_{i+1} \sin 2\alpha_{i+1}] L$$

$$P_{beam(infill)} = \frac{1}{4} \times 1.1 \times 350 \text{ MPa} \times [2.0 \text{ mm} \times \sin 90^\circ - 1.0 \text{ mm} \times \sin 90^\circ] \times (7600 \text{ mm} - 425 \text{ mm})$$

$$P_{beam(infill)} = 691 \text{ kN}$$

$$P_{beam(column)} = \frac{1}{2} R_y F_y [w_i h_i \sin^2 \alpha_i + w_{i+1} h_i \sin^2 \alpha_{i+1}]$$

$$P_{beam(column)} = \frac{1}{2} \times 1.1 \times 350 \text{ MPa} \times [2.0 \text{ mm} \times \sin^2 45^\circ \times 3800 \text{ mm} + 1.0 \text{ mm} \times \sin^2 45^\circ \times 3800 \text{ mm}]$$

$$P_{beam(column)} = 1097 \text{ kN}$$

$$P_{beam} = P_{beam(column)} + P_{beam(infill)}$$

$$P_{beam} = 1097 \text{ kN} + 691$$

$$P_{beam} = 1790 \text{ kN}$$

It can be seen from the calculation of $P_{beam(infill)}$ that if the infill plate thickness is the same above and below the beam, the axial force component from the panel above the beam is equal and opposite to the force component from the panel below the beam, resulting in no net axial force from the infill plate component. The length of the beam element, L , is the centre to centre distance between the columns less half the column depth, d_c , from each end.

The design moment at the beam midspan due to yielding of the infill panel above and below the beam, $M_{beam(infill)}$, is calculated assuming simple support conditions using the following equation:

$$M_{beam(infill)} = \frac{1}{8} R_y F_y [w_i \cos^2 \alpha_i - w_{i+1} \cos^2 \alpha_{i+1}] L^2$$

$$M_{beam(infill)} = \frac{1}{8} \times 1.1 \times 350 \text{ MPa} \times [2.0 \text{ mm} \times \cos^2 45^\circ - 1.0 \text{ mm} \times \cos^2 45^\circ] \times (7600 \text{ mm} - 425 \text{ mm})^2$$

$$M_{beam(infill)} = 1240 \text{ kN}\cdot\text{m}$$

$$M_{beam} = M_{beam(infill)} + M_{beam(gravity)}$$

$$M_{beam} = 1240 \text{ kN}\cdot\text{m} + 212 \text{ kN}\cdot\text{m} = 1450 \text{ kN}\cdot\text{m}$$

The reduced plastic moment capacity for the beam sections, M_{rpb} , is calculated according to Clause 27.9.3.4 of S16-09. The total axial beam force, P_{beam} , is used as the factored compressive force C_f , and C_y is the axial yield resistance of the beam, calculated as $A_g F_y$. The reduced plastic moment capacity is calculated as:

$$M_{rpb} = 1.18 \left(1.1 R_y Z_x F_y \right) \left(1 - \frac{C_f}{\phi C_y} \right) \leq Z_x F_y$$

$$M_{rpb} = 1.18 \times \left(1.1 \times 1.1 \times 4750 \times 10^3 \text{ mm}^3 \times 350 \text{ MPa} \right) \times \left(1 - \frac{1790 \text{ kN}}{0.9 \times 8610 \text{ kN}} \right) \\ \leq 4750 \times 10^3 \text{ mm}^3 \times 350 \text{ MPa}$$

$$M_{rpb} = 1830 \text{ kN}\cdot\text{m} > 1660 \text{ kN}\cdot\text{m}$$

Therefore, the plastic moment capacity is not reduced by the presence of the axial force and $M_{rpb} = 1660 \text{ kN}\cdot\text{m}$.

The beam design shear consists of $V_{beam(infill)}$, which is the maximum shear force in the beam due to yielding of the infill panel, $V_{beam(MF)}$, the shear in the beam resulting from the formation of plastic hinges at the ends of the beam under frame sway action, and $V_{beam(gravity)}$, which is the shear due to the gravity loads. While plastic hinges typically form $d_b/2$ from the column face (Berman and Bruneau, 2008), where d_b is the beam depth, for the purpose of calculating the force effects, it is assumed that the hinges form at the beam-to-column intersection. The first component, $V_{beam(infill)}$, is calculated using the following equation, which assumes yielding of the infill plates above and below the beam:

$$V_{beam(infill)} = \frac{1}{2} R_y F_y \left[w_i \cos^2 \alpha_i - w_{i+1} \cos^2 \alpha_{i+1} \right] L$$

$$V_{beam(infill)} = \frac{1}{2} \times 1.1 \times 350 \text{ MPa} \times [2.0 \text{ mm} \times \cos^2 45^\circ - 1.0 \text{ mm} \times \cos^2 45^\circ] \\ \times (7600 \text{ mm} - 425 \text{ mm})$$

$$V_{beam(infill)} = 691 \text{ kN}$$

$$V_{beam(MF)} = \frac{2M_{rpb}}{L}$$

$$V_{beam(MF)} = \frac{2 \times 1660 \text{ kN} \cdot \text{m}}{(7.6 \text{ m} - 0.425 \text{ m})}$$

$$V_{beam(MF)} = 463 \text{ kN}$$

$$V_{beam(gravity)} = \frac{w_g L}{2}$$

$$V_{beam(gravity)} = \frac{32.8 \text{ kN/m} \times (7.6 \text{ m} - 0.425 \text{ m})}{2}$$

$$V_{beam(gravity)} = 118 \text{ kN}$$

$$V_{beam} = V_{beam(MF)} + V_{beam(infill)} + V_{beam(gravity)}$$

$$V_{beam} = 463 \text{ kN} + 691 \text{ kN} + 118 \text{ kN}$$

$$V_{beam} = 1270 \text{ kN}$$

The component of shear for the beam, $V_{beam(MF)}$, at level 15 (roof level) must be modified since the plastic hinge at that location will form in the column rather than in the beam, which is heavier than the column due to the stiffness requirement of S16-09. The calculated shear from moment frame action for top level uses the reduced plastic moment for the column instead.

The design force effects for the columns are determined using the same free body diagram approach as the beams and separating the forces into individual components. The axial force components are summed from the top storey to the storey under

consideration (not shown in the sample calculations below). The summed axial forces are presented in Table 5.5 and Table 5.7 for the preliminary and final design force effects, respectively.

The design force effects for the column at storey 10 are calculated using a W360x421 section as shown in Table 5.4. The gravity load, $P_{column(g)}$, for the columns at each floor is calculated to be:

$$P_{column(g)} = p_t A_t$$

$$P_{column(g)} = (1.0 \times 4.26 \text{ kPa} + 0.5 \times 2.4 \text{ kPa}) \times (6.0 \text{ m} \times 7.6 \text{ m}) = 249 \text{ kN}$$

where A_t is the tributary area of the column and p_t is the total pressure on the tributary area.

The capacity design axial forces at mid-height of the 10th storey columns consists of the component from yielding of the infill panel, $P_{column(infill)}$, and the component from the beams, $P_{column(beam)}$. The individual storey loads are calculated as:

$$P_{column(infill)} = \frac{1}{2} w_i h_i R_y F_y \sin 2\alpha_i$$

$$P_{column(infill)} = \frac{1}{2} \times 2.0 \text{ mm} \times 3800 \text{ mm} \times 1.1 \times 350 \text{ MPa} \times \sin(2 \times 45^\circ)$$

$$P_{column(infill)} = 1460 \text{ kN}$$

$$P_{column(beam)} = (V_{beam(MF)} + V_{beam(infill)} + V_{beam(gravity)})$$

$$P_{column(beam)} = 463 \text{ kN} + 691 \text{ kN} + 118 \text{ kN}$$

$$P_{column(beam)} = 1270 \text{ kN}$$

$$P_{column} = P_{column(infill)} + P_{column(beam)} + P_{column(g)}$$

$$P_{column} = 1460 \text{ kN} + 1270 \text{ kN} + 249 \text{ kN}$$

$$P_{column} = 2980 \text{ kN}$$

The column design moments are the sum of the component from the uniformly distributed force from the tension field in the infill plate, $M_{column(infill)}$, the moment frame action, $M_{column(MF)}$, assuming the columns are fixed at their ends, and $M_{column(beam)}$, which is the component from the beam shear. The components are calculated as follows:

$$M_{column(infill)} = \frac{1}{12} wh^2 R_y F_y \sin^2 \alpha$$

$$M_{column(infill)} = \frac{1}{12} \times 2.0 \text{ mm} \times (3800 \text{ mm})^2 \times 1.1 \times 350 \text{ MPa} \times \sin^2 45^\circ$$

$$M_{column(infill)} = 463 \text{ kN} \cdot \text{m}$$

$$M_{column(MF)} = \frac{1}{2} \text{Max}(M_{pbr,i} : M_{pbr,i+1})$$

$$M_{column(MF)} = \frac{1}{2} (1660 \text{ kN} \cdot \text{m})$$

$$M_{column(MF)} = 830 \text{ kN} \cdot \text{m}$$

$$M_{column(beam)} = \frac{1}{2} \text{Max}(V_{beam,i} : V_{beam,i+1}) \frac{d_c}{2}$$

$$M_{column(beam)} = \frac{1}{2} \times 1270 \text{ kN} \times \frac{0.425 \text{ m}}{2}$$

$$M_{column(beam)} = 135 \text{ kN} \cdot \text{m}$$

$$M_{column} = M_{column(infill)} + M_{column(MF)} + M_{column(beam)}$$

$$M_{column} = 463 \text{ kN} \cdot \text{m} + 830 \text{ kN} \cdot \text{m} + 135 \text{ kN} \cdot \text{m}$$

$$M_{column} = 1430 \text{ kN} \cdot \text{m}$$

For the column moment component due to the plastic hinging of the beams, $M_{column(MF)}$, half of the reduced plastic moment from each beam (at the top or at the bottom of a specific column) can be attributed to the column end connected to that beam. Thus, at

each storey i , the column moment from the plastic hinging of the beams is half of the plastic moment from the bounding beam elements. A similar procedure is used for the column moment due to the beam shear, $M_{column(beam)}$. The component of the column moment from frame action at the top and bottom levels is modified to account for the plastic hinge forming in the column rather than in the beam (because stiff beams are required to anchor the tension field at the top and the bottom panels). While the moment components, $M_{column(infill)}$ and $M_{column(MF)}$, oppose one another at one end of each storey and are additive at the other, the summation is conservative. The reduced plastic moment capacity of the column must be greater than half of the reduced plastic moment capacity of the beam to ensure that plastic hinges form in the beams instead of the column. The reduced plastic capacity of the column is calculated as:

$$M_{rpc} = 1.18 \left(1.1 R_y Z_x F_y \right) \left(1 - \frac{C_f}{\phi C_y} \right) \leq Z_x F_y$$

$$M_{rpc} = 1.18 \times \left(1.1 \times 1.1 \times 8880 \times 10^3 \text{ mm}^3 \times 350 \text{ MPa} \right) \times \left(1 - \frac{11200 \text{ kN}}{0.9 \times 18800 \text{ kN}} \right)$$

$$\leq 8880 \times 10^3 \text{ mm}^3 \times 350 \text{ MPa}$$

$$M_{rpc} = 1500 \text{ kN} \cdot \text{m} < 3108 \text{ kN} \cdot \text{m}$$

Thus the reduced plastic capacity of the column is $1500 \text{ kN} \cdot \text{m}$, which is greater than half of the reduced plastic capacity of the beam, $0.5 M_{rpb} = 830 \text{ kN} \cdot \text{m}$.

The column shear forces are calculated assuming fixed end columns and a uniformly distributed force from the tension field in the infill plate, which yields the following equations:

$$V_{column(infill)} = \frac{1}{2} w h R_y F_y \sin^2 \alpha$$

$$V_{column(infill)} = \frac{1}{2} \times 2.0 \text{ mm} \times 3800 \text{ mm} \times 1.1 \times 350 \text{ MPa} \times \sin^2 45^\circ$$

$$V_{column(infill)} = 732 \text{ kN}$$

$$V_{column(beam)} = \frac{1/2(M_{pbri} + M_{pbri+1})}{h}$$

$$V_{column(beam)} = \frac{1}{2} \left(\frac{1660 \text{ kN}\cdot\text{m} + 1150 \text{ kN}\cdot\text{m}}{3.8 \text{ m}} \right)$$

$$V_{column(beam)} = 370 \text{ kN}$$

$$V_{column} = V_{column(infill)} + V_{column(beam)}$$

$$V_{column} = 732 \text{ kN} + 370 \text{ kN}$$

$$V_{column} = 1100 \text{ kN}$$

The selected beam and column sections are verified to be Class 1 using the axial forces previously calculated. Each of the elements selected satisfied the cross-sectional strength compression and bending interaction check according to Clause 13.8 of S16-09. As both static and dynamic analyses accounted for $P-\Delta$, $P-\delta$ effects, and inelastic behaviour, the overall strength (in-plane behaviour) check was not necessary. Additionally, the lateral torsional buckling interaction check was ignored as the SPSW requires lateral bracing according to Clause 13.7(b) of S16-09, which is discussed in Section 5.6.3.

5.4.4 Detailed Design

The detailed design was implemented by constructing a model in the analysis program SAP2000® V14.0.0 using the infill plate thickness and beam and column sections selected in the preliminary design. The frame is constructed using rigid beam-to-column connections and the infill plate is modeled using the strip model proposed by Thorburn *et al.* (1983). When the equivalent static load approach is used for seismic design, the tension strips are all inclined in a single direction because the loading is applied in one direction only.

Using the plate thicknesses selected in Section 5.4.3, appropriate tension strips are created using custom sections. Previous research (Thorburn *et al.* 1983; Driver *et al.* 1997; Shishkin *et al.* 2005) has indicated that 10 strips are adequate to describe the

behaviour of SPSWs. In this example, 11 strips were selected for the model and the spacing of the strips is determined based on the number of strips and the geometry of the SPSW calculated as:

$$\Delta_x = \frac{1}{n}(L + h \sin \alpha)$$

$$\Delta_x = \frac{1}{11}(7600 \text{ mm} + 3800 \text{ mm} \times \sin 45^\circ)$$

$$\Delta_x = 935 \text{ mm}$$

where Δ_x is the spacing of the strips and all other terms are as previously defined. The strip spacing, as well as the number of strips, can be modified to simplify the model. For the model used in this example, 11 strips at a spacing of 950 mm, are used in a crosshatched pattern, which simplifies the generation of the model. Using the strip spacing, Δ_x , the required area of the strips, A_s , for a 1.0 mm thick infill plate is determined using the following equation:

$$A_s = \Delta_x w \cos \alpha$$

$$A_s = 950 \text{ mm} \times 1.0 \text{ mm} \times \cos 45^\circ$$

$$A_s = 672 \text{ mm}^2$$

The tension strips in the model are modeled as rectangular sections with cross sectional areas of 672 mm², 1344 mm², and 2016 mm² for the 1.0 mm, 2.0 mm, and 3.0 mm thick infill panels, respectively. The tension strips are pinned at each end and are made of G40.21 350W steel.

Using these dimensions and the preliminary sections, a model of the structure is created and loaded with the loads presented in Section 5.4.2. Two models of the SPSW are shown in Figure 5.4: the model in Figure 5.4 (a) with unidirectional tension strips for the static analysis and the model in Figure 5.4 (b) with bidirectional tension strips for the dynamic analysis. The lateral loads from the equivalent static force procedure are applied as point loads at each diaphragm level, at the beam-to-column intersection. Gravity loads are applied as distributed loads on the beams and concentrated forces on the columns. Plastic hinges with bending-axial interaction are inserted at the beam-to-

column intersections (rigid joint assumed) and hinge offsets are ignored as it has been shown to have a negligible effect (Shishkin *et al.* 2005). Axial hinges are inserted at the midpoint of the tension strips. The hinge definitions, presented in Section 4.3.3, are defined according to FEMA 356 (2000) guidelines.

5.4.4.1 Stability and Second Order Effects

Methods to incorporate second order effects as well as inelastic contributions prescribed by NBCC 2005 and S16-09 are considered here. As previously mentioned, the notional load was incorporated into the static loads. However, the notional load as described by S16-09 is modified to 0.2% of the factored gravity loads as inelastic action was accounted for by the NBCC amplification factor, $R_d R_o / I_E$, which is applied to the elastic deflections.

The NBCC requires that the storey shears and overturning moments be amplified to account for the $P-\Delta$ effects by a method proposed by Pauley and Priestly, (1992). The proposed method considers seismically induced $P-\Delta$ effects and includes inelastic deformations. The seismic effects are amplified through a stability factor, θ_x , which, if less than 0.10, can be neglected according to Commentary J of the NBCC (NBCC 2005). The amplification factor, θ_x , used to amplify the design storey shear, V_x^* , and the overturning moment, M_x^* , is defined as:

$$\theta_x = \frac{P_x \Delta_{mx}}{R_o V_x h_{sx}} \quad 5.7$$

where P_x is the building gravity load at and above level x ; Δ_{mx} is the maximum inelastic interstorey drift of the storey directly below level x ; and h_{sx} is the storey height immediately below level x . The amplified shear and moment are then defined as:

$$V_x^* = V_x (1 + \theta_x) \quad 5.8$$

$$M_x^* = M_x (1 + \theta_x) \quad 5.9$$

S16-09 requires that stability effects be accounted for by the addition of the notional loads and the inclusion of $P-\Delta$ effects. The notional loads were included to account for initial out-of-plumb and any partial yielding at the factored load. S16-09 requires that

$P-\Delta$ effects be determined using either a second order analysis or an amplification factor.

As SAP2000® includes a second order analysis option, it was decided to use the nonlinear analysis option in SAP2000® to account for the $P-\Delta$ effects. Additionally, Bhowmick *et al.* (2009) found that for SPSWs that met the drift requirements of the NBCC, the amplification factor approach tends to over-estimate the second order effects.

5.4.5 Analysis Results

The interstorey and base shears, the member forces, moments and displacements are obtained from the analysis. A comparison of the member forces from the analysis with the design forces from the previous section indicated that the selected elements are adequate for the design. The comparisons are presented in Chapter 6, Section 6.3. According to the NBCC, the elastic interstorey drifts obtained from the analysis are to be multiplied by $R_d R_o / I_E$ to account for inelastic behaviour. Using the infill panel thickness and member sizes from the preliminary analysis, it was seen that the interstorey deflections exceeded the limit of $0.025 h_s$. To meet the deflection requirements, the infill panel thickness is increased in 1.0 mm increments beginning with the 1.0 mm infill plate at the 11th storey and continuing upwards towards the 15th storey. After each increase in plate thickness, the capacity design equations are updated and the SAP2000® analysis is repeated using the new tension strip elements. The final panel thickness required to meet the NBCC 2005 inelastic deflection requirements of the majority of the floors is determined to be 3.0 mm, and, for convenience, 3.0 mm infill plates are used over the full height of the structure. The final section sizes and design force effects are presented in Table 5.6 and Table 5.7 respectively.

5.5 Dynamic Analysis

The dynamic design procedure requires a base shear estimate to begin the design procedure. An estimate of the base shear was made using the equivalent static force procedure as described in Section 5.4.2. With an estimate of the base shear, a model for analysis can be created. The model was implemented in SAP2000® and subjected to four nonlinear time history analyses following the procedure outlined in Chapter 4. Using the

results from the analysis the model was refined to meet the requirements of the NBCC and S16-09.

5.5.1 Design

The equivalent static force procedure and capacity design principles outlined in Section 5.4.2 and 5.4.3, respectively, were used as a starting point to size the beam and column elements as shown in Table 5.4.

A rigid frame was modeled in SAP2000® using the building dimensions and the selected sections. The infill panel was modeled using tension strips which are created using the same technique as the equivalent static force procedure. The distinction between the model used for the equivalent static force procedure and the dynamic procedure is the inclusion of pinned tension strips in both directions for the dynamic model. Tension strips in both directions are required in the dynamic model due to the load reversals that occur from seismic loading, which would not be resisted by tension-only elements in a single direction. Once the model was constructed, bilinear, moment-axial load interaction hinges are assigned at each end of the beam and column elements. Axial hinges are inserted at the midpoint section in the tension strips. The hinge definitions are defined in Chapter 5 of the FEMA 356 (2000) guidelines.

As the analysis method was dynamic, the mass of the building is included in the model by inserting lumped masses at the columns acting in the direction of lateral motion. The masses do not contribute to the gravity loads. The lumped masses applied on each column of the model correspond to one quarter of the total storey weights presented in Table 5.2. Gravity loads were added to the columns and beams to simulate tributary dead and live loads.

The model was subjected to four spectrum compatible time histories for analysis. The time histories were made spectrum compatible by the computer program SYNTH (Naumoski, 2001). The histories were as follows: N-S component of the 1940 El-Centro earthquake; the 1995 Nahanni region earthquake located in Canada; the 1966 Parkfield earthquake record; and the 1992 Petrolia station record of the Cape Mendocino earthquake. These records are illustrated in Figure 5.5.

The roof displacement, base shear, and moment, and the interstorey displacements from the four earthquake records can be seen in Table 5.8 and Table 5.9 respectively.

It can be seen that the interstorey displacements are well under the maximum allowable drift of 95 mm allowed by the NBCC 2005. The analysis results also indicate that the beams and columns selected in the preliminary design are adequate as the peak axial force and moment interactions for the individual elements are below the values for the design forces. The values for the design forces are presented along with the analysis results in Section 6.3. The results of the analysis can be seen in Chapter 6. The analysis indicates that plastic hinges formed in the majority of the tension strips in the lower floors (1st storey through 6th). In 7th through 15th storey, plastic hinges formed in at least 2 tension strips. None of the time histories induced plastic hinging in the beams or columns.

5.6 Connection and Welding Details

The SPSW used in this example requires rigid beam-to-column connections throughout the steel plate shear wall to comply with the S16-09 Type D classification. This section reviews the connection design requirements of S16-09 as well as the CISC document “Moment Connections for Seismic Applications” (CISC 2008). The beam-to-column connections used for this example are extended end plate moment connections. However, other rigid connections are acceptable provided they meet the requirements of S16-09. The connection design illustrates several components of the connection between the beam and the column at level 14 of the SPSW designed according to the equivalent static force procedure as described in Section 5.4.2. The welding procedure of the infill panel depends on the thickness of the selected plate. Typically, earlier research on SPSW has focused on infill panel with a thickness of at least 3.0 mm. The upper floors of the SPSW designed using the nonlinear analysis requires plates that are less than 3.0 mm, and thus a different welding procedure is recommended.

5.6.1 Connection Details

The CISC document on seismic connections (CISC 2008) provides details for three types of connections: bolted unstiffened extended end plate moment connections, bolted stiffened extended end plate moment connections, and reduced beam section

connections. For the SPSW designed according to the equivalent static force procedure, bolted stiffened extended end plate connections are selected as the CISC guide allows for a beam flange thickness of up to 25 mm, which is close to the beam sections selected. For the beams selected based on the nonlinear dynamic analysis results, the beam flange thickness is smaller than 19 mm, which indicates that bolted unstiffened extended end plate moment connections can be used.

The beam-to-column connection is designed to have a factored resistance greater than the effect of the gravity loads and tension forces developed by the probable yield capacity of the infill panel as described in Clause 27.9.2.2 of CSA-S16-09, which occurs both above and below the beam. The beam element selected for the final design was a W410x149 section and the column was a W360x463 section both above and below the connection. The connection must also resist the shear introduced by a moment equal to $1.1R_y M_{pb}$ acting at the plastic hinge location where M_{pb} is the nominal plastic moment capacity, $Z_x F_y$. The reduced moment at the plastic hinge location is calculated using Clause 27.9.3.4 of S16-09 as:

$$M_{rpb} = 1.18 (1.1R_y M_{pb}) \left(1 - \frac{C_f}{\phi C_y} \right)$$

$$M_{rpb} = 1.18 \left(1.1 \times 1.1 \times [3280 \times 10^3 \text{ mm}^3 \times 350 \text{ MPa}] \right) \left(1 - \frac{2190 \text{ kN}}{0.9 \times 6720 \text{ kN}} \right)$$

$$M_{rpb} = 1046 \text{ kN} \cdot \text{m}$$

The column joint panel zone must resist the shear introduced by the plastic moment from the beam as well as the distributed load, w_g , from the beam and is calculated as:

$$V' = \frac{M_{rpb}}{d_b} + \frac{w_g L}{2}$$

$$V' = \frac{1046 \text{ kN} \cdot \text{m}}{0.381 \text{ m}} + \frac{32.8 \text{ kN/m} \times (7.6 \text{ m} - 0.435 \text{ m})}{2}$$

$$V' = 2860 \text{ kN}$$

with the length of the beam, L , considering the column depth on each side. The required thickness of the panel zone, w' , to resist the shear is calculated according to Clause 27.2.4.2 of S16-09 as:

$$V_r = 0.55 \times \phi \times d_c \times w' \times F_{yc} \geq V'$$

from which,

$$w' \geq \frac{V'}{0.55 \times \phi \times d_c \times F_{yc}}$$

$$w' \geq \frac{2860 \text{ kN} \times 1000 \text{ N/kN}}{0.55 \times 0.9 \times 435 \text{ mm} \times 350 \text{ MPa}}$$

$$w' \geq 38.0 \text{ mm}$$

where w' is the total column web thickness required; F_{yc} is the yield strength of the column; and all other terms as previously defined. The web of the column selected is 57.3 mm, which is adequate. For column panel zones that would require the web to be reinforced by the addition of doubler plates, the width-to-thickness ratio of the doubler plate is to be checked according to Clause(s) 27.2.4.3(b) and 13.4.1.1(a) of S16-09.

CISC (2008) recommends that the panel zone thickness with single sided connections be a minimum of:

$$w' \geq \frac{C_y M_{cf} \left(\frac{h - d_b}{h} \right)}{0.9 (0.6 R_{yc} F_{yc} d_c) (d_b - t_b)}$$

$$w' \geq \frac{0.774 \times 1150 \text{ kN} \cdot \text{m} \times \left(\frac{3800 \text{ mm} - 431 \text{ mm}}{3800 \text{ mm}} \right) \times 10^6 \text{ N} \cdot \text{mm/kN} \cdot \text{m}}{0.9 \times (0.6 \times 1.1 \times 350 \text{ MPa} \times 435 \text{ mm}) \times (431 \text{ mm} - 25.0 \text{ mm})}$$

$$w' \geq 21.5 \text{ mm}$$

where w' is the required panel zone thickness; h is the average storey height above and below the connection; $R_{yc} F_{yc}$ is the probable yield strength of the column; d_c and d_b are the respective depths of the column and beam; t_b is the thickness of the beam flange; and M_{cf} is the moment at the column centerline, defined by CISC (2008) as:

$$M_{cf} = M_{pb} + V_h (x + d_c / 2) = Z_x F_{yc} + V_h (x + d_c / 2)$$

$$M_{cf} = 3280 \times 10^3 \text{ mm}^3 \times 350 \text{ MPa} + 410 \text{ kN} \times (216 \text{ mm} + 435 \text{ mm} / 2)$$

$$M_{cf} = 1150 \text{ kN} \cdot \text{m}$$

where M_{pb} is the plastic moment resistance of the beam (the column plastic moment must be used for the top level due to heavy beam section); V_h is the shear at the plastic hinge location as defined in Figure 5.6; and x is the distance from the column face to the plastic hinge which can be assumed to form at $d_b/2$ from the column face. C_y is calculated as follows:

$$C_y = \frac{S_e}{C_{pr} Z_x}$$

$$C_y = \frac{2900 \times 10^3 \text{ mm}^3}{1.143 \times 3280 \times 10^3 \text{ mm}^3}$$

$$C_y = 0.774$$

where S_e is the elastic section modulus of the beam at the plastic hinge location; C_{pr} is a factor to account for the effects of strain hardening, local restraint and other connection conditions. C_{pr} is calculated as:

$$C_{pr} = \frac{F_y + F_u}{2F_y}$$

$$C_{pr} = \frac{350 \text{ MPa} + 450 \text{ MPa}}{2 \times 350 \text{ MPa}}$$

$$C_{pr} = 1.143$$

Since the required panel zone thickness is 21.5 mm and the actual thickness is 35.8 mm, the panel zone thickness for the selected column satisfies the CISC (2008) design guide requirement.

The strength of the beam to column connection is outlined in Clause(s) 27.9.6, which references Clause 27.4.4 of S16-09. Clause 27.4.4.1 requires the connection to maintain a resistance of at least M_{pb} through a minimum interstorey rotation of 0.02 rad, which is to be confirmed by physical testing. S16-09 offers an alternative to this clause in

Clauses 27.4.4.2 through 27.4.4.6. Clause 27.4.4.2 requires that the beam-to-column connection be designed for a moment resistance of at least $R_y M_{pb}$ and Clause 27.4.4.3 requires the column to be an I-shape section. Clause 27.4.4.4 gives specific details on the welding procedures for the connection, which are in accordance with the CISC moment connections guide. The clause requires that backing bars and runoff tabs be removed and replaced with fillet welds with the exceptions of top flange backing bars provided that they are continually fillet welded to the column flange on the edge below the complete penetration groove weld. S16-09 does not allow partial penetration groove or fillet to resist tensile forces in the connections. Clause 27.4.4.5 requires that the shear resistance of the connection be sufficient to resist the shear generated by the gravity load combined with the shear introduced by the moments at each end of $R_y M_{pb}$.

The CISC connection guide (CISC 2008) also has several provisions for welded joints used in the connections. The beam flange-to-plate joint requires a complete penetration groove weld, but weld access holes are not permitted. Each single bevel T-joint requires an 8 mm fillet weld on the inner flange face which serves as a backing. The root of the backing is then gouged to sound metal and the groove weld is completed in the horizontal position. The stiffeners in the bolted stiffened endplate connection require complete joint penetration double-bevel groove welds for the connection to the end plate and the beam flange. A complete joint penetration groove or fillet weld is required for the beam web to end plate joint. If fillet welds are used they must be placed on both sides of the web and the connection will be required to resist the flexural capacity of the web and the shear force at the column face.

Continuity plates, or column transverse stiffeners, are required on the column web at the location of the tension and compression flange of the beam if the bearing resistance of the column web and the tensile capacity of the column flange are exceeded. The demand on the column requires the full tensile and bearing capacity of the beam flanges, T_f and B_f respectively, which is calculated as:

$$T_f = B_f = 1.1 R_y F_y b_b t_b$$

$$T_f = B_f = 1.1 \times 1.1 \times 350 \text{ MPa} \times 265 \text{ mm} \times 25.0 \text{ mm}$$

$$T_f = B_f = 2800 \text{ kN}$$

The bearing and tensile capacities of the column, B_r and T_r respectively, are calculated according to Clause 27.4.4.3 and 21.3 of S16-09 as:

$$B_r = \phi_{bt} w_c (t_b + 10t_c) F_{yc}$$

$$B_r = 0.8 \times 35.8 \text{ mm} \times (25.0 \text{ mm} + 10 \times 57.4 \text{ mm}) \times 350 \text{ MPa}$$

$$B_r = 6000 \text{ kN} > 2800 \text{ kN}$$

and

$$0.6T_r = 7\phi t_c^2 F_{yc}$$

$$0.6T_r = 7 \times 0.9 \times (57.4 \text{ mm})^2 \times 350 \text{ MPa}$$

$$T_r = 12100 \text{ kN} > 2800 \text{ kN}$$

which indicates that continuity plates are not required.

CISC (2008) recommends the following equations to select the bolt grade and size to preclude bolt failure in tension (Equations 5.10 and 5.11) and shear (Equation 5.12) :

$$0.75A_b F_u \geq \frac{M_{cf}}{3.4(d_2 + d_3)} \quad 5.10$$

$$0.75A_b F_u \geq \frac{3.25 \times 10^{-6} p_f^{0.591} P_{cf}^{2.58}}{t_p^{0.895} d_{bt}^{1.91} t_s^{0.327} b_p^{0.965}} + T_b \quad 5.11$$

$$6A_b (0.5F_u) \geq V_{cf} \quad 5.12$$

where T_b is the minimum bolt tension given in Table 7 of S16-09; d_{bt} is the bolt diameter; P_{cf} is defined as $M_{cf} / (d_b - t_b)$; t_p is the thickness of the end plate; and F_u is the tensile strength of the bolt. The other terms in the equation are dependent on the connection details as shown in Figure 5.7 and are left to the designer to determine a suitable configuration. For bolted connections subjected to seismic loading, the bolts must be pre-tensioned (CISC 2008). They can be either of grade ASTM A490 or A325 and their size must not exceed 1-1/2 in.

Once the bolt diameter is selected, the end plate thickness can be selected to resist flexure and shear. To resist flexural forces, the end plate thickness is selected to be the larger of the following equations:

$$t_p \geq \frac{154 \times 10^{-6} \rho_f^{0.9} g^{0.6} P_{cf}^{0.9}}{d_{bt}^{0.9} t_s^{0.1} b_p^{0.7}} \quad 5.13$$

$$t_p \geq \frac{267 \times 10^{-6} \rho_f^{0.25} g^{0.15} P_{cf}}{d_{bt}^{0.7} t_s^{0.15} b_p^{0.3}} \quad 5.14$$

where t_p is the thickness of the endplate; and all other terms are based on the dimensions as shown in Figure 5.7. The CISC guide requires that the column flanges be at least as thick as the required endplate thickness.

5.6.2 Infill Panel Welding

Several methods and procedures for connecting the infill panel to the boundary members have been studied in the past including: welding, bolting, and epoxy connections (Schumacher *et al.* 1999, Berman and Bruneau 2005, 2008). The connection method of the infill panel to the boundary elements described in this report consisted of welding the infill panel to fishplates that are in turn welded to the beams and columns. The selected fish plate thickness is 6 mm, which is sufficient to allow commonly used flux-cored welding process for the fishplate to boundary member welds. A gap between the vertical and horizontal fish plate of 6 mm was recommended by Schumacher *et al.* (1999). The fish plate width selected is 100 mm to simplify alignment issues with the infill panel and for ease of handling. The fish plate detail can be seen in Figure 5.8.

The infill plate thickness used for the SPSW designed according to the equivalent static force procedure was 3.0 mm throughout the structure. The following outlines the basic procedure for welding of the 1.0 mm thick infill plate used in the SPSW designed according to the dynamic analysis procedure. For complete welding details regarding the connection of the thin infill panel to the fish plates, the reader should refer to the welding procedure implemented by Neilson *et al.* (2010), which was developed specifically for thin infill plates.

The welding procedure to connect the 1.0 mm infill panel to the fish plates requires attention due to the thickness of the infill panel. Neilson *et al.* (2010) found that short-

circuited gas metal arc welding was a suitable method of welding the thin plates due to the lower heat input and smaller weld sizes. The welding procedure consists of tack welding the plate to the fish plate at specific intervals, then stitch welding the plates at alternating intervals. This procedure helps to minimize distortion and burn through issues. Because of the limited widths available of cold rolled thin steel plates, the infill plate may have to be placed in two or more sections, requiring a splice between the plate sections. The largest plate width locally available at the time of writing were 1219mm (4') wide. A procedure used to splice the panels together is suggested by Neilson *et al.* (2010). Using a matching electrode, a fillet weld the same size as the plate thickness is sufficient to develop the capacity of the plate, thus a 1.0 mm fillet weld can be used.

The welds connecting the fish plates to the bounding elements are designed to be capable of yielding the infill panel. The probable yield of a unit strip of infill, 1.0 mm thick, is calculated as:

$$T_y = 1.1AR_yF_y$$

$$T_y = 1.1 \times 1.0 \text{ mm} \times 1.0 \text{ mm} \times 1.1 \times 350 \text{ MPa}$$

$$T_y = 424 \text{ kN/m}$$

The weld required to connect the fish plate to the boundary element is calculated according to Clause 13.13.2.2 of S16-09. For a weld metal compatible with the base metal, the required weld size, D , is obtained from:

$$V_{r, \text{weld metal}} = 0.67 \phi_w A_w X_u (1.00 + 0.50 \sin^{1.5} \theta) M_w$$

$$424 \text{ N/mm} = 0.67 \times 0.67 \times .707 \times D \times 1.0 \text{ mm} \times 490 \text{ MPa} \times (1.0 + 0.5 \sin^{1.5} 45^\circ) \times 1.0$$

$$D = 2.1 \text{ mm}$$

The welds selected for the fish plate-to-bounding element connection are selected as 6 mm double sided fillet welds.

5.6.3 Miscellaneous Requirements

The final beam and column sections selected are required by Clause 27.9.3.2 of S16-09 to form a moment resisting frame capable of resisting 25% of the applied factored storey shear force. This requirement is to ensure that, in the higher displacement cycles, when the infill plate has stretched, that the rigid frame can carry a significant portion of the seismic shear forces, thus avoiding excessive pinching of the hysteresis curves, which is one of the main characteristics of Type D plate walls. When calculating the beams flexural resistance for this condition, S16-09 allows the axial force in the beams and the effects due to gravity loads to be neglected (Clause 27.9.3.2). A moment frame consisting of the final beam and column sections is modeled in the analysis program SAP2000® and the loads applied to this model consist of 25% of the loads from the equivalent static force procedure applied as lateral loads at the beam-to-column connections. The resulting internal forces and displacements met the requirements of S16-09 and the NBCC 2005.

Clause 27.9.2.2 of S16-09 places an upper limit on the capacity design forces in that the forces need not exceed values corresponding to $R_d R_o = 1.3$. The analysis using the equivalent static force procedure is repeated on the final model in SAP2000® using the upper bound limit of $R_d R_o = 1.3$. The results of the analysis indicated that the forces in the beam and column elements calculated using capacity design principles were lower than the forces obtained from the upper bound analysis and do not require any further modification.

When flexural members are expected to form plastic hinges and remain stable through large deformations pass the point of plastic hinging, special attention must be paid to lateral bracing to ensure that these members remain stable during cyclic loading. The allowable laterally unsupported bracing length, L_{cr} , is determined from Clause 13.7(b) of S16-09 and is calculated as follows:

$$L_{cr} = \frac{r_y (17250 + 15500 \kappa)}{F_y}$$
$$L_{cr} = \frac{63.6 \text{ mm} \times (17250 + 15500 \times (1.0))}{350 \text{ MPa}}$$

$$L_{cr} = 5950\text{mm} < 7600\text{mm}$$

where r_y is the radius of gyration of the member about the weak axis and $\kappa = M_p / M_p = +1$ for double curvature (see Clause 13.6(a)). Thus lateral bracing is required for the beam elements as the beam span exceeds the allowable unsupported bracing length L_{cr} .

The column splices are selected according to Clause 27.9.4.3 of S16-09 to develop the flexural resistance of the smaller section at the splice together with the shear force imparted from plastic hinging at the column ends. S16-09 requires the splices to be located as close as possible to $0.25h_s$ (25% of the storey height) above the floor level.

The protected zones of the SPSW, as defined by S16-09, are to be free of structural and other attachments and any discontinuities created during fabrication and construction are required to be repaired. The protected zones on the SPSW include the infill panel, the beam ends and the column bases and their connections. The protected zones of the beams are limited to the area where inelastic straining is anticipated which is defined as the area from the face of the column flange to half of the beam depth past the theoretical beam hinging location. The protected zones in the columns include the areas where inelastic deformations are anticipated to occur. In addition, the columns are required to be stiffened at their base according to Clause 27.9.4.4 of S16-09 such that plastic hinging in the columns occurs above the baseplate or foundation beam. As a guide, Clause 27.8.2.7 of S16-01 is referenced, which requires columns to be stiffened to ensure plastic hinges form at a minimum distance of 1.5 times the column depth above the base plate. The section selected for the base column (W360x1086) has a depth of 570 mm, indicating that the columns be stiffened a minimum of 850 mm above the base of the SPSW.

Table 5.1 - Dead Loads

Roof Loads [kPa]		Storey Loads [kPa]	
Steel deck	0.10	Steel deck	0.10
Insulation	0.10	Carpeting	0.10
Steel allowance	0.15	Suspended ceiling	0.20
Suspended ceiling	0.20	HVAC/Wiring	0.25
HVAC/Wiring	0.25	Partitions	0.50
Asphalt and gravel	0.32	Steel allowance	0.56
		Concrete deck slab	2.55
Total	1.12	Total	4.26

Table 5.2 - Storey Weights and Seismic Information for a Single SPSW

Storey	W_x [kN]	h_x [m]	F_x [kN]	V_x [kN]	J_x	M_x [kN·m]
1	4260	3.8	15	1820	0.90	64400
2	4260	7.6	31	1810	0.92	58900
3	4260	11.4	46	1780	0.93	53300
4	4260	15.2	61	1730	0.94	47600
5	4260	19.0	77	1670	0.95	42000
6	4260	22.8	92	1590	0.96	36400
7	4260	26.6	107	1500	0.98	31000
8	4260	30.4	123	1390	0.99	25700
9	4260	34.2	138	1270	1.00	20700
10	4260	38.0	153	1130	1.00	18300
11	4260	41.8	169	980	1.00	11600
12	4260	45.6	184	810	1.00	10300
13	4260	49.4	199	630	1.00	4800
14	4260	53.2	214	430	1.00	2400
15	1490	57.0	213	210	1.00	800

Table 5.3 - Initial Infill, Beam and Column Selection

Storey	Level	V_x [kN]	w_{calc} [mm]	w_{select} [mm]	I_c [10^6 mm^4]	I_b [10^6 mm^4]	Column	Beam
	0					1340.71		W360x382
1	1	1940	2.03	3.0	255.15	—	W360x101	W410x100
2	2	1920	2.00	3.0	255.15	—	W360x101	W410x100
3	3	1880	1.96	3.0	255.15	—	W360x101	W410x100
4	4	1830	1.91	3.0	255.15	—	W360x101	W410x100
5	5	1760	1.83	3.0	255.15	—	W360x101	W410x100
6	6	1670	1.74	2.0	170.10	—	W310x129	W410x100
7	7	1570	1.64	2.0	170.10	—	W310x129	W410x100
8	8	1450	1.52	2.0	170.10	—	W310x129	W410x100
9	9	1320	1.38	2.0	170.10	—	W310x129	W410x100
10	10	1180	1.23	2.0	170.10	—	W310x129	W410x100
11	11	1020	1.06	1.0	85.05	—	W310x45	W410x100
12	12	840	0.88	1.0	85.05	—	W310x45	W410x100
13	13	650	0.67	1.0	85.05	—	W310x45	W410x100
14	14	440	0.46	1.0	85.05	—	W310x45	W410x100
15	15	220	0.23	1.0	85.05	1340.71	W310x45	W360x382

Table 5.4 - Preliminary Element Selection

Storey	Level	w [mm]	Column	Beam
	0			W760x582
1	1	3.0	W360x990	W410x149
2	2	3.0	W360x990	W410x149
3	3	3.0	W360x990	W410x149
4	4	3.0	W360x677	W410x149
5	5	3.0	W360x677	W460x193
6	6	2.0	W360x677	W410x149
7	7	2.0	W360x509	W410x149
8	8	2.0	W360x509	W410x149
9	9	2.0	W360x509	W410x149
10	10	2.0	W360x421	W460x193
11	11	1.0	W360x421	W410x149
12	12	1.0	W360x421	W410x149
13	13	1.0	W360x216	W410x149
14	14	1.0	W360x216	W410x149
15	15	1.0	W360x216	W760x582

Table 5.5 - Preliminary Design Force Effects

Storey	Level	Beam			Column		
		Axial [kN]	Shear [kN]	Moment [kN·m]	Axial [kN]	Shear [kN]	Moment [kN·m]
	0	3130	4510	3800			
1					39000	3430	9080
	1	2190	412	212			
2					32000	1370	1270
	2	2190	412	212			
3					29200	1370	1270
	3	2190	410	212			
4					26400	1370	1270
	4	2190	410	212			
5					23500	1450	1650
	5	2510	1250	1430			
6					19800	1090	1190
	6	1460	438	212			
7					17700	1030	1090
	7	1460	438	212			
8					15500	1030	1090
	8	1460	438	212			
9					13400	1030	1090
	9	1460	438	212			
10					11200	1100	1430
	10	1790	1270	1450			
11					8220	735	940
	11	732	438	212			
12					6800	668	850
	12	732	436	212			
13					5390	668	850
	13	732	436	212			
14					3970	668	850
	14	732	436	212			
15					2550	1430	3860
	15	1060	1770	1470			

Table 5.6 - Final Element Selection

Storey	Level	w [mm]	Column	Beam
	0			W760x582
1	1	3.0	W360x1086	W410x149
2	2	3.0	W360x1086	W410x149
3	3	3.0	W360x1086	W410x149
4	4	3.0	W360x990	W410x149
5	5	3.0	W360x990	W410x149
6	6	3.0	W360x990	W410x149
7	7	3.0	W360x900	W410x149
8	8	3.0	W360x900	W410x149
9	9	3.0	W360x900	W410x149
10	10	3.0	W360x744	W410x149
11	11	3.0	W360x744	W410x149
12	12	3.0	W360x744	W410x149
13	13	3.0	W360x463	W410x149
14	14	3.0	W360x463	W410x149
15	15	3.0	W360x463	W760x582

Table 5.7 - Final Design Force Effects

Storey	Level	Beam			Column		
		Axial [kN]	Shear [kN]	Moment [kN·m]	Axial [kN]	Shear [kN]	Moment [kN·m]
1	0	3130	4510	3780	49500	3430	10300
	1	2190	412	212			
2	2	2190	412	212	42500	1370	1280
	3	2190	412	212			
3	4	2190	412	212	39600	1370	1280
	5	2190	412	212			
4	6	2190	412	212	36800	1370	1270
	7	2190	412	212			
5	8	2190	412	212	33900	1370	1270
	9	2190	412	212			
6	10	2190	411	212	31000	1370	1270
	11	2190	411	212			
7	12	2190	411	212	28200	1370	1270
	13	2190	411	212			
8	14	2190	411	212	25400	1370	1270
	15	2190	411	212			
9	16	2190	410	212	22500	1370	1270
	17	2190	410	212			
10	18	2190	410	212	19700	1370	1270
	19	2190	410	212			
11	20	2190	410	212	16800	1370	1270
	21	2190	410	212			
12	22	2190	410	212	14000	1370	1270
	23	2190	409	212			
13	24	2190	409	212	11100	1370	1260
	25	2190	409	212			
14	26	2190	409	212	8250	1370	1260
	27	2190	409	212			
15	28	2190	409	212	5400	2140	4500
	29	3170	3150	3920			

Table 5.8 - Dynamic Analysis Results

Earthquake	Roof Displacement [mm]	Base Shear [kN]	Base Moment [kN·m]
El Centro	489	4437	134000
Nahanni	513	5102	151000
Parkfield	548	5047	131000
Petrolia	538	5090	143000

Table 5.9 - Peak Interstorey Displacements in Millimeters

Level	Earthquake Record			
	El Centro	Nahanni	Parkfield	Petrolia
1	16	16	16	19
2	20	22	21	25
3	21	24	22	25
4	24	29	26	29
5	31	36	33	35
6	36	39	38	37
7	41	40	43	37
8	45	41	46	38
9	46	41	48	41
10	51	44	52	49
11	61	56	66	67
12	58	56	67	67
13	52	51	63	58
14	46	43	54	49
15	37	33	42	38

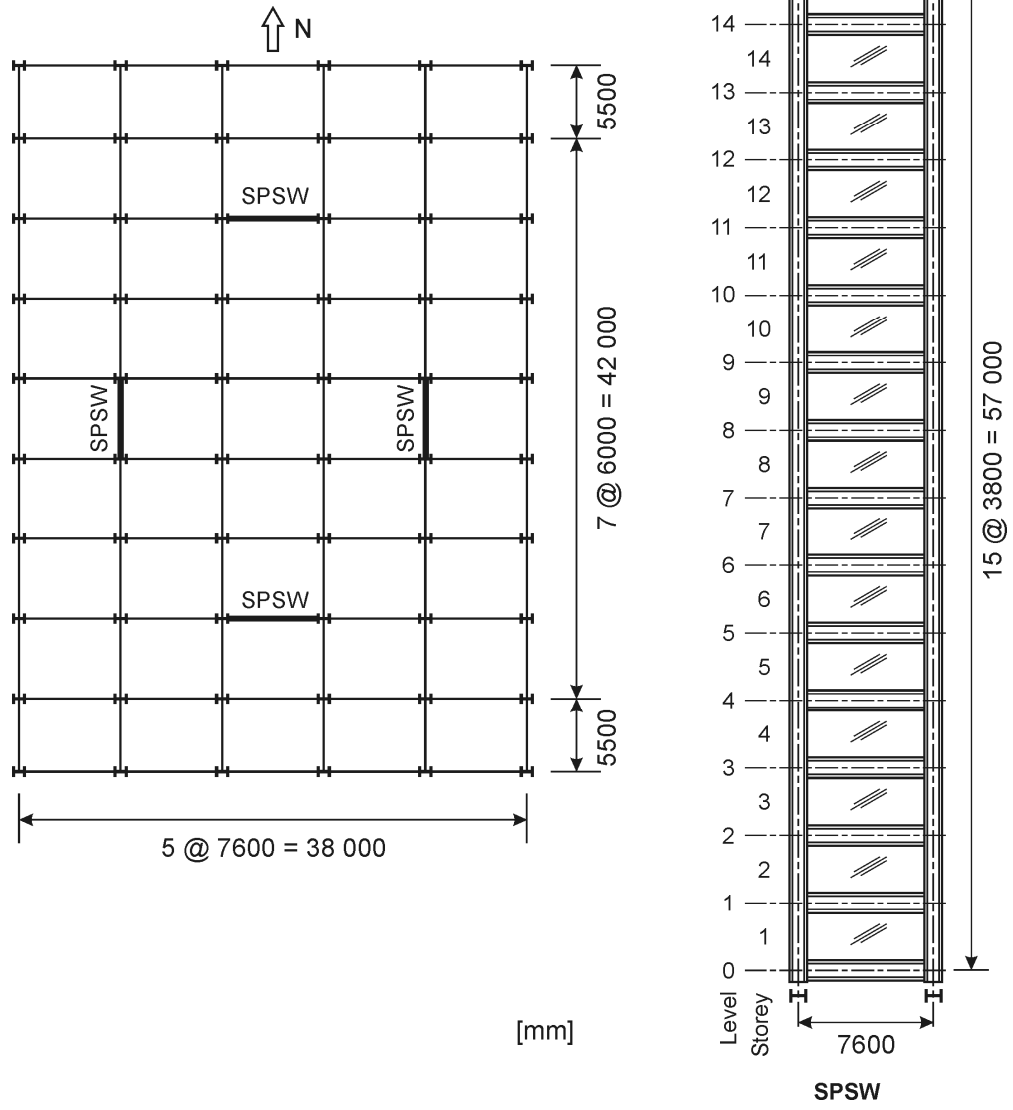


Figure 5.1 - Example Building Layout

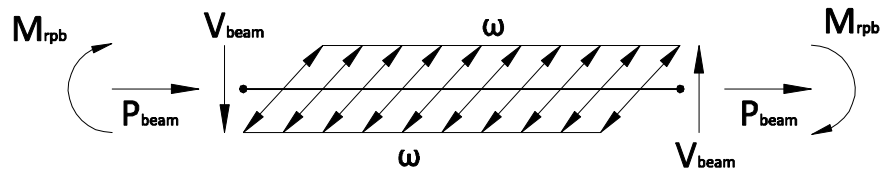


Figure 5.2 - Beam Forces Due to Infill Plate Yielding

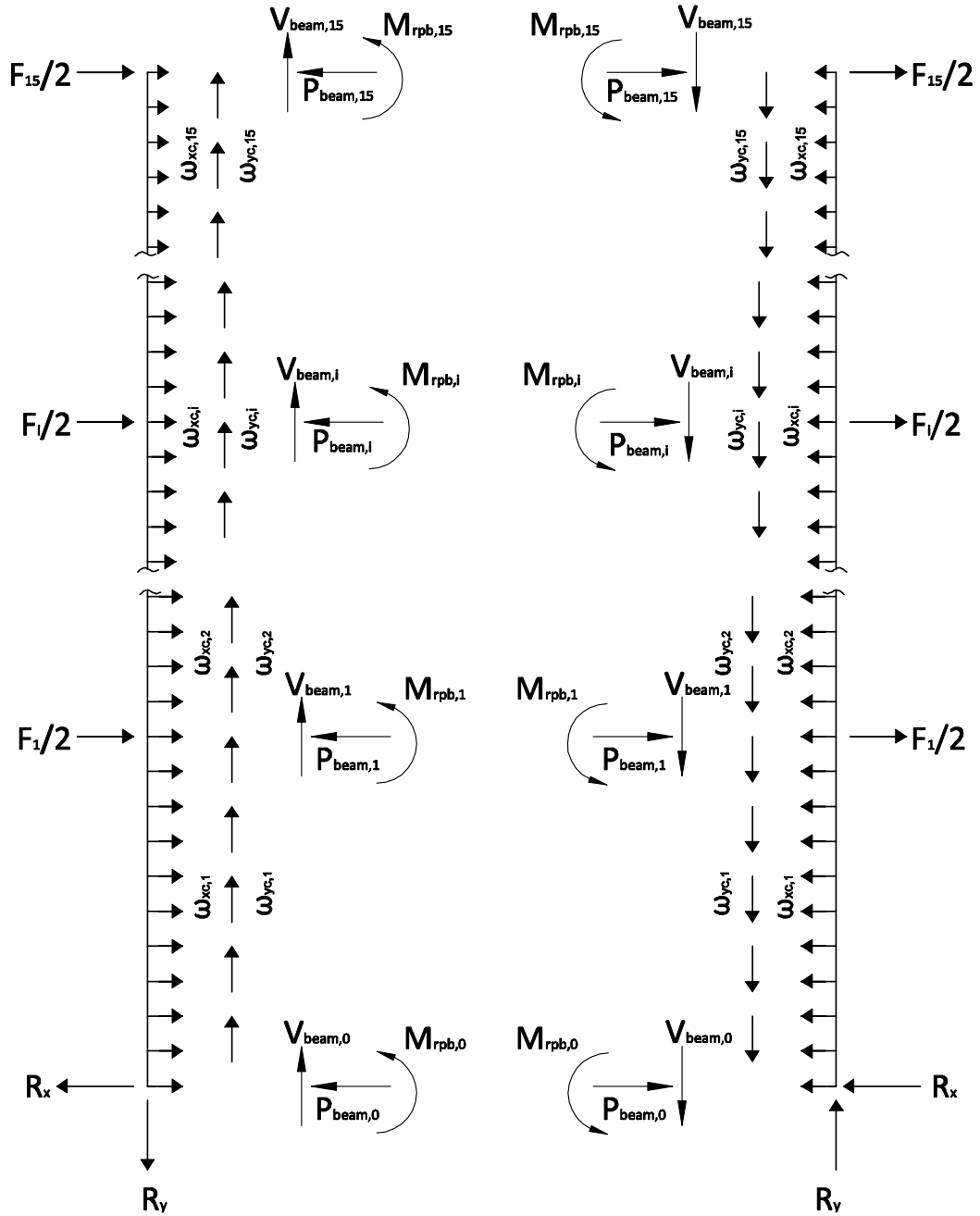


Figure 5.3 - Column Forces from Yielding of Infill Panel

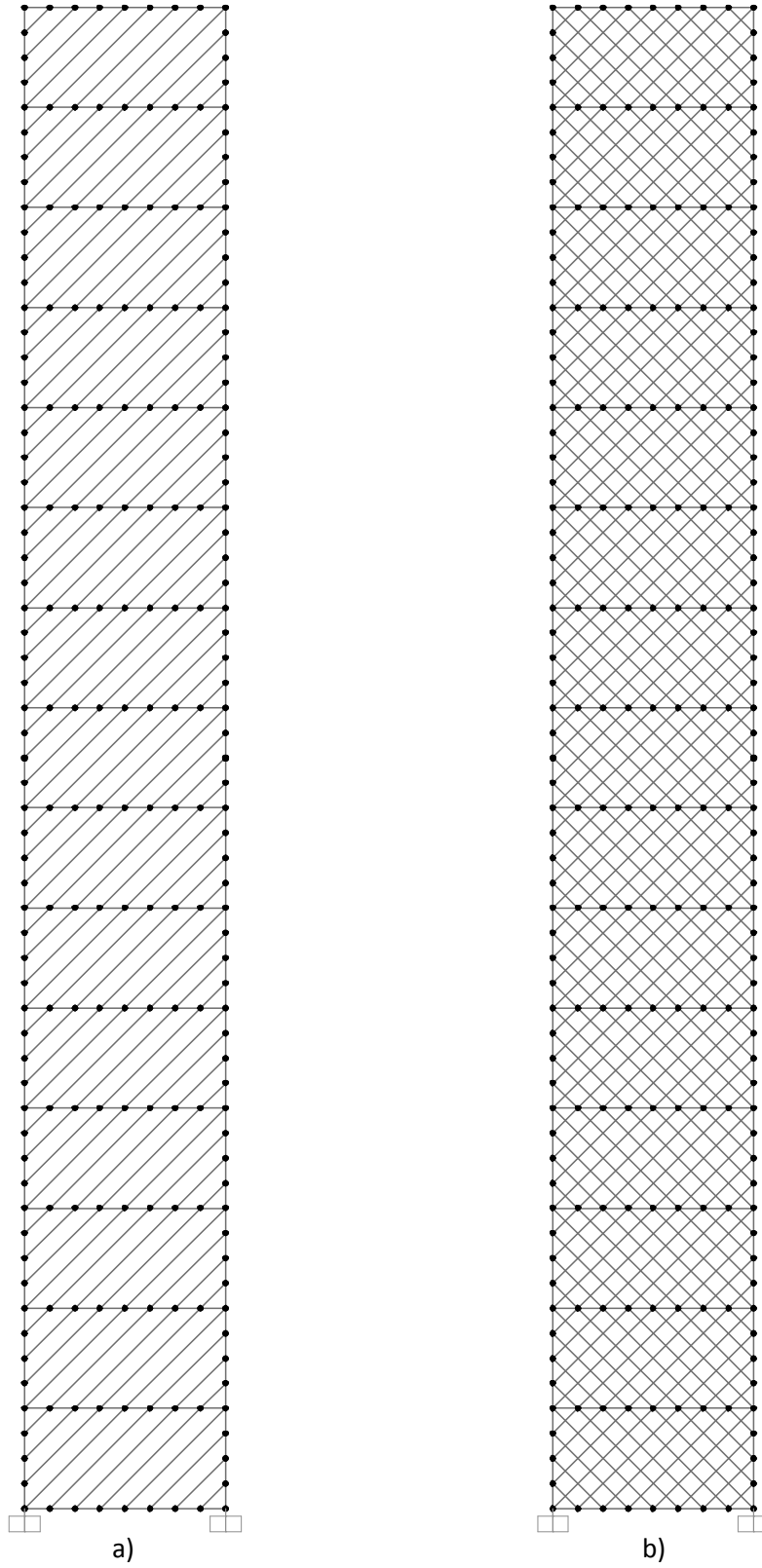


Figure 5.4 – 15-Storey Analysis Model Using; a) ESFP and b) Dynamic Analysis

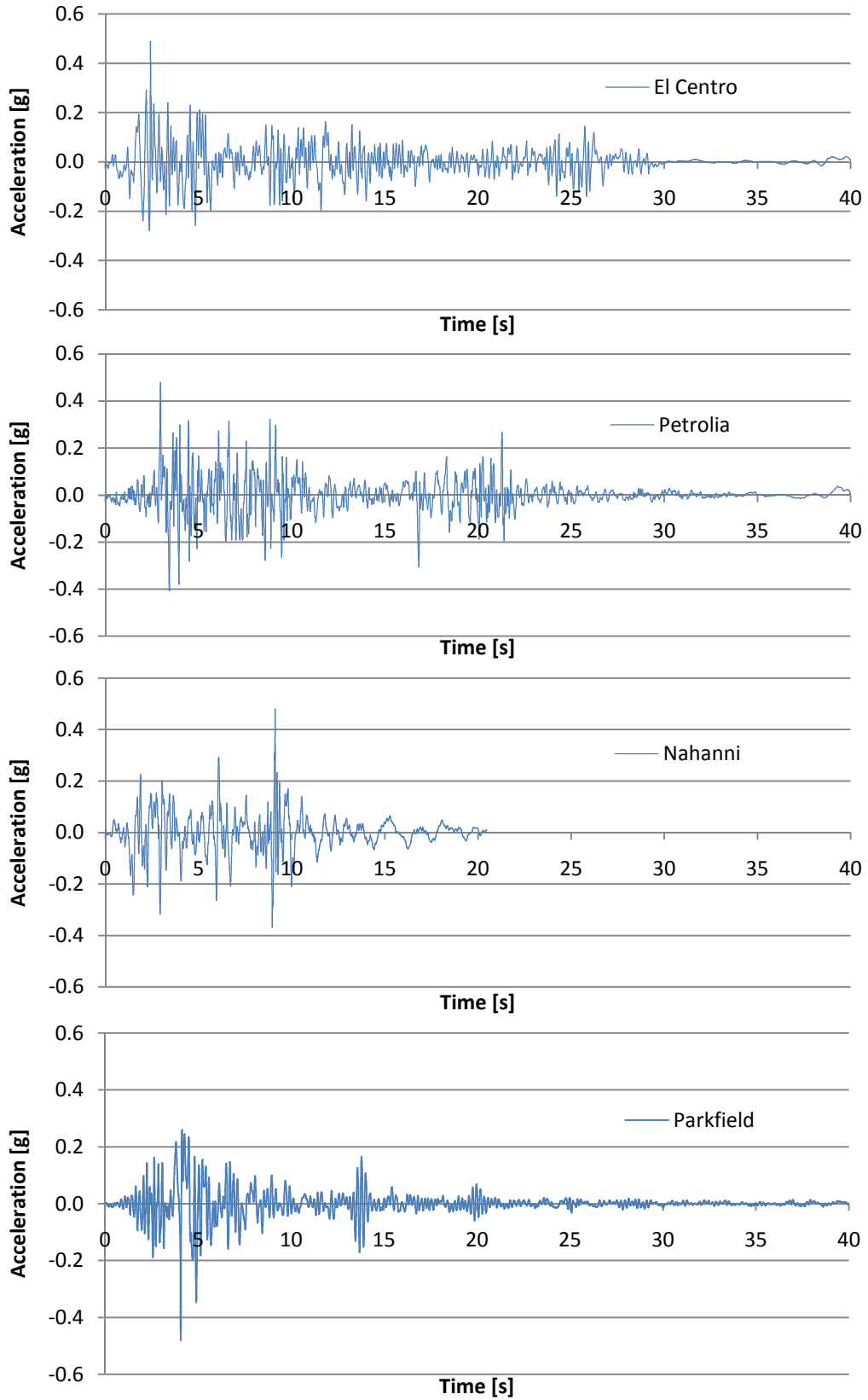
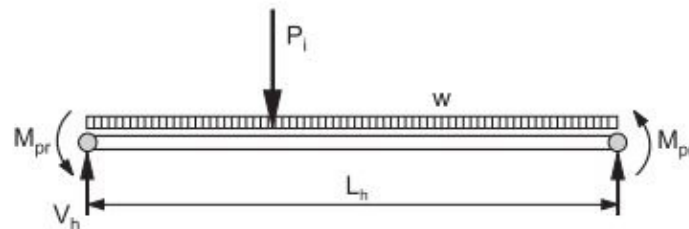
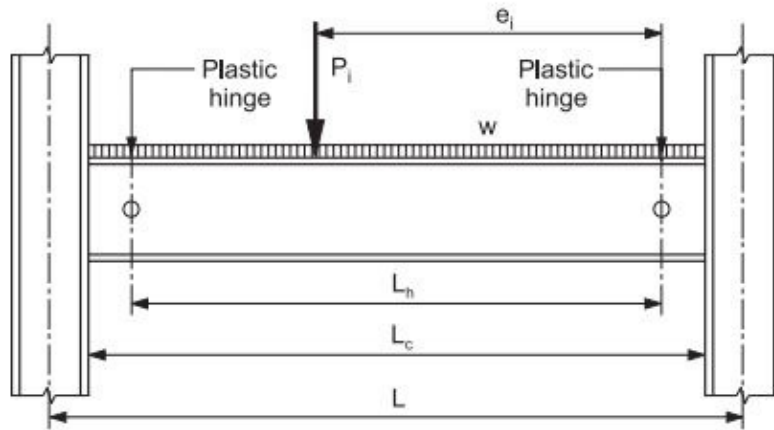


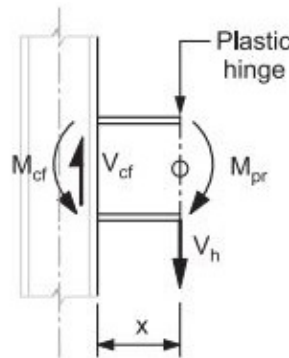
Figure 5.5 - Vancouver Spectrum Compatible Ground Motion Histories



Free-Body Diagram of Beam Segment between Plastic Hinges

$$V_h = V_E + V_G$$

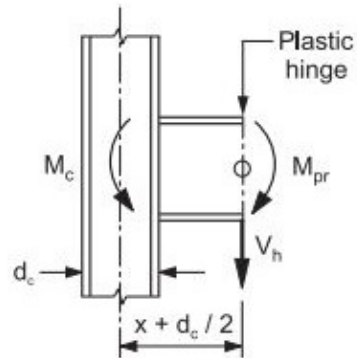
$$= \frac{2M_{pr}}{L_h} + \left(\frac{\sum e_i P_i}{L_h} + \frac{wL_h}{2} \right)$$



$$M_{cf} = M_{pr} + V_h x$$

$$V_{cf} = V_h + xw$$

Critical Section at Column Face



$$M_c = M_{pr} + V_h (x + d_c / 2)$$

Critical Section at Column Centreline

Figure 5.6 - CISC Seismic Connection Guide Shear and Moment Definitions (CISC 2008)

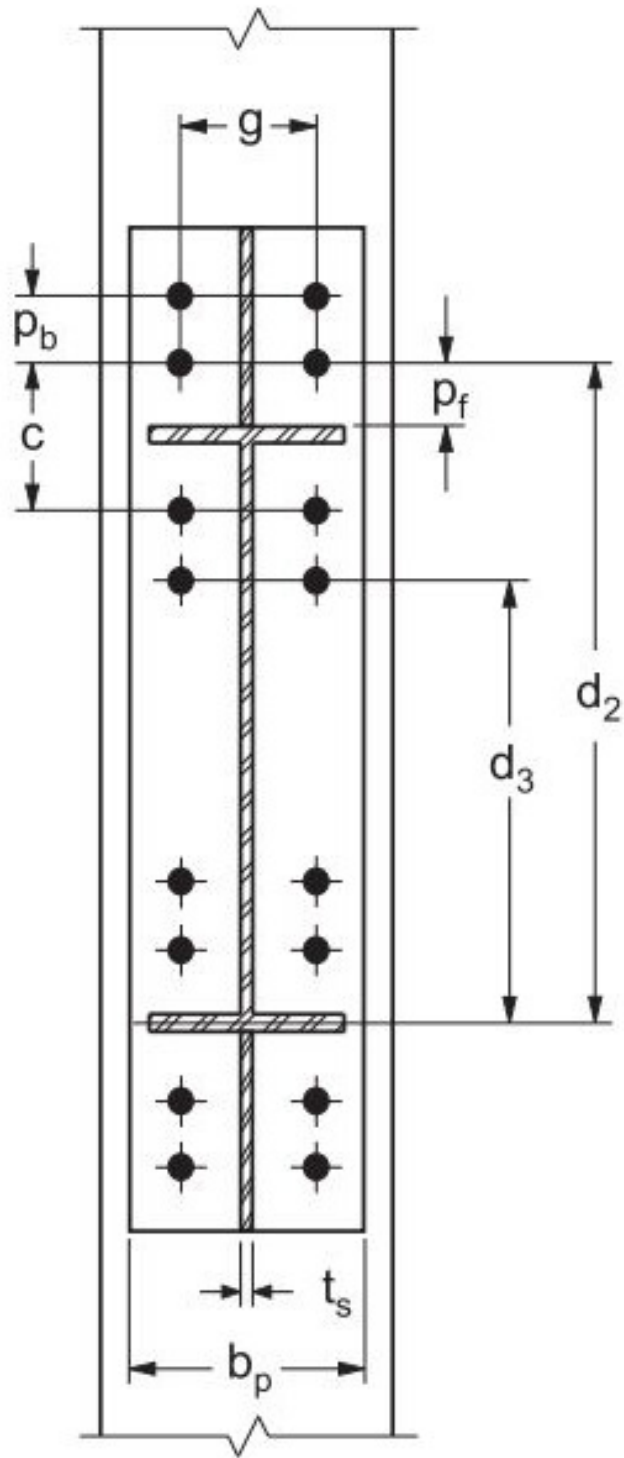


Figure 5.7 - Bolted Stiffened Connection Detail (CISC 2008)

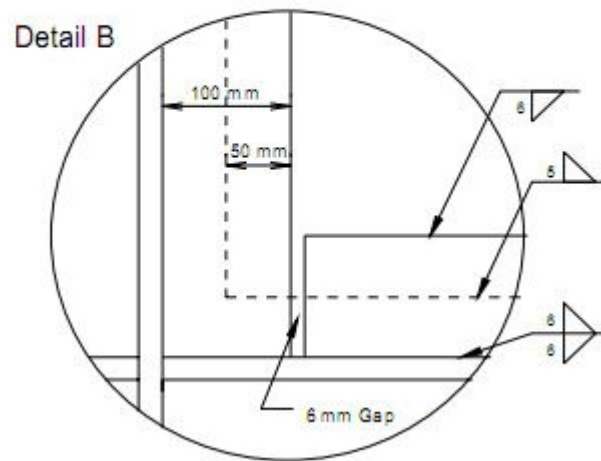
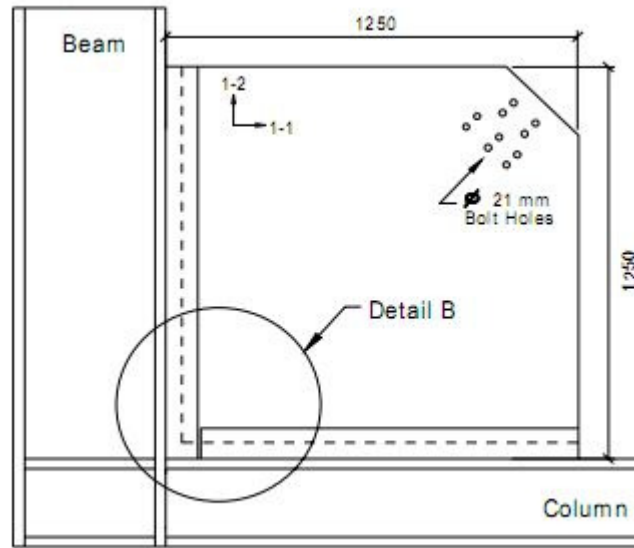


Figure 5.8 - Fish Plate Detail - Schumacher et al. (1999)

6. DISCUSSION

6.1 Introduction

This chapter discusses the results of both the static and dynamic analyses of the 15-storey SPSW designed in Chapter 5. It also presents a comparison of the dynamic analysis model with a similar model developed using the general purpose finite element program ABAQUS®. The ABAQUS® model was validated against several test results including quasi-static cyclic tests and a dynamic test.

6.2 Validation of the Dynamic Model

The strip model has been mostly used for conducting monotonic pushover analysis of SPSWs (Driver *et al.*, 1997; Shishkin *et al.*, 2005). This model has been shown to accurately capture the initial stiffness, ultimate capacity and hysteresis envelope of cyclic tests. Several methods have been proposed to reproduce the degradation of SPSWs after reaching the ultimate capacity (Driver *et al.*, 1997; Shishkin *et al.*, 2005; Choi and Park, 2009), however, the monotonic and quasi static tests are unable to capture certain aspects related to dynamic behaviour, such as the Bauschinger effect and participation from higher vibrational modes.

Recently, a few research projects have attempted to utilize tension only strips in both directions for dynamic and cyclic analysis of SPSWs. An eight storey SPSW model was created by Kulak *et al.* (2001) and used tension strips in both directions. The model was subjected to a nonlinear static pushover analysis as well as a nonlinear dynamic time history analysis using the program DRAIN-2DX (Prakash *et al.*, 1993). The static pushover analysis results were compared to the hysteresis envelope of the quasi-static cyclic test from Driver *et al.* (1997). The dynamic model was not validated against any dynamically tested specimens. The models created by Lubell (1997) used tension only strips in both directions using the software CANNY-E (Canny Consultants, 1996). The modeling was done for both monotonic and reverse cyclic loading, but not dynamic loading. The dynamic model was not validated against any other dynamically tested specimens. Elgaaly and Liu (1997) also conducted an analysis of four quasi-static cyclic tested specimens using bi-directional strips with the software ANSR-III (Oughourlian and Powell, 1982). Finally, Choi and Park (2010) performed a quasi-static cyclic analysis of

the 4-storey test specimen by Driver *et al.* (1997) and two 3-storey test specimens by Park *et al.* (2007) using bi-directional strips using the software OpenSees (Mazzoni *et al.*, 2006). It is clear that dynamic analysis models using the strip model have seldom been used in research despite being the preferred method by the NBCC 2005 and CSA-S16-09.

Bhowmick *et al.* (2009) modeled SPSWs using the FE software ABAQUS®. The infill panels, beams and columns were modeled using large displacement, finite strain, shell elements to capture all secondary effects, the infill panel buckling behaviour, and local buckling of the beams and columns. The model was validated using several monotonic and cyclic test results as well as a dynamic test. The dynamic validation was done using the results of a dynamic test on a 4-storey, reduced scale, steel plate shear wall conducted by Rezai (1999). The test specimen was subjected to a scaled time history record of the Tarzana Hill earthquake, shown in Figure 6.1, using a shake table. The ground motions from the earthquake were scaled to 140% of the recorded data. The same ground motion data was used as a time history input for the ABAQUS® model, and the top storey displacement results, shown in Figure 6.2, showed excellent agreement with the test results. The finite element analysis was able to predict the maximum top storey displacement test result to within 1%; however, due to the limitation of the shake table, the test specimen remained in the elastic region for the duration of the experiment. The same model parameters were used by Bhowmick *et al.* (2009) for a 15-storey SPSW, herein referred to as the shell model, which was subjected to four Vancouver spectrum compatible time history records previously shown in Figure 5.5.

A strip model similar to the shell model was created in SAP2000®, herein referred to as the strip model, and presented in detail in Chapter 3 and Chapter 4. The strip model was created using the same beam and column sections, and storey masses as those used by Bhowmick *et al.* (2009), and was subjected to the same four time history records. A comparison between the shell model and the strip model using peak base moment, shear, and top storey displacement for each earthquake record are presented in Table 6.1. The average displacement, base shear and base moment predicted by the strip model for the four time history records were within 12%, 9.0% and 5.0%, respectively, of the average results predicted by the shell model.

A comparison of the El Centro time history analysis between the shell model and the strip model is presented using the top storey displacement, base moment and base shear shown in Figure 6.3, Figure 6.4 and Figure 6.5, respectively. The strip model was able to capture the peak value for the base moment to within 5% and the top storey displacement and base shear to within 10%. In addition to the peak values, the strip model produced similar results over the entire range of the analysis.

A comparison of the first four periods of the shell model and the strip model is presented in Table 6.2, as well as the first four periods for the building designed in Chapter 5 (Design Building), which made use of lighter column sections than for the shell model and the strip model. Also presented in Table 6.2 are the periods determined using the NBCC equation (Equation 3.5) and by the equation proposed by Bhowmick *et al.* (2009) (Equation 3.6). The strip model displays a lower period than the shell model in all four modes, underestimating by 7.0%, 8.5%, 9.5% and 24% for the 1st through 4th modes, respectively. Part of the discrepancy between the periods may be attributed to the modeling of the infill plate as independent elements by the strip model. It can also be seen that the building designed in Chapter 5 exhibits slightly longer periods, which is expected due to the increased flexibility from the columns selected. As the period of the structure is required by the strip model to determine the Rayleigh damping coefficients for the dynamic analysis, the periods obtained for the shell model were used instead of those determined from the modal analysis of the strip model. The change of periods (and corresponding damping coefficients) did not have a significant effect on any of the subsequent force effects determined from the analyses and thus the periods obtained from the modal analysis were used.

The shell element model has several advantages over the strip models; it allows the user to ignore the angle of the tension field, α , and it accounts for the spread of plasticity instead of concentrating it at discrete points. However, shell element models are time consuming to implement and require a robust nonlinear solver to deal with cyclic buckling of the infill panel and overall yielding of the SPSW. The strip model offers a simplified approach and has been demonstrated to give results that are similar to the shell element model. The strip model with its discrete plastic hinges can be implemented on more economically accessible software.

6.3 Analysis Results

The analysis results are presented for the 15-storey SPSW designed using the dynamic method and the equivalent static force procedure modeled with the elements from Table 5.4 and Table 5.6, respectively. The deflections and element force effects that are presented are the peak values of the interstorey displacements, storey shear and moments, column moments and column axial loads. The peak values presented do not necessarily occur simultaneously. Also presented are the capacity design force effects for the buildings designed using the dynamic analysis and the equivalent static force procedure as determined in Chapter 5 (Table 5.5 and Table 5.7, respectively).

6.3.1 Storey Displacement

The elastic storey and interstorey displacements for the wind analysis and equivalent static force procedure using the final design elements are shown in Table 6.3. The inelastic interstorey drifts for the equivalent static force procedure are also presented. The inelastic interstorey drifts were obtained by multiplying the elastic interstorey drifts by $R_d R_o / I_E = 8.0$ as required by the NBCC. The elastic drifts from the wind and seismic analysis are almost identical which is expected given how close the loading pattern and total base shear for the two loading methods. The interstorey drifts for the dynamic analysis are presented in Table 6.4. The drift values for the dynamic analysis fall well below the NBCC limit using lighter sections and infill panels compared with the static analysis results.

Figure 6.6 shows the peak interstorey drifts from the wind loading analysis, the equivalent static force procedure (with inelastic amplification) and the dynamic analysis. The dynamic analysis results for the four time history records fall well below the NBCC limit of $0.025h_s$, which is defined by the vertical red line in the figure. All four of the time history drifts have similar curves, each indicating that the maximum drifts occur between the 11th and 13th floors. The “ESFP – Prelim” and “ESFP – Final” curve are the inelastic storey drifts of the building designed using the equivalent static force procedure. The “ESFP – Prelim” curve uses elements selected by the capacity design equations, which uses the same beams, columns, and infill plate thickness as the model used in the dynamic analyses. It can be seen that while the dynamic model is well under

the NBCC limit, the same model, using the loads from the equivalent static force procedure, has much higher interstorey drifts, and falls on or outside the acceptable limit at several storeys. The “ESFP – Final” curve represents the inelastic interstorey drifts of the model with the increased column and beam sizes and the increased infill plate thickness to meet the drift requirements. While the peak dynamic interstorey drifts occur at the upper levels, the “ESFP – Final” exhibits smaller interstorey drift ratios in the top stories due to the significant overstrength of the infill plates used (3.0 mm used vs. 1.0 mm required) to meet the NBCC drift requirements. The curve labelled Wind represents the interstorey drifts from the static wind analysis. The deflections obtained are from an elastic analysis and do not require any inelastic modifications. Design for the wind loads does not require capacity design principles.

6.3.2 Structure and Element Force Effects

The base shear, base moment, and the roof displacement obtained from the dynamic analysis are presented in Table 6.5 for all four time histories as well as for the static analyses (wind and seismic). The dynamic base shear and moment that occurred are significantly higher than the reactions predicted by the equivalent static force procedure for the structure which will be discussed later. Additionally, it can be seen that despite using four distinct time histories, the displacements, shears and moments are within 10% of each other, indicating the efficacy of the program SYNTH used to make the time history records spectrum compatible.

Figure 6.7 and Figure 6.8 show the peak storey moment and peak storey shear, respectively, from the dynamic analysis and equivalent static force procedure using the final design elements. The four results for both the shear and moment from the dynamic analyses are grouped together indicating that the spectrum compatible earthquakes obtain similar behaviour from the structure. The average base moment and shear from the dynamic analyses, 140000 kN·m and 4890 kN, respectively, are 2.2 and 2.5 times larger, respectively, than the values from the equivalent static force procedure. This is partially attributed to using thicker infill plates than required to resist the storey shear as well as the shear strength prediction for SPSWs in S16-09, which assumes that the infill panel resists 100% of the shear. It was observed that the average shear in the boundary columns at the base for the dynamic analyses was 1590 kN, which

represents 32% of the average base shear exhibited by the models. These results are similar to the results obtained by Bhowmick *et al.* (2009) where 30% of total average base shear was resisted by columns. These results indicate that a significant amount of shear strength can be overlooked by the Canadian standard. The storey shears from the dynamic analyses exhibit significantly larger values compared to the equivalent static force procedure, particularly in the upper four storeys.

The maximum moment in the left and right columns for the dynamic and static analyses can be seen in Figure 6.9 and Figure 6.10, respectively. The column moments from all four dynamic analyses follow similar patterns, and the left and right columns peak results for each storey are similar. The column moments from the wind and equivalent static force procedure analyses exhibit almost identical behaviour, which is expected as the loading pattern and total base shears are similar. In the case of the equivalent static force procedure and wind loading column moments, the left column exhibits a peak moment at the base which is 50% larger than the moment in the right column at the same location. The column results would be reversed had the static loads been applied on the opposite side of the SPSW. The dynamic moments are considerably larger than the static moments which can be attributed to the static storey shear estimation. As the storey shear forces were underestimated, the resulting moments from the shears are also significantly less than those seen determined from the dynamic analysis.

The peak axial forces in the left and right columns can be seen in Figure 6.11 and Figure 6.12, respectively, where tension is plotted as a positive value. The column axial force from each of the dynamic analyses is separated into peak compressive and tensile forces as each column undergoes full load reversals. Similar to the column moments, the dynamic analysis results show similar peak axial forces in the left and right columns. For the column forces from the static analyses, the equivalent static force procedure and the wind loading, only single curves are required as the loads were applied in only one direction. It can be seen in Figure 6.11 that for the static analyses methods, the axial force in the left column has compressive peaks in the upper floors and tensile peaks in the lower floors. This is due to the influence of the gravity loads combined with weaker tensile forces from the overturning moments in the upper storeys. The tensile forces from overturning moments in the lower storeys become sufficiently large to overcome

the effects from the gravity loads. In the right column, the overturning moment acts in conjunction with the gravity loads and it can be seen that the column axial force is compressive throughout the entire height of the structure. The left and right column axial forces from the static analysis are dependent on the direction of loading. Had the static loads been applied on the opposite side of the structure, the axial force effects of the left and right columns would be reversed.

6.3.3 Capacity Design Forces

The axial and shear forces and the bending moments derived using the capacity design equations for the left and right columns are presented in Figure 6.13, Figure 6.14, and Figure 6.15, respectively. Two curves are shown for the capacity design force effects in each figure, namely, “Capacity Design – Prelim” and “Capacity Design – Final”. These are the preliminary and final design force effects calculated in Chapter 5, Tables 5.5 and Table 5.7, respectively. The average force effects from the dynamic analysis are also presented as the “Dynamic Average” curve, and the column force effects from the equivalent static force procedure is presented as the “ESFP” curve. Finally, the force effects from a static analysis using the equivalent static force procedure and a ductility and overstrength modification factor of $R_d R_o = 1.3$ is presented.

The figures show that the column force effects obtained from a dynamic analysis or a static analysis are smaller than the force effects obtained from the capacity design equations. The large values of shear and moment observed at the top and bottom of the SPSW from the capacity design are due to the large stiffness of the beams required at the top and the bottom of the SPSW. The top and bottom level beam stiffness is significantly larger than the adjacent storey column stiffness resulting in the column forming a plastic hinge before the beam. Apart from the high shear force and bending moment at the top and bottom of the SPSW, the “Capacity Design – Final” curve increases in a linear fashion down the building height for the axial loads, and remains constant for the moment and shear force effects. This is due to the infill plate and beam sections remaining the same for all stories. The converse is observed for the “Capacity Design – Prelim” curve. At the storey locations where there is a change in infill plate thickness, and subsequent beam section size increase, small peaks can be seen in the shear and the moment curves.

S16-09 places a limit on the design force effects determined using capacity design principles. According to Clause 27.9.2.2, the limiting factor of $R_d R_o = 1.3$ is used in the calculation of the base shear for the structure. With this limit, the calculation of the seismic forces using the equivalent static force procedure, and subsequent analysis, result in the column force effects identified as "S16-09 - Limit". It can be seen that the axial force in the upper stories using the capacity design equations are slightly larger than the S16-09 limit. While a reduction in column size may be possible, the deflection requirements of the NBCC must still be satisfied. The moments and shear forces from the capacity design calculations fall under the S16-09 limit except in the top storey of the preliminary design, and the upper four storeys of the final design. The upper storey force effects are significantly larger than the S16-09 limit due to the required stiffness of the upper beam.

6.3.4 System Overstrength

The analysis using the equivalent static force procedure indicated that no hinges formed in the beam, column, or tension strip elements. The analysis using the dynamic method indicated that hinging did not occur in any of the beams or columns, however, the majority of the strips in the lower floors (1st through 6th floor) yielded. This is partly due to the fact that the frame was overdesigned. The capacity design equations are based on the assumption of all infill panels yielding simultaneously (Berman and Bruneau, 2003). Research has shown that this is unlikely to happen, especially in the upper stories of taller structures (Bhowmick *et al.*, 2009). Additionally, as it is unlikely that the upper storey infill plate will yield, the stiffness requirement of the top storey beam adds significant overstrength to the frame. As well, neglecting the column shear strength contribution by the design equations, both design methods, specifically the equivalent static force procedure, had infill plates larger than required, and consequently, beams and columns that were larger than required. This was also a contributing factor to the overstrength of the system.

6.4 Comparisons of Analysis Methods

A SPSW was designed and analyzed using two different methods accepted by the NBCC. The preferred method of analysis, the dynamic procedure, resulted in a design that used

thinner infill plates and lighter beams and columns throughout the entire structure. The equivalent static force procedure resulted in a preliminary design that satisfied the capacity design equations, but failed to satisfy the NBCC drift requirement after inelastic effects were accounted for by the inelastic amplification factor.

The ratio of dynamic analysis results to the equivalent static force procedure results for storey shears and moments, shown in Table 6.6 and Table 6.7, respectively, varied from 1.68 to 3.90, with an average of 2.45 for the storey shear and 2.54 for the storey moments. These ratios are comparable to the results obtained by Kulak *et al.* (1999), where an average ratio of 2.46 was obtained for the storey shears using 20 time histories. Kulak *et al.* (1999) concluded that these results indicate weak storeys do not appear at these load levels and small interstorey drifts. Additionally, the inelastic straining in the beams and columns are restricted as the storey drifts remain small.

The natural period of the building for the equivalent static force procedure determined using the NBCC equation was significantly lower than the value determined using the strip model as well as the shell model. Using Equation 3.6 would result in a 64% increase in the natural period to 1.71 s (NBCC equation gives 1.04 s), which reduces the base shear from the equivalent static force procedure by approximately 25%. The reduction in base shear, and consequently, storey shear, would allow for a SPSW design comparable to that obtained by the dynamic design.

Table 6.1 - Comparison of 15-Storey Models; Shell Model and Strip Model

Earthquake Record	Shell Model			Strip Model		
	Roof Displacement [mm]	Base Shear [kN]	Base Moment [kN]	Roof Displacement [mm]	Base Shear [kN]	Base Moment [kN]
El Centro	489	6260	228000	521	5690	212000
Nahanni	487	6950	196000	526	6550	214000
Parkfield	450	6260	197000	514	6450	199000
Petrolia	437	6400	209000	554	7550	204000

Table 6.2 - Periods of SPSWs

Mode	Calculated periods of 15-Storey SPSWs [s]			Predicted Periods [s]	
	Shell Model	Strip Model	Design Building	NBCC	Bhowmick
1 st	3.01	2.8	3.33	1.04	1.71
2 nd	0.82	0.75	0.94	—	—
3 rd	0.42	0.38	0.47	—	—
4 th	0.29	0.22	0.26	—	—

Table 6.3 - Drift Values from Static Analyses; Final Design

Level	Wind Drift [mm]		ESFP Drift [mm]		
	Storey Drift	Interstorey Drift	Storey Drift	Interstorey Drift	Inelastic Drift
1	6.8	6.8	6.9	6.9	55.2
2	16.3	9.5	16.5	9.6	76.8
3	25.7	9.4	26.0	9.5	76.0
4	35.4	9.7	35.8	9.8	78.4
5	45.3	9.9	45.8	10	80.0
6	55.3	10.0	55.8	10	80.0
7	65.3	10.0	65.8	10	80.0
8	75.1	9.8	75.7	9.9	79.2
9	84.7	9.6	85.4	9.7	77.6
10	94.1	9.4	94.8	9.4	75.2
11	103.1	9.0	103.9	9.1	72.8
12	111.8	8.7	112.6	8.7	69.6
13	120.1	8.3	121.0	8.4	67.2
14	127.9	7.8	128.8	7.8	62.4
15	134.7	6.8	135.7	6.9	55.2

Table 6.4 - Interstorey Drift Values from Dynamic Analysis

Level	Earthquake Record			
	El Centro [mm]	Nahanni [mm]	Parkfield [mm]	Petrolia [mm]
1	16	16	16	19
2	20	22	21	25
3	21	24	22	25
4	24	29	26	29
5	31	36	33	35
6	36	39	38	37
7	41	40	43	37
8	45	41	46	38
9	46	41	48	41
10	51	44	52	49
11	61	56	66	67
12	58	56	67	67
13	52	51	63	58
14	46	43	54	49
15	37	33	42	38

Table 6.5 - Base Reactions and Top Storey Displacements of Dynamic and Static Models

Earthquake Record	Design Building		
	Roof Displacement [mm]	Base Shear [kN]	Base Moment [kN · m]
El Centro	489	4437	134000
Nahanni	513	5102	151000
Parkfield	548	5047	131000
Petrolia	538	5090	143000
ESFP	136 ¹	1940	64400
Wind	135	2100	63800

¹ The roof displacement given is the elastic displacement without the NBCC inelastic amplification factor

Table 6.6 - Storey Shear Ratio; Dynamic Analysis/ESFP

Storey	El Centro	Nahanni	Parkfield	Petrolia
15	1.92	1.82	2.30	2.10
14	3.08	2.99	3.74	3.39
13	3.07	3.07	3.78	3.38
12	2.76	2.86	3.44	3.00
11	2.42	2.54	3.05	2.79
10	2.19	2.27	2.78	2.42
9	2.00	2.25	2.71	2.20
8	1.82	2.22	2.58	2.01
7	1.70	2.19	2.40	2.02
6	1.68	2.18	2.26	2.15
5	1.76	2.21	2.17	2.28
4	1.84	2.23	2.10	2.39
3	2.01	2.40	2.19	2.48
2	2.13	2.52	2.35	2.55
1	2.23	2.63	2.60	2.62
Minimum	Maximum	Average	Standard Deviation	
1.68	3.78	2.45	0.49	

Table 6.7 - Storey Moment Ratio; Dynamic Analysis/ESFP

Storey	El Centro	Nahanni	Parkfield	Petrolia
15	1.92	1.84	2.31	2.11
14	3.39	2.67	3.35	3.05
13	3.90	2.93	3.65	3.30
12	3.16	2.27	2.80	2.49
11	3.55	2.85	3.47	3.03
10	2.69	2.34	2.82	2.49
9	2.78	2.49	3.01	2.74
8	2.57	2.32	2.83	2.62
7	2.39	2.25	2.68	2.48
6	2.23	2.25	2.55	2.34
5	2.10	2.25	2.42	2.21
4	2.01	2.26	2.30	2.12
3	1.96	2.28	2.19	2.12
2	1.94	2.31	2.08	2.15
1	2.09	2.35	2.03	2.21
Minimum	Maximum	Average	Standard Deviation	
1.84	3.90	2.54	0.48	

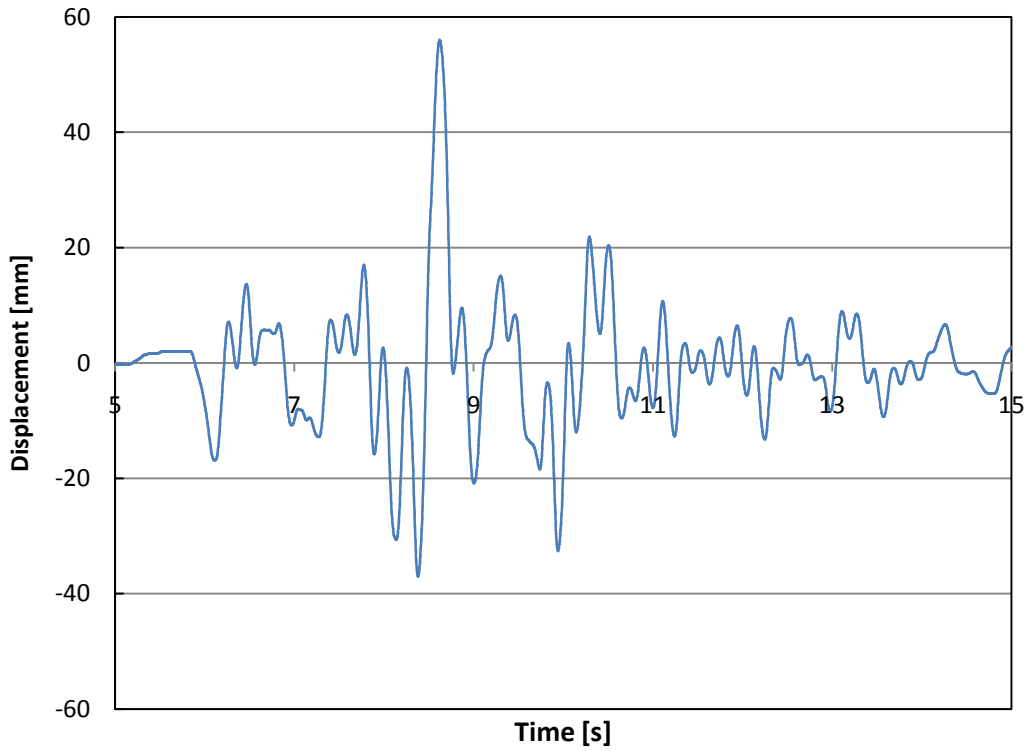


Figure 6.1 - 140% Tarzana Hill Ground Displacement Record

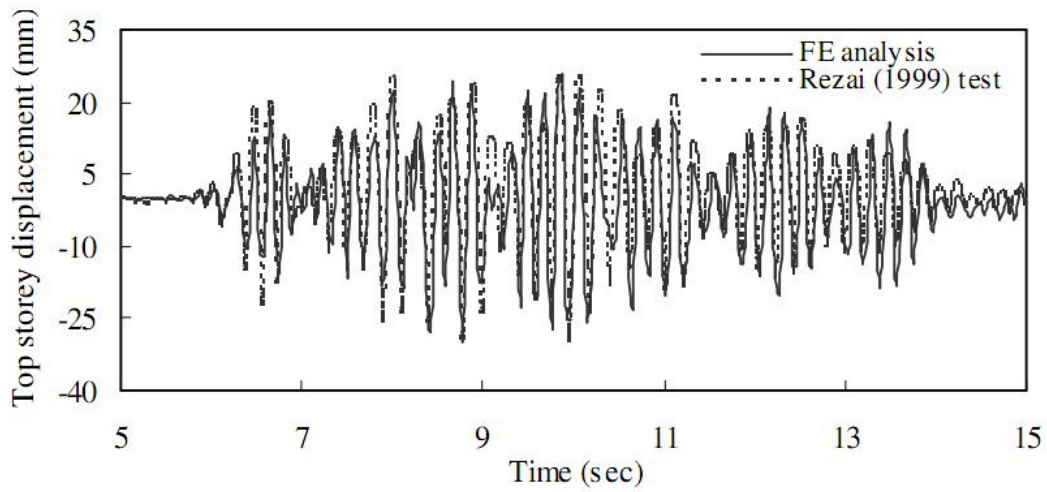


Figure 6.2 - Time History Comparison of Top Storey Displacement from the 4-storey Model; 140% Tarzana Hill Record (Bhowmick et al., 2009)

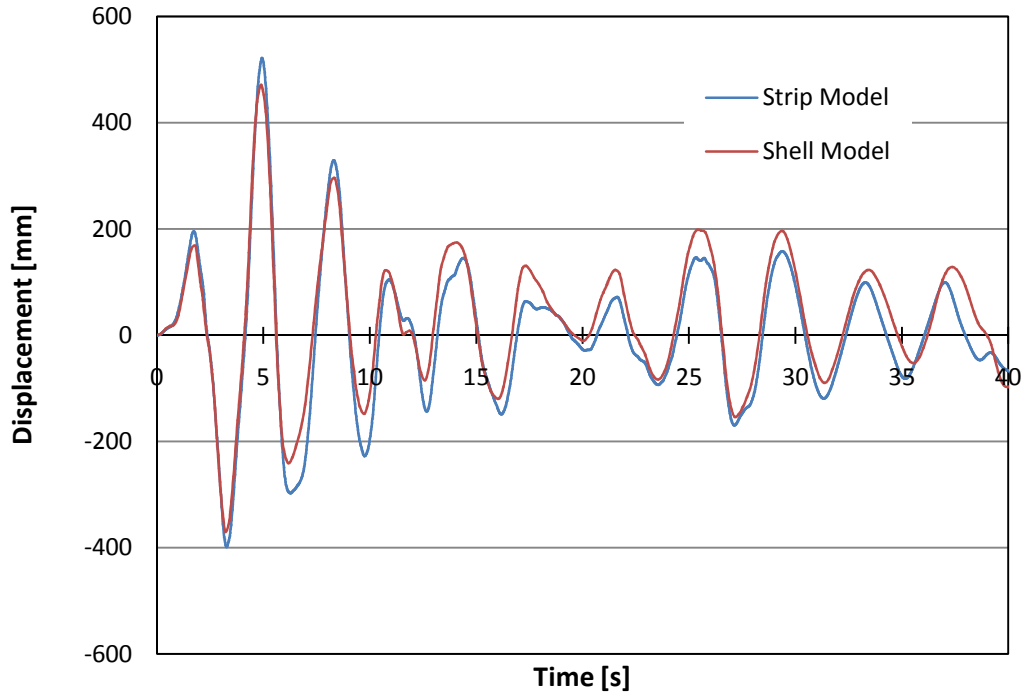


Figure 6.3 - Time History Comparison of the Top Storey Displacement from the 15-Storey Model (El Centro Earthquake)

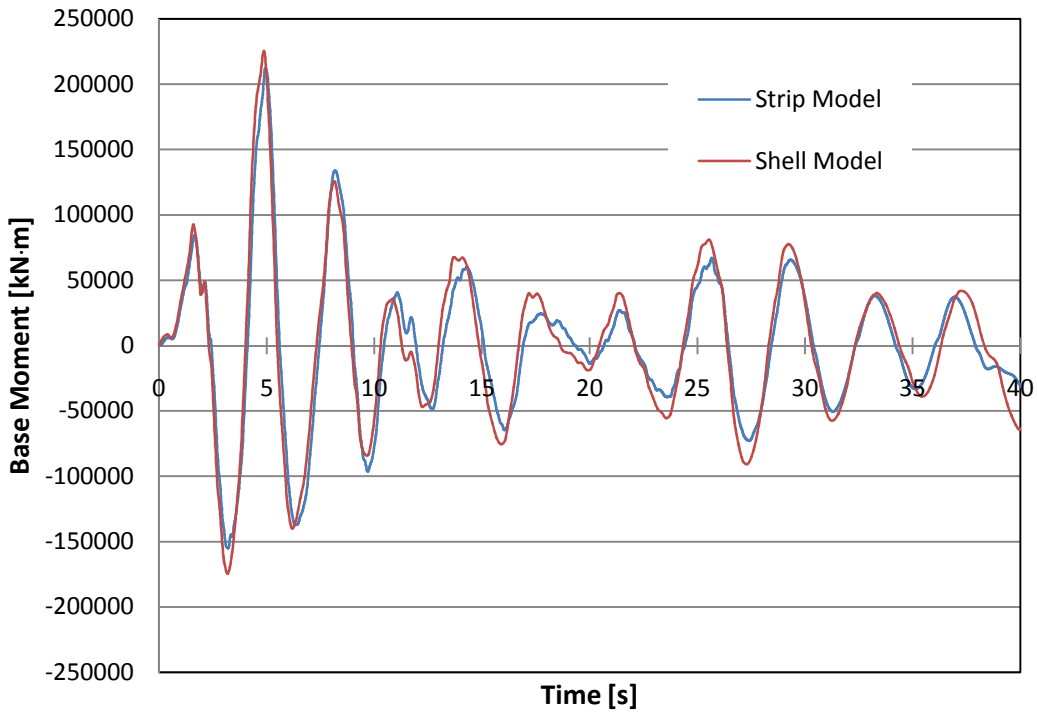


Figure 6.4 - Time History Comparison of the Base Moment from the 15-Storey Model (El Centro Earthquake)

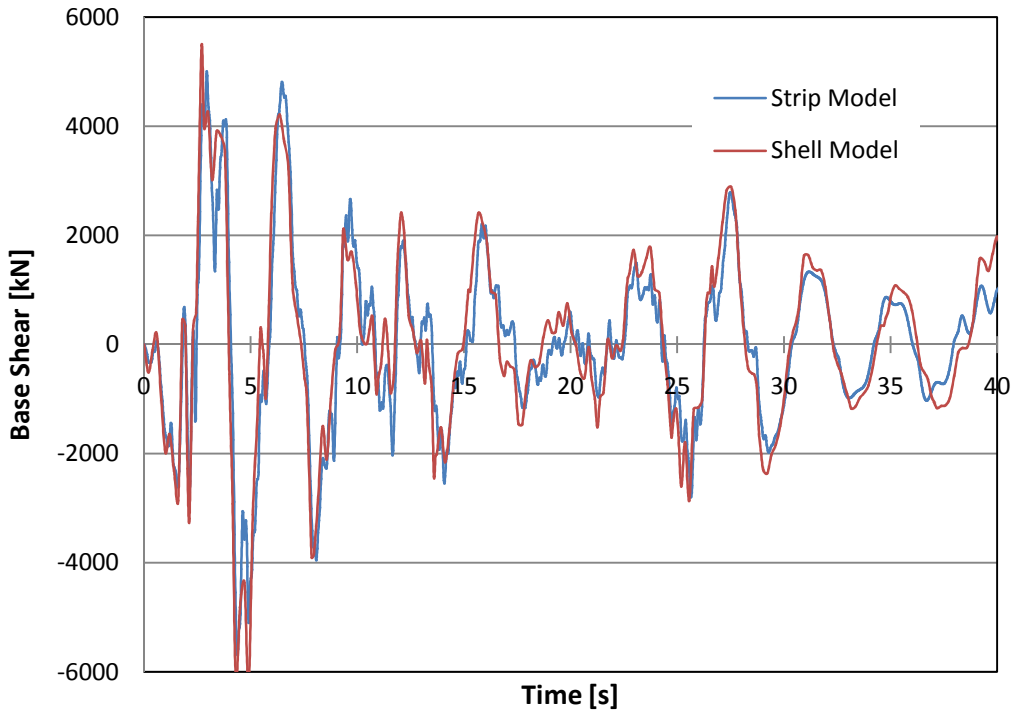


Figure 6.5 - Time History Comparison of the Base Shear from the 15-Storey Model (El Centro Earthquake)

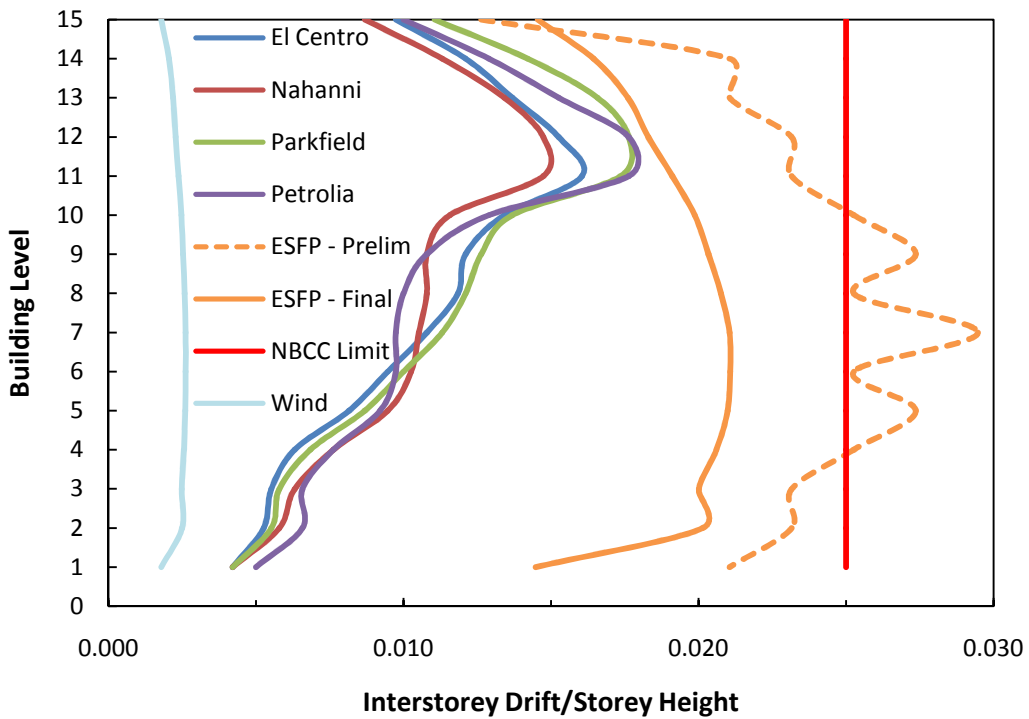


Figure 6.6 - Interstorey Drift from Dynamic and Static Analyses, and NBCC Limit

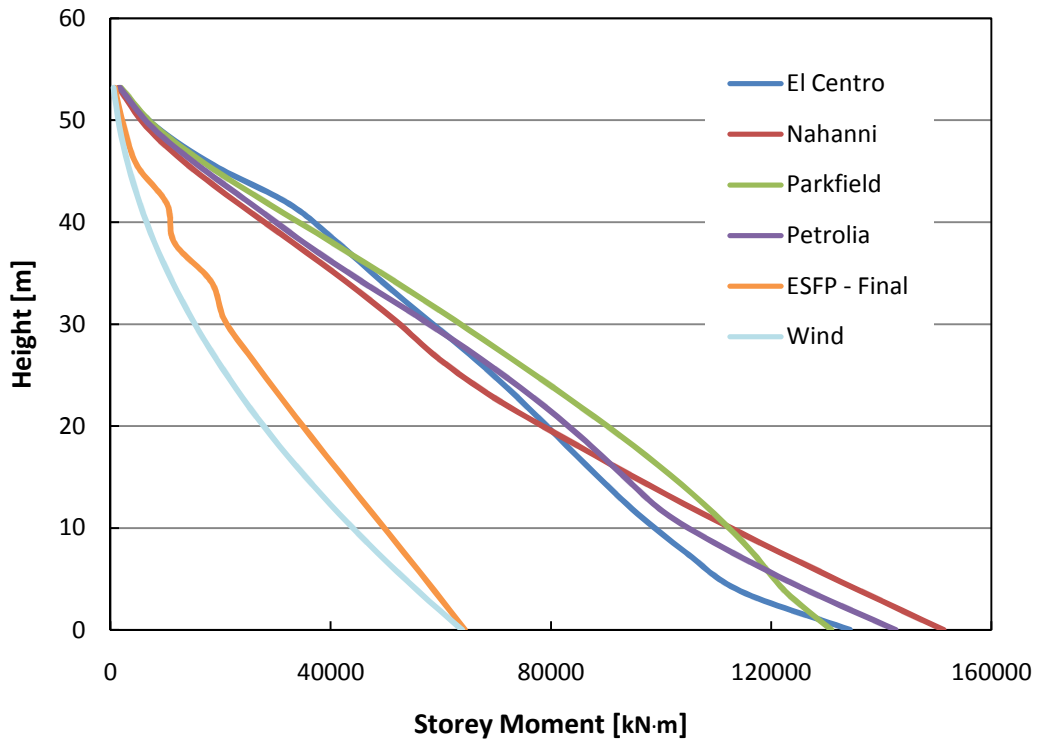


Figure 6.7 - Peak Storey Moments

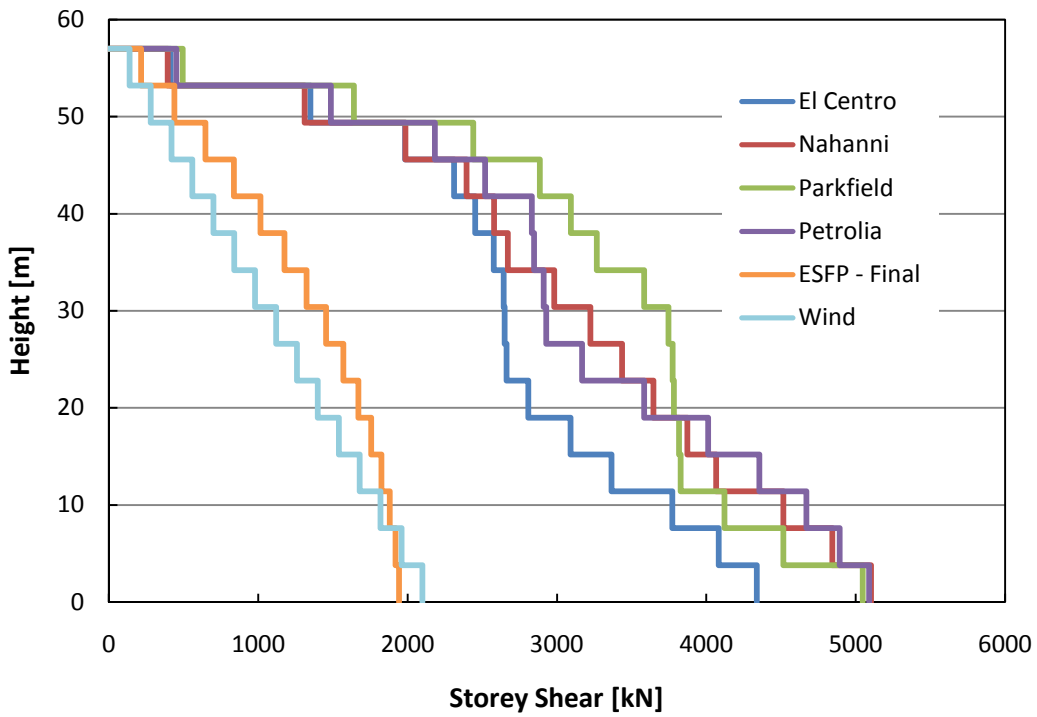


Figure 6.8 - Peak Storey Shears

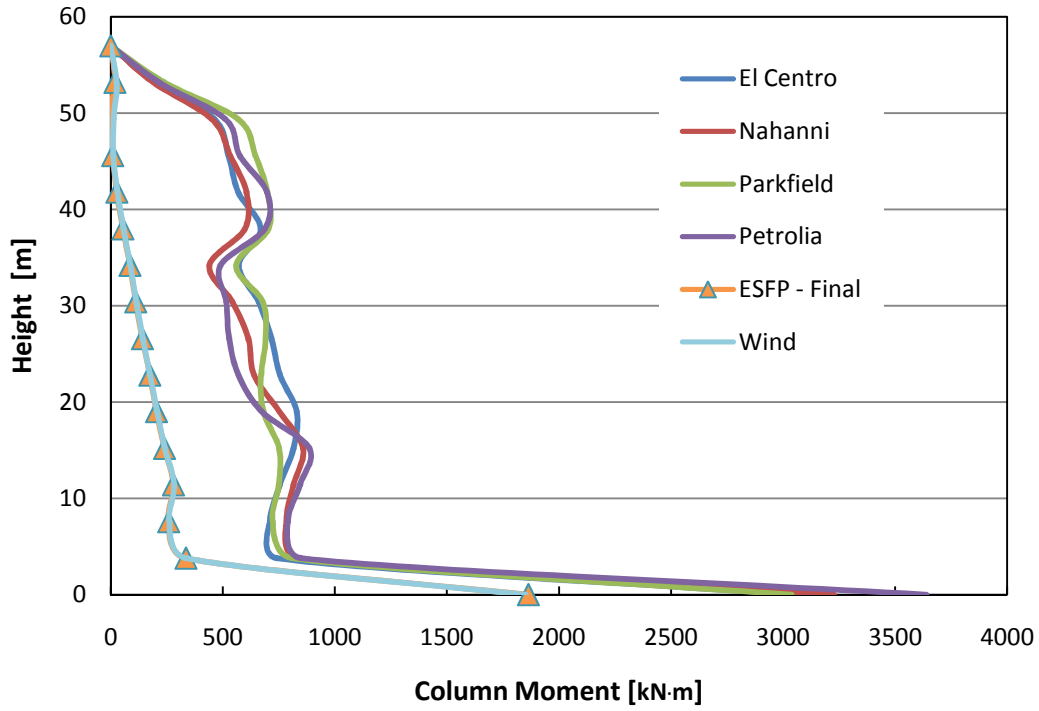


Figure 6.9 - Maximum Moment; Left Column

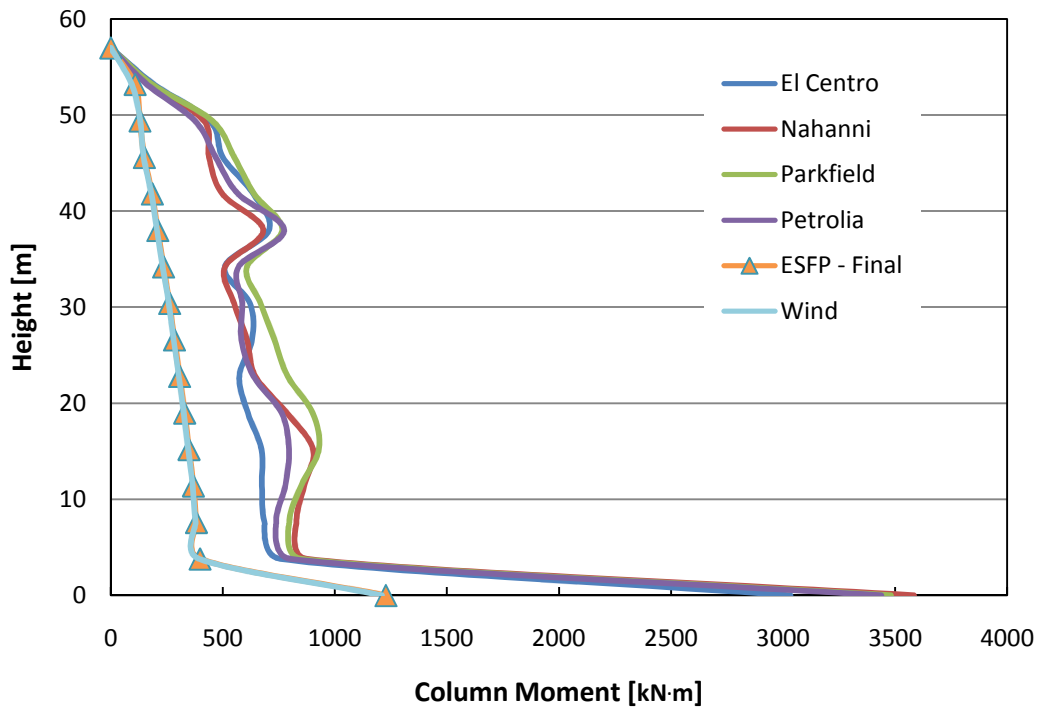


Figure 6.10 - Maximum Moment; Right Column

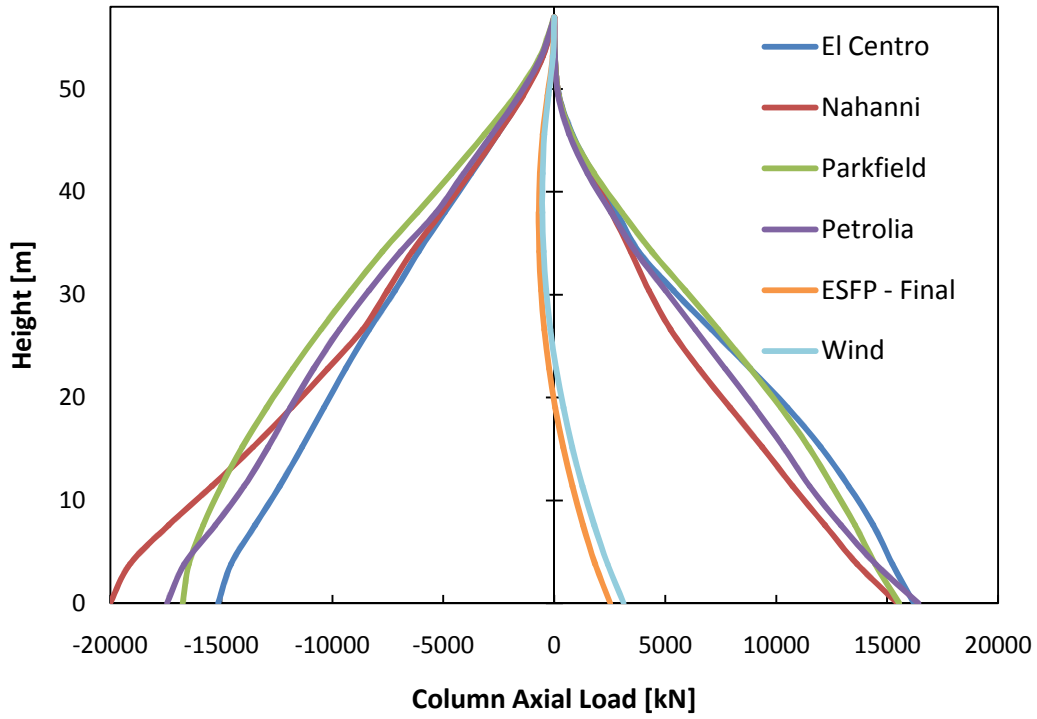


Figure 6.11 - Maximum and Minimum Axial Load; Left Column

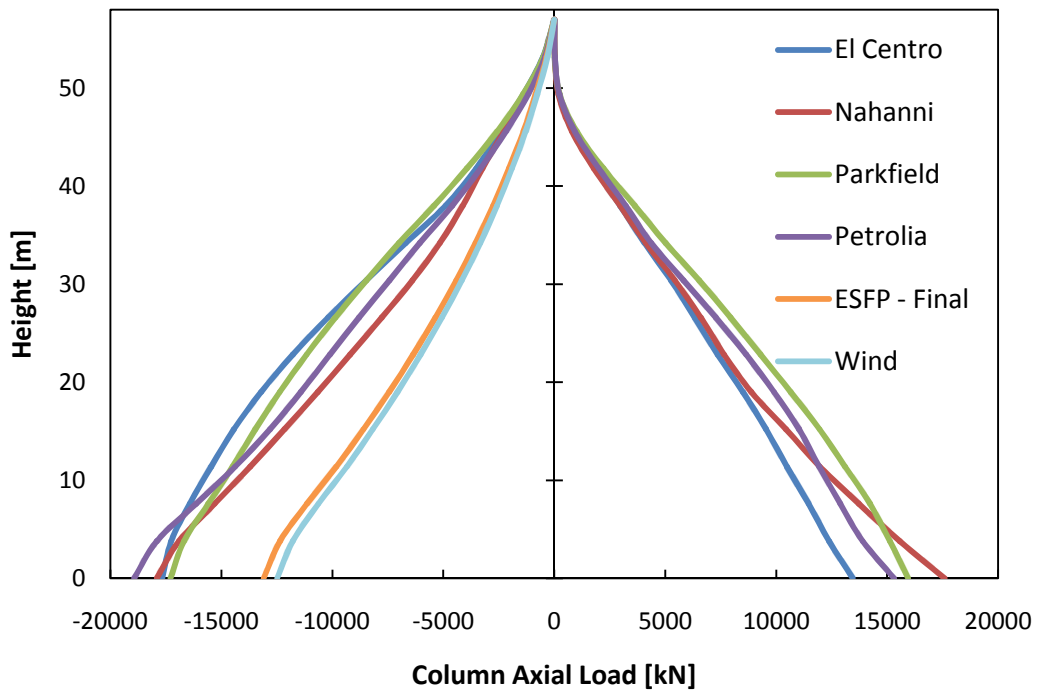


Figure 6.12 - Maximum and Minimum Axial Load; Right Column

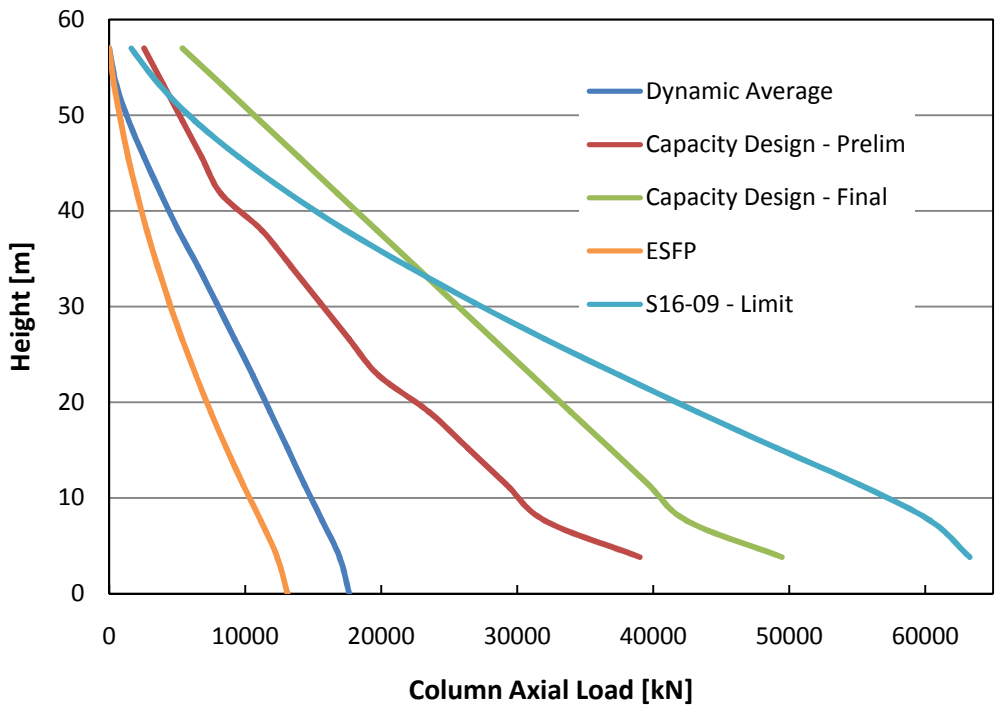


Figure 6.13 - Capacity Design and Analysis Force Effects; Column Axial Loads

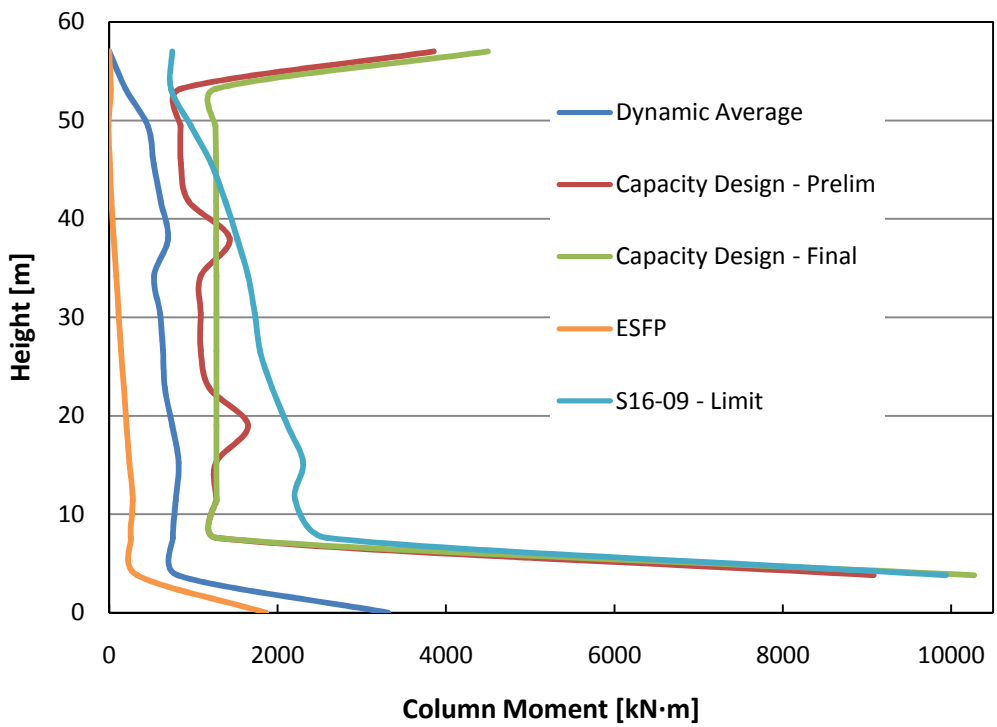


Figure 6.14 - Capacity Design and Analysis Force Effects; Column Moments

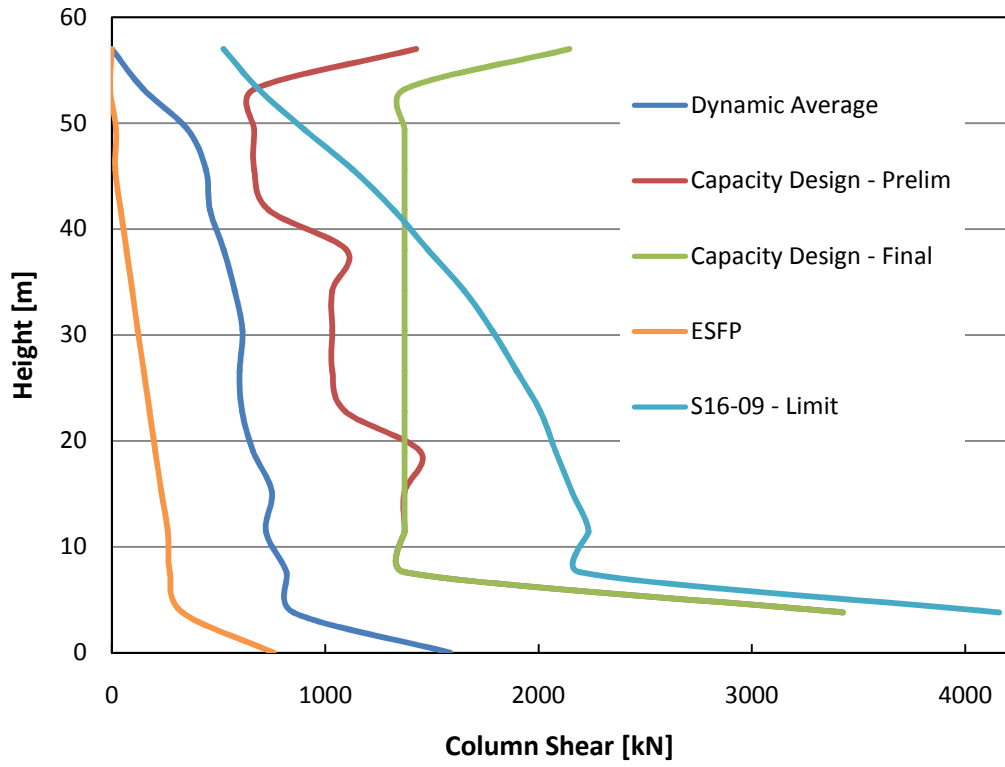


Figure 6.15 - Capacity Design and Analysis Force Effects; Column Shear

7. SUMMARY AND CONCLUSIONS

7.1 Summary

Steel plate shear walls have been used effectively as lateral load resisting systems since the early 1970's. SPSWs comprise of a steel plate which has been fixed to the bounding beams and columns to provide additional lateral resistance and ductility. They have been used in several countries including Canada, Japan, Mexico, and the United States. Typically, the infill plate is assumed to resist the entire shear loading by forming a diagonal tension field upon loading. The compressive resistance is considered to be negligible as the shear buckling of the panel occurs at a low loading.

The literature review presented in Chapter 2 outlined the trend of SPSWs from thick or stiffened infill plates in the early 1970's to the current thin, unstiffened panels most commonly used in new buildings. The research has shown that unstiffened SPSWs offer high initial lateral stiffness for wind loads and provide excellent energy absorption and ductility for seismic loads. Additionally, it has been shown that the capacity of the SPSW degrades in a gradual and stable manner after the ultimate capacity has been reached during cyclic testing. The research has shown that SPSWs with a rigid frame offer higher redundancy and better energy dissipation than SPSWs with shear beam to column connections. Early analysis methods involved the use of the strip model developed by Thorburn *et al.* (1983), which discretized the infill plate by a series of pin ended tension only strips. With the advance of computers and software capabilities, the use of complex FEA software (ABAQUS®, ANSYS®) using shell elements and large deformation formulations have become the preferred method for researchers. The analysis methods used have typically been either static nonlinear pushover analysis, or quasi-static cyclic loading routines. Recently, researchers have begun to use dynamic methods for the analysis of SPSWs.

Chapter 3 outlined the current guidelines for load determination and SPSW design according to the NBCC (2005) and S16-09. The lateral loading due to wind and earthquakes are covered from the NBCC. The NBCC has two methods of determining the seismic loads; the equivalent static force procedure and a dynamic procedure, which is the preferred method of analysis. The equivalent static force procedure approximates

the dynamic loads as static forces, but it has limited applicability. The static and dynamic analysis approaches were compared in terms of deflections and drift limits. The design requirements for SPSWs using the S16-09 guidelines for Type D and Type LD SPSWs were reviewed and applied to the design of a 15-storey SPSW. Finally, a comparison between the AISC design and the S16-09 design requirements is made.

The modeling procedure for a SPSW was outlined in Chapter 4 using commonly used structural analysis software. The infill panel of the SPSW was represented using the strip model proposed by Thorburn *et al.* (1983) to resist the lateral loads from wind and earthquakes. The SPSW model used tension strips inclined at an angle of 45° as it has been shown that the analysis results are insensitive to angles between 38° and 50° . The strips were provided in a single direction to model the effects of wind loading as well as the effects from the equivalent static force procedure from the NBCC (2005). The model was modified to include strips in both directions for the dynamic analysis. The static analysis incorporated the $P-\Delta$ and $P-\delta$ effects and the dynamic analysis was done using a nonlinear direct integration time history analysis using the time history records from four earthquakes. The earthquake records were made to be spectrum compatible for the Vancouver region as required by the NBCC. A nonlinear analysis was required due to the method of implementing the strip model, which used tension only strips to model the infill panel. Material nonlinearities were incorporated by inserting axial-moment interaction plastic hinges (FEMA 2000) in the beams and columns and axial hinges in the tension strips. The dynamic model was validated using the results from a similar SPSW modeled using finite strain shell elements by Bhowmick *et al.* (2009).

In Chapter 5, a 15-storey office building located in Vancouver Canada was selected to illustrate the design procedure of a Type D SPSW. The wind and earthquake loading for the structure were determined according to NBCC (2005). The infill panels were selected based on calculated seismic base shear and according to S16-09 and capacity design principles. The model as described in Chapter 4 was implemented in SAP2000® for both static and dynamic analysis and the results presented in Chapter 6. The preliminary analysis results indicated that the element sizes selected using capacity design were adequate for the structure analyzed dynamically, however, for the model analysed using

the equivalent static force procedure, the structure did not satisfy the NBCC maximum storey deflection requirements. To satisfy the requirements, the infill plate thickness was increased in an iterative process. The capacity design equations to select the boundary elements were repeated and the analysis was repeated for each iteration. The final design elements selected for the SPSW using the equivalent static force procedure resulted in beams and columns that were significantly larger than the beams and columns selected for the dynamic design.

Chapter 6 presents the validation of the dynamic strip model by comparing its results with the results of a shell element model presented by Bhowmick *et al.* (2009). The shell element model was validated using several monotonic tests, cyclic tests, and a dynamic test result. The tension strip model was validated against the shell model using four time history analysis results. The results of the validated dynamic analysis were compared to the equivalent static analysis results. Results from the wind loading were also presented. The force effects from the dynamic and static analyses were compared with the capacity design force effects determined in Chapter 5 as well as the S16-09 limit on the capacity design forces.

7.2 Conclusions

For design purposes, software programs such as ABAQUS® and ANSYS® are not ideal for use by design offices due to the complexity, cost, and time restraints in implementing a shell element model. Additionally, while the analysis methods typically used in research are able to predict monotonic and cyclic loading envelopes, these results are not indicative of the dynamic nature of earthquake loading and the subsequent behaviour of the structure.

The design and analysis of a 15-storey SPSW has shown that the strip model provides accurate dynamic analysis results. The SPSW designed using the dynamic analysis resulted in a frame that used lighter columns and thinner infill plates. The storey shears and storey moments determined from the dynamic design were significantly higher than the prescribed NBCC values determined from the equivalent static force procedure, indicating that the structure is capable of resisting significantly larger forces.

Additionally, these larger force effects did not cause any plastic hinge formation in the beam or column elements.

Using the equivalent static force procedure, the SPSW was required to have significant overstrength in order to satisfy the NBCC inelastic deflection requirements. It is recommended that the dynamic analysis procedure be used as the modeling procedure does not require significantly more effort than the static procedure. Additionally, the static procedure is only available for structures that meet certain requirements. These limitations restrict the procedure to structures that are relatively short with high stiffness and regular footprints. It was also seen that the S16-09 stiffness requirement of the top floor beam introduced significant overstrength to the design of the frame. The stiffness requirement for the top beam appears to be overly conservative given that the top storey infill panel in taller structures is unlikely to yield. Also seen was the overstrength introduced from assumption in the design equation that the infill plate resists 100% of the shear. Both the static and dynamic analyses indicated that significant portions of the storey shears were resisted by the columns.

The analyses of the SPSWs indicated that the period of the structure as determined using the NBCC equivalent static force procedure was significantly lower than what was determined analytically by the strip model and other models. In the case of the equivalent static force procedure, using the equation proposed by Bhowmick *et al.* (2009) would significantly reduce the static loads applied to the structure resulting in reduced deflections. With the smaller deflections, the structure would not have required the significant stiffening (infill plates, beams, and columns) that was needed to meet the NBCC interstorey drift limits.

7.3 Future Research

The methods typically used for testing SPSW are limited to monotonic and quasi static cyclic loading for the specimen. Analysis methods have been able to predict the initial stiffness and ultimate capacity to a relatively high degree of accuracy. However, these tests are not representative of dynamic loading that occurs during seismic events. Increasing the number of dynamic tests performed on SPSWs would increase our

understanding of the behaviour from dynamic excitations, as well as providing needed test results for the validation of analysis models for dynamic analysis.

The focus of this thesis was on the design and analysis of SPSW using thin infill plates as the lateral load resisting system. Provisions in S16-09 allow for perforations and cut-outs to weaken the infill panel, thus reducing the overstrength, as well as providing local access points. Reduced beam sections are also allowed in the design to encourage the beams to develop plastic hinging prior to the columns. These effects could be incorporated into the dynamic design procedure and validated against dynamic models.

REFERENCES

- AISC, 2007. Steel Plate Shear Walls. American Institute of Steel Construction, Chicago, IL.
- AISC, 2005. ANSI/AISC 341-05, Seismic Provisions for Structural Steel Buildings. American Institute of Steel Construction, Chicago, IL.
- AISC, 1999. Load and Resistance Factor Design Specification. American Institute of Steel Construction, Chicago, IL.
- Applied Technology Council, 1992. Guidelines for Cyclic Seismic Testing of Component of Steel Structures. ATC-24, Redwood City, CA.
- ASCE, 2005. SEI/ASCE 7-05, Minimum Design Loads for Buildings and Other Structures, American Society of Civil Engineers, Reston, VA.
- Astaneh-Asl, A., 2001. Seismic Behaviour and Design of Steel Shear Walls. Steel TIPS Report, Structural Steel Educational Council, July, Moraga, CA.
- Basler, K., 1961. Strength of Plate Girders in Shear. ASCE Journal of the Structural Division, Vol. 87, No. ST7, 151-180.
- Behbahanifard, M.R., Grondin, G.Y., and Elwi, A.E., 2003. Experimental and Numerical Investigation of Steel Plate Shear Walls. Structural Engineering Report No. 254, Department of Civil and Environmental Engineering, University of Alberta, Edmonton, Canada.
- Berman, J., and Bruneau, M., 2003. Plastic Analysis and Design of Steel Plate Shear Walls." ASCE Journal of Structural Engineering, November, 1448-1456.
- Berman, J. W. and Bruneau, M. 2003. Experimental Investigation of Light-Gauge Steel Plate Shear Walls. Journal of Structural Engineering, ASCE, 131 (2):259-267.
- Berman, J., and Bruneau, M., 2008. Capacity Design of Vertical Boundary Elements in Steel Plate Shear Walls. Engineering Journal, AISC, first quarter, 57-71.

- Bhowmick, A.K., Driver, R.G., and Grondin, G.Y., 2009. Seismic Analysis and Design of Steel Plate Shear Walls. Ph.D Dissertation, Department of Civil and Environmental Engineering, University of Alberta, Edmonton, Canada.
- Bing, Q., and Bruneau, M., 2009. Design of Steel Plate Shear Walls Considering Boundary Frame Moment Resisting Action. *Journal of Structural Engineering, ASCE*, 135 (12):1511-1521.
- Caccese, V., Elgaaly, M., and Chen, R., 1993. Experimental Study of This Steel-Plate Shear Walls Under Cyclic Load. *ASCE Journal of Structural Engineering*, 119 (2): 573-587.
- Canny Consultants, 1996. Canny-E Users' Manual, Win 95 Version (October). Canny Consultants Pty Ltd., Singapore.
- Chen, R., 1991. Cyclic Behaviour of Unstiffened Thin Steel Plate Shear Walls. Ph. D. Thesis. University of Maine, Orono, ME.
- Chen, W.F., Goto, Y., and Liew, J.Y.R., 1996. *Stability Design of Semirigid Frames*. Wiley, Ney York.
- Chien, E., 1987. *Multi-Storey Steel Building Design Aide*. Canadian Institute of Steel Construction, Willowdale, ON.
- Choi, I.R., Park, H.G., 2010. Hysteresis Model of Thin Infill Plate for Cyclic Nonlinear Analysis of Steel Plate Shear Walls. *ASCE Journal of Structural Engineering*, 136 (11):1423-1434.
- Chopra, A.K., 2001. *Dynamics of Structures: Theory and Applications to Earthquake Engineering*. Prentice-Hall, Inc., Englewood Cliffs, N.J.
- CSA, 2009. *Limit States Design of Steel Structures*. CAN/CSA S16-09, Canadian Standards Association, Toronto, ON., Canada.
- CSA, 2001. *Limit States Design of Steel Structures*. CAN/CSA S16-01, Canadian Standards Association, Toronto, ON., Canada.

- CISC, 2008. Moment Connections for Seismic Applications. Canadian Institute of Steel Construction, Markham, ON.
- Computers and Structures, Inc., 1984-2010. SAP2000® Nonlinear, Computers and Structures, Inc., Berkeley, CA.
- Dastfan, M., and Driver, R.G., 2008. Flexural Stiffness Limits for Frame Members of Steel Plate Shear Wall Systems. Proc., Annual Stability Conference, Structural Stability Research Council, April 2-5, Nashville, Tennessee, U.S.A.
- DeVall, R.H., 2003. Background Information for Some of the Proposed Earthquake Design Provisions for the 2005 Edition of the National Building Code of Canada. Canadian Journal of Civil Engineering, 30:279-286.
- Driver, R.G., Kulak, G.J., Kennedy, D.J.L., and Elwi, A.E., 1997. Seismic Behaviour of Steel Plate Shear Walls. Structural Engineering Report No. 215, Department of Civil and Environmental Engineering, University of Alberta, Edmonton, Canada.
- Driver, R.G., Kulak, G.J., Kennedy, D.J.L., and Elwi, A.E., 1998a. Cyclic Test of a Four-Storey Steel Plate Shear Wall. ASCE Journal of Structural Engineering, 124 (2): 112-120.
- Driver, R.G., Kulak, G.J., Kennedy, D.J.L., and Elwi, A.E., 1998b. FE and Simplified Models of Steel Plate Shear Walls. ASCE Journal of Structural Engineering, 124 (2): 121-130.
- Elgaaly, M., Caccese, V., 1990. Steel Plate Shear Walls. Proc., AISC Nat. Steel Constr. Conf., American Institute of Steel Construction Inc., Chicago, ILL. 4-1-4-28.
- Elgaaly, M., Caccese, V., and Du, C., 1993a. Postbuckling Behaviour of Steel-Plate Shear Walls under Cyclic Loads. ASCE Journal of Structural Engineering, 119 (2): 588-605.
- Elgaaly, M., Liu, Y., 1997. Analysis of Thin-Steel-Plate Shear Walls. ASCE Journal of Structural Engineering, 123 (11): 1487-1496.

- FEMA, 2000. Prestandard and Commentary for the Seismic Rehabilitation of Buildings (FEMA 356). Washington, D.C.
- Fragiacomo, M., Amadio, C., and Rajgelj, S., 2006. Evaluation of the Structural Response Under Seismic Actions Using Non-Linear Static Methods. *Earthquake Engineering and Structural Dynamics*, 35 (12), 1511-1531.
- Fujitani, H., Yamanouchi, H., Okawa, I., Sawai, N., Uchida, N., and Matsutani, T., 1996. Damage and Performance of Tall Buildings in the 1995 Hyogoken Nanbu Earthquake. Proceedings of 67th Regional Conference (in conjunction with ASCE Structures Congress XIV), Council on Tall Buildings and Urban Habitat, Chicago. 103-125.
- Heidebrecht, A.C., 2003. Overview of Seismic Provisions of the Proposed 2005 Edition of the National Building Code of Canada. *Canadian Journal of Civil Engineering*, 30:241-254.
- Hibbitt, Karlsson, and Sorenson, 2007. ABAQUS/Standard User's Manual. Version 6.8, HKS Inc., Pawtucket, RI.
- Humar, J., and Kumar, P., 1998. Torsional Motion of Buildings During Earthquakes. I. Elastic Response. *Canadian Journal of Civil Engineering*, 25:898-916.
- Humar, J., and Kumar, P., 1998. Torsional Motion of Buildings During Earthquakes. II. Inelastic Response. *Canadian Journal of Civil Engineering*, 25:917-934.
- Humar, J., and Mahgoub, M.A., 2003. Determination of Seismic Design Forces by Equivalent Static Load Method. *Canadian Journal of Civil Engineering*, 30:287-307.
- Humar, J., Yavari, S., and Saatcioglu, M., 2003. Design for Forces Induced by Seismic Torsion. *Canadian Journal of Civil Engineering*, 30:328-337.
- Kennedy, D.J.L., Kulak, G.L., and Driver, R.G., 1994. Discussion to "Postbuckling Behaviour of Steel-Plate Shear Walls," by Elgaaly, M., Caccese, V. and Du, C. *Journal of the Structural Division, ASCE*, 120 (7): 2250-2251.

- Kharrazi, M.H.K., Ventura, C.E., Prion, G.L., and Sabouri-Ghomi, S., 2004. Bending and Shear Analysis and Design of Ductile Steel Plate Walls. Proceedings of the 13th World Conference on Earthquake Engineering, August, Vancouver, B.C., Canada.
- Krawinkler, H., and Seneviratna, G.D.P.K., 1998. Pros and Cons of a Pushover Analysis of Seismic Performance Evaluation. *Engineering Structures*, 20 (4-6): 452-464.
- Kulak, G.L., and Grondin, G.Y., 2009. Limit States Design in Structural Steel. Canadian Institute of Steel Construction, Willowdale, ON.
- Kulak, G.L., Kennedy, D.J.L., and Driver, R.G., 1994. Discussion of "Experimental Study of Thin Plate Shear Walls Under Cyclic Load." *ASCE Journal of Structural Engineering*, 120 (10): 3072-3073.
- Kulak, G.L., Kennedy, D.J.L., Driver, R.G., and Medhekar, M., 2001. Steel Plate Shear Walls – An Overview" *American Institute of Steel Construction Engineering Journal*, First Quarter: 50-62.
- Kuhn, P., Peterson, J.P., and Levin, L.R., 1952. A Summary of Diagonal Tension, Part I – Methods of Analysis. Technical Note 2661, National Advisory Committee for Aeronautics, Washington, DC.
- Kurban, C.O., and Topkaya, C., 2009. A numerical Study on Response Modification, Overstrength, and Displacement Amplification factors for Steel Plate Shear Walls. *Earthquake Engineering and Structural Dynamics*, 38 (4):497-516.
- Lubell, A.S., 1997. Performance of Unstiffened Steel Plate Shear Walls Under Cyclic Quasi-Static Loading. M.Sc. Thesis, Department of Civil Engineering, University of British Columbia, Vancouver, B.C., Canada.
- Lubell, A.S., Prion, H.G.L., Ventura, C.E., and Rezai, M., 2000. Unstiffened Steel Plate Shear Wall Performance Under Cyclic Loading. *Journal of Structural Engineering*, 126 (4):453-460.
- Mazzoni, S. McKenna, F., and Fenves, G.L., 2006. Open System for Earthquake Engineering Simulations, Version 1.7.3. Pacific Earthquake Engineering Research Center, Univ. of California, Berkeley, CA.

- Mimura, H., and Akiyama, H., 1977. Load-Deflection Relationship of Earthquake-Resistant Steel Shear Walls With a Developed Diagonal Tension Field. Transactions, Architectural Institute of Japan, 260, October: 109-114.
- Mitchell, D., Tremblay, R., Karacabeyli, E., Paultre, P., Saaticioglu, M., and Anderson, D.L., 2003. Seismic Force Modification Factors for the Proposed 2005 Edition of the National Building Code of Canada. Canadian Journal of Civil Engineering, 30:308-327.
- Naumoski, N. 2001. Program SYNTH, Generation of Artificial Accelerogram History Compatible with a Target Spectrum. Dept. of Civil Engineering, University of Ottawa, On.
- NEHRP, 2000. National Earthquake Hazards Reduction Program, Recommended Provisions for Seismic Regulations for New Buildings and Other Structures. Building Seismic Safety Council, Washington, D.C. 2 vols., FEMA 368 and 369.
- Neilson, D.A.H., Grondin, G.Y., and Driver, R.G. 2010. Welding of Light Gauge Infill Panels for Steel Plate Shear Walls. Structural Engineering Report No. 290, Department of Civil and Environmental Engineering, University of Alberta, Edmonton, AB.
- NRCC, 1995. National Building Code of Canada 1995. Canadian Commission on Building and Fire Codes, National Research Council of Canada, Ottawa, ON.
- NRCC, 2005. National Building Code of Canada. Canadian Commission on Building and Fire Codes, National Research Council of Canada, Ottawa, ON.
- Oughourlian, C.V., and Powell, G.H., 1982. ANSR-III, General Purpose Computer Program for Nonlinear Analysis. EERC – Rep. No. UCB/EERC-82/21.
- Park, H. G., Kwack, J.H., Jeon, S.W., Kim, W.K., and Choi, I.R., 2007. Framed Steel Plate Wall Behaviour Under Cyclic Lateral Loading. ASCE Journal of Structural Engineering, 133 (3):378-388.
- Paulay, T. and Priestley, M.J.N., 1992. Seismic Design of Reinforced Concrete and Masonry Buildings. John Wiley & Sons, Inc., New York, N.Y.

- Prakash, V., Powell, G.H., and Campbell, S., 1993. DRAIN-2DX Base Program Description and User Guide, Version 1.10. Report No. UCB/SEMM-93/17, Department of Civil Engineering, University of California, Berkeley, California.
- Purba, R.H., 2006. Design Recommendations for Perforated Steel Plate Shear Walls. M.Sc. Thesis, State Univ. of New York at Buffalo, Buffalo, N.Y.
- Redwood, R.G. and Channagiri, V.S., 1991. Earthquake-Resistant Design of Concentrically Braced Steel Frames. Canadian Journal of Civil Engineering, 18 (5):839-850.
- Rezai, M., 1999. Seismic Behaviour of Steel Plate Shear Walls by Shake Table Testing. PhD Dissertation, Department of Civil Engineering, University of British Columbia, Vancouver, B.C., Canada.
- Roberts, T.T. and Sabouti-Ghomi, S., 1992. Hysteretic Characteristics of Unstiffened Perforated Steel Plate Shear Panels. Thin Walled Structures, 14: 139-151.
- Sabelli, R. and Bruneau, M., 2007. Steel Design Guide 20: Steel Plate Shear Walls. American Institute of Steel Construction, Chicago, IL.
- Saatcioglu, M. and Humar, J., 2003. Dynamic Analysis of Buildings for Earthquake Resistant Design. Canadian Journal of Civil Engineering, 30:338-359.
- Seal, C.K., Hodgson, M.A., and Ferguson, W.G., 2007. Cyclic Plasticity of Steel. Materials Science and Technology Conference and Exhibition. Exploring Structure, Processing and Applications Across Multiple Materials Systems. September 16-20, Detroit, Michigan, U.S.A.
- Schumacher, A., Grondin, G.Y., and Kulak, G.L., 1999. Connection of Infill Panels in Steel Plate Shear Walls. Canadian Journal of Civil Engineering, 26:549-563.
- Shishkin, J.J., Driver, R.G., and Grondin, G.Y., 2005. Analysis of Steel Plate Shear Walls Using the Modified Strip Model. Structural Engineering Report No. 261, Department of Civil and Environmental Engineering, University of Alberta, Edmonton, AB.

- Takahashi, Y., Takemoto, Y., Takeda, T., and Takago, M., 1973. Experimental Study on Thin Steel Shear Walls and Particular Bracings Under Alternative Horizontal Load. Preliminary report, IABSE Symposium on Resistance and Ultimate Deformability of Structures Acted on by Well-Defined Repeated Loads, Lisbon, Portugal, 185-191.
- Thorburn, L.J., Kulak, G.L., and Montgomery, C.J., 1983. Analysis of Steel Plate Shear Walls. Structural Engineering Report No. 107, Department of Civil and Environmental Engineering, University of Alberta, Edmonton, Canada.
- Timler, P.A., Kulak, G.L., 1983. Experimental Study of Steel Plate Shear Walls. Structural Engineering Report No. 114, Department of Civil and Environmental Engineering, University of Alberta, Edmonton, Canada.
- Timler, P.A., 1998. Design Procedures Development, Analytical Verification, and Cost Evaluation of Steel Plate Shear Wall Structures. Earthquake Engineering Research Facility Technical Report No. 98-01.
- Timler, P.A., Ventura, C.E., Prion, H., and Anjam, R., 1998. Experimental and Analytical Studies of Steel Plate Shear Walls as Applied to the Design of Tall Buildings. Structural Design of Tall Buildings, 7:233-249.
- Topkaya, C., and Kurban, O.C., 2009. Natural Periods of Steel Plate Shear Wall Systems. Journal of Constructional Steel Research, 65 (3):542-551.
- Tromposch, E.W., Kulak, G.L., 1987. Cyclic and Static Behaviour of Thin Panel Steel Plate Shear Walls. Structural Engineering Report No. 145, Department of Civil and Environmental Engineering, University of Alberta, Edmonton, Canada.
- Vian, D., 2005. Steel Plate Shear walls for Seismic Design and Retrofit of Building Structures. Ph.D. dissertation, State Univ. of New York at Buffalo, Buffalo, N.Y.
- Wagner, H., 1931. Flat Sheet Metal Girders with Very Thin Webs, Part 1 – General Theories and Assumptions. Technical Memo No. 604, National Advisory Committee for Aeronautics, Washington, D.C.

Xue, M., and Lu, L.W., 1994. Interaction of Infilled Steel Shear Wall Panels with Surrounding Frame Members. Proceedings, Structural Stability Research Council Annual Technical Session, Bethlehem, PA, 339-354.

Youssef, N., Wilkerson, R., Fischer, K., Tunick, D., 2009. Seismic Performance of a 55-Storey Steel Plate Shear Wall Building. The Structural Design of Tall and Special Buildings. 19 (1-2): 139-165